uOttawa

L'Université canadienne
Canada's university

FACULTÉ DES ÉTUDES SUPÉRIEURES ET POSTOCTORALES

uOttawa

L'Université canadienne
Canada's university

FACULTY OF GRADUATE AND POSDOCTORAL STUDIES

Katherine V. Clark-Knowles

AUTEUR DE LA THÈSE / AUTHOR OF THESIS

Ph.D. (Cellular and Molecular Medicine)

GRADE / DEGREE

Department of Cellular and Molecular Medicine

FACULTÉ, ÉCOLE, DÉPARTEMENT / FACULTY, SCHOOL, DEPARTMENT

Conditional Inactivation of the BRCA1 Tumour Suppressor Gene in the Mouse Ovarian Surface Epithelium In Vitro and In Vivo

TITRE DE LA THÈSE / TITLE OF THESIS

Barbara Vanderhyden

DIRECTEUR (DIRECTRICE) DE LA THÈSE / THESIS SUPERVISOR

CO-DIRECTEUR (CO-DIRECTRICE) DE LA THÈSE / THESIS CO-SUPERVISOR

EXAMINATEURS (EXAMINATRICES) DE LA THÈSE / THESIS EXAMINERS

Patricia Kruk

Jonathan Lee

Douglas Gray

Bruce McKay

Gary W. Slater

Le Doyen de la Faculté des études supérieures et postdoctorales / Dean of the Faculty of Graduate and Postdoctoral Studies

CONDITIONAL INACTIVATION OF THE *BRCA1* TUMOUR SUPPRESSOR GENE IN THE MOUSE OVARIAN SURFACE EPITHELIUM *IN VITRO* AND *IN VIVO*

by

Katherine Victoria Clark-Knowles

Thesis submitted to the Faculty of Graduate and Postdoctoral Studies in partial fulfillment of the requirements for the degree of Doctor of Philosophy

Department of Cellular and Molecular Medicine
University of Ottawa
Ottawa, Ontario, Canada
January 2007

Your file Votre référence
ISBN: 978-0-494-49333-5
Our file Notre référence
ISBN: 978-0-494-49333-5

Table of Contents

Abstract

Epithelial ovarian cancer (EOC) is thought to arise from the ovarian surface epithelium (OSE); however the molecular events underlying this transformation are poorly understood. Germline mutations in the *BRCA1* tumor suppressor gene result in a significantly increased risk of developing EOC and a large proportion of sporadic EOCs display some sort of *BRCA1* dysfunction.

Using mice with conditional expression of *Brca1*, we inactivated *Brca1* in the murine OSE and demonstrate that this inactivation results in the development of preneoplastic changes, such as hyperplasia, epithelial invaginations, and inclusion cysts, which arise earlier and are more numerous than in control ovaries. These changes resemble the premalignant lesions that have been reported in human prophylactic oophorectomy specimens from women with *BRCA1* germline mutation.

While tumourigenesis was not observed when *Brca1* was inactivated on its own, it was found that inactivation of *Brca1* accelerated tumour progression in animals in which the *p53* tumour suppressor had also been inactivated in the OSE, an effect that was not observed with concomitant inactivation of the *Rb* tumour suppressor gene.

Inactivation of *Brca1* in primary cultures of murine OSE cells led to a suppression of proliferation due to increased apoptosis that could be rescued by concomitant inactivation of *p53* and/or *Rb*, however only concomitant inactivation of *p53* led to the ability of *Brca1*-deficient MOSE cells to grow in an anchorage-independent manner. *Brca1*-deficient MOSE cells displayed an increased sensitivity to the DNA damaging agent cisplatin and were modestly less sensitive to the mitotic spindle poison paclitaxel, effects which could both be modulated via inactivation of *p53* and/or *Rb*

These observations indicate that loss of function of *Brca1* in OSE cells impacts both cellular growth control and DNA-damage repair which results in altered cell behavior manifested as morphological changes *in vivo* that arise earlier and are more numerous than what can be attributed to ageing. It is postulated that loss of *Brca1* in the OSE renders these cells susceptible to further genetic aberrations such as loss of other tumour suppressors or activation of oncogenes that could lead to transformation and tumourigenesis.

Acknowledgements

I would like to take this opportunity to thank all those who were a part of my graduate school journey, without whom I could not have made it out the other side.

Firstly, thank you to my supervisor Dr. Barbara Vanderhyden, whose guidance and encouragement and complete love of science made my graduate school experience such a positive one. Her ability to always put a positive spin on any result, to remind me that these results were always interesting and of value, helped me get through the bumps in the road that come with a PhD project. She embodies all of the qualities one hopes for in a supervisor; enthusiasm, availability, letting you figure things out for yourself, but never leaving you high and dry. Barb took a chance on me, in that I did not arrive in her lab under the normal circumstances, something I feel we've all but forgotten. I like to think I was a "surprise", something she didn't know she really wanted until she got it. Thanks for taking me in and restoring my faith when it had been shaken.

Thank you to my advisory committee, Dr. Bruce McKay, Dr. Ben Tsang, and Dr. Chris Kennedy, for your critiques, suggestions, recommendations, and support throughout my degree. Special thanks as well to Dr. Mary Senterman for her assistance and time with helping us determine the pathology of the tumours. A very big thank you to Donna Hooper, the graduate secretary for the CMM department, for answering so many questions over the years. I would also like to thank the scientists, students, and staff of the 3rd floor Cancer Research Group at the Cancer Centre for making it a great place to work and learn.

I would also like to thank some key members of the Vanderhyden lab who were an integral part of my success as a graduate student. To Ken Garson, for insightful talks,

encouragement, and invaluable opinions. To Olga Collins for struggling with the MOSE cultures with me, and never giving up on our quest to make them grow. To Kerri Courville, for teaching me everything there is to know about mice and more. To Liz Macdonald, our PCR guru, for always knowing a way to make it work. To Colleen Crane, for cutting seemingly endless sections and helping so much with troublesome immunohistochemistry, and for being a great friend at and away from the lab.

To my fellow graduate students who were there when I started, Tanya Shaw and Lisa Vandermeer. You are two of my greatest friends and I have missed having you around so much. Thank you for all the great talks, great times, support and encouragement, for sharing much laughter, a few tears, and so many big events in our lives. Lisa, I could not have asked for a better co-coordinator for Let's Talk Science. A special thank you to Tanya as well, for introducing me to my husband!

To my current lab mates, David Pepin, Laura Laviolette, Rita Shamoon, Lisa Turchet, and Valerie Snoulten. Thanks for making the lab a fun place to be. We had some great scientific discussions, some great life discussions, and also a lot of joking around.

To Elizabeth Hadwen and Natacha Gagnon, a summer student and co-op student respectively, who worked on various aspects of my project with me during their stints in the lab. I hope you learned as much about science and research from me as I learned from you about leadership and teaching.

To my parents, Janet and Cameron Clark, and my sister Jenny. Thank you for your unwavering support and encouragement, I truly could not have done this without you. You have cheered me on the whole way through, telling me to never give up, to

always do my best, and to keep things in perspective. Thank you for never letting me doubt that I was making you very proud.

Finally, I want to thank my husband and best friend, Jason Knowles, for standing by me through the best and worst of this degree and for often being the voice of reason. For telling me you'd help me find my second, third, one-hundredth winds, whatever it took, to get through. For turning into a domestic god, making sure I was fed, washed, and clothed, so I could get as much work done as possible. Thank you for helping me relax and reminding me what life is really all about. It's been quite the adventure together!

List of Figures

List of Tables

List of Abbreviations and Chemical Formulae

°C	degrees Celsius
λ	wavelength
1st	first
α	alpha
β	beta
Δ	delta
α-MEM	alpha minimum essential medium
AdCre	adenoviral Cre recombinase
AdGFP	adenoviral green fluorescent protein
AdLacZ	adenoviral LacZ
ANOVA	analysis of variance
BASC	BRCA1-associated genome surveillance complex
BRCA1	breast cancer 1 early onset
BRCA2	breast cancer 2 early onset
bp	base pair
$C_6H_8O_7$	citric acid
CA125	cancer antigen 125
cDNA	complementary DNA
CK19	cytokeratin 19
cm	centimetre(s)
CO_2	carbon dioxide
DAB	diaminobenzidine
dH_2O	distilled water
DNA	deoxyribonucleic acid
dNTPs	deoxynucleoside triphosphate
Dox	doxycycline
DTT	dithiothreitol
E-cadherin	epithelial cadherin
EDTA	ethylenediaminetetraacetic acid
eGFP	enhanced green fluorescent protein
EOC	epithelial ovarian cancer
ES	embryonic stem
FIGO	International Federation of Gynecology and Obstetrics
FSH	follicle-stimulating hormone
g	gram(s)
GAPDH	glyceraldehyde-3-phosphate dehydrogenase
GFP	green fluorescent protein

H_2O	water
H_2O_2	hydrogen peroxide
hCG	human chorionic gonadotropin
H&E	hematoxylin and eosin
HI-FBS	heat inactivated fetal bovine serum
HPV	human papilloma virus
HRP	horseradish peroxidase
IHC	immunohistochemistry
I.U.	international unit
ITSS	insulin-transferrin-sodium-selenite
KCl	potassium chloride
kD	kiloDalton
LH	luteinizing hormone
LOH	loss of heterozygosity
LoxP	locus of X over P1
µl	microlitre(s)
µM	micromolar
µm	micrometre(s)
M	molar
$MgCl_2$	magnesium chloride
mg	milligram(s)
MISIIR	Mullerian Inhibiting Substance Type II Receptor
ml	millilitre(s)
mM	millimolar
MMP	matrix metalloproteinase
MOI	multiplicity of infection
MOPS	3-(N-morpholino) propanesulfonic acid
MOSE	mouse ovarian surface epithelium (epithelial)
mRNA	messenger ribonucleic acid
$Na_3C_6H_5O_7$	sodium citrate
Na_3VO_4	sodium orthovanadate
NaCl	sodium chloride
NaF	sodium fluoride
NaPP	sodium pyrophosphate
ng	nanogram(s)
nM	nanomolar
OSE	ovarian surface epithelium (epithelial)

p53	tumour protein 53
P	probability
PBS	phosphate-buffered saline
PCR	polymerase chain reaction
pfu	plaque forming unit
PMSF	phenylmethylsulphonylfluoride
PMSG	pregnant mare serum gonadotropin
PTT	protein truncation test
RB	retinoblastoma
RIPA	radioimmunoprecipitation assay
RNA	ribonucleic acid
rTA	tetracycline-controlled transactivator protein
rtTA	reverse tetracycline-controlled transactivator protein
RT-PCR	reverse transcription-polymerase chain reaction
rpm	rotations per minute
SEM	standard error of the mean
SDS	sodium dodecylsulphate
SMA	smooth muscle actin
S-PBS	Stockholm's phosphate-buffered saline
SSCA	single-stranded conformation analysis
SV40	simian virus 40
TAE	Tris acetate ethylenediaminetetraacetic acid
TAg	large T antigen
Taq	thermophilic DNA polymerase
TBS/T	tris-buffered saline+Tween
TE	Tris-buffered EDTA
Tet	tetracycline
TRE	tetracycline responsive element
Trp53	transforming related protein 53
WAP	whey acidic protein
WHO	World Health Organization
X	multiplied by
X-Gal	5-bromo-4-chloro-3-indolyl-beta-D-galactopyranoside

Chapter 1: Introduction

1.1 Ovarian Cancer: General overview

Ovarian cancer is the fifth leading cause of cancer death of women in the Western world and is the most fatal of all the gynecologic malignancies. This year in Canada approximately 2300 women will be diagnosed with ovarian cancer and 1600 will die from this disease. One in seventy Canadian women will be diagnosed with ovarian cancer in her lifetime (Canadian Cancer Society 2006). If the disease is diagnosed when it is still confined to the ovaries, the five-year survival rate is greater than ninety percent, however less than twenty-five percent of patients are diagnosed this early in disease progression (Moloughney, et. al., 2000). Once the disease has spread to the rest of the reproductive tract and the other organs and tissues within the peritoneal cavity, the five-year survival rate is only 30-40%. This statistic has not changed in over thirty years. The dismal prognosis for ovarian cancer can be attributed to a lack of effective screening methods as well as the frequent development of drug resistance.

1.2 Ovarian Cancer: Classification

Ninety percent of ovarian carcinomas are epithelial in origin and are thought to arise from the ovarian surface epithelium (OSE), a single-cell layer that comprises the outer surface of the ovary. These epithelial neoplasms can be further subtyped based on their resemblance to other tissues of the reproductive tract. The most common subtype is the serous adenocarcinoma, so-named because of its resemblance to the cells of the inner lining of the fallopian tube. The other subtypes include: mucinous, which resemble the

endocervical epithelium; endometrioid, which as the name suggests, are similar to the cells of the endometrium; clear cell tumours, with cells with a large, clear cytoplasm; and transitional cell tumours, whose cells can be likened to those of the bladder epithelium (Chen, et. al., 2003). The other ten percent of malignant ovarian tumours originate from the other tissues of the ovary, such as the granulosa cells, the theca cells, the stromal cells, and the oocytes. Such tumours include sex cord-stromal tumours, granulosa tumours, theca tumours, fibromas, and germ cell tumours .

The International Federation of Gynecology and Obstetrics (FIGO) has developed guidelines for the staging of ovarian carcinomas (Benedet, et. al., 2000). This encompasses four stages and 3 grades, with grade only being applicable to tumours of epithelial pathology. Stage I disease indicates that one or both ovaries are involved, but there is no dissemination beyond this point. Stage II disease presents with pelvic implants on the uterus or fallopian tubes or other pelvic structures. Stage III disease is indicated by the presence of micro or macroscopic peritoneal disease outside of the pelvic area. Stage IV disease is classified by the presence of metastases to distant sites.

Grading of epithelial tumours is done based on features such as architectural patter, cytologic atypia, and/or mitotic index (Malpica, et. al., 2004), however there currently does not exist a universally accepted grading system. The widely used FIGO grading system utilizes level of differentiation as well as the ratio of glandular or papillary structures versus solid tumour growth for the further classification of epithelial ovarian tumours. Grade 0 tumours are those of low malignant potential and are the most well differentiated. A grade I tumour is well differentiated with less than 5% solid tumour, grade II indicates moderate differentiation with 5-50% solid component, and

grade III tumours are poorly differentiated withh greater than 50% solid tumour growth (Benedet, et. al., 2000). The system developed by the World Health Organization (WHO) is based on the qualitative observations of the architectural and cytologic features, but is not quantitative (Brugghe, et. al., 1995). Finally, the Silverberg grading system classifies epithelial ovarian tumours based on a combination of tissue architecture, cytology, and the number of mitotic figures in ten high power fields. With this system, Grade 1 tumours are glandular with slight cytologic atypia and less than 10 mitotic figures, Grade 2 tumours are papillary with moderate atypia and 10-24 mitotic figures, and Grade 3 tumours are solid with significant cytologic atypia and $\geq$25 mitotic figures (Silverberg, 2000).

1.3 Ovarian Cancer: Etiology

The events that lead to the malignant transformation of the OSE and the development of ovarian cancer are not well understood. There are, however, several factors that have been implicated, including ovulation, reproductive hormones, environmental agents, and genetics, all of which will be addressed here.

1.3.1 The Incessant Ovulation Theory

One of the more popular theories regarding the development and progression of ovarian cancer is the "incessant ovulation hypothesis", first proposed by Fathalla in 1971. This hypothesis proposed that the continuous rupture and repair of the OSE with each ovulation render this tissue more sensitive to transformation due to the constant cell turnover; thus the more ovulatory cycles the OSE is subjected to, the more likely it is for a neoplasm to develop (Fathalla, 1971). Several lines of evidence from animal models

and epidemiological data support this hypothesis. Domestic hens, that when forced to lay eggs and hence ovulate continuously, were found to be more prone to the development of spontaneous ovarian tumours (Fredrickson, 1987). Conversely, animals that ovulate only when they mate (reflex ovulators, which comprises most domestic animals) display a decreased tendency towards the development of spontaneous ovarian tumours (MacLachlan, 1987). Epidemiologic data also supports this theory in the human female. When the number of ovulatory cycles over time was compared in a sample of women, it was found that an increase in ovulation number correlated with an increased risk for the development of ovarian cancer, and this increased risk was strongest in women who had increased ovulations between the ages of 20-29 (Purdie, et. al., 2003). This effect is also seen in women who underwent induced ovulations with the aid of fertility drugs (Rossing, et. al., 2004) and in a mouse model it has been shown that superovulation increases the proliferation of OSE cells (Burdette, et. al., 2006). There is also considerable evidence that indicates that factors which prevent ovulation, such as pregnancy, lactation, and the use of oral contraceptives, decrease a woman's risk of developing ovarian cancer (Cramer, et. al., 1983; Gwinn, et. al., 1990; Siskind, et. al., 1997).

1.3.2 The Gonadotropin Theory

One of the other main theories proposed to explain the development of epithelial ovarian cancer (EOC) is the "gonadotropin theory". This theory postulates that elevated levels of the pituitary gonadotropins luteinizing hormone (LH) and follicle-stimulating hormone (FSH) are responsible for excessive stimulation of ovarian tissue that ultimately leads to transformation. This hypothesis stems from the fact that the majority of EOCs

are diagnosed in peri- or postmenopausal women, when endogenous levels of LH and FSH are their highest (Yancik, 1993). It was originally derived based on experiments involving the transplantation of ovaries into the splenic pulp of rats, which lead to ovarian tumour formation. The tumourigenesis was thought to be due to the fact that estrogen was inactivated in the liver and thus gonadotropin levels would rise due to lack of pituitary feedback (Vanderhyden 2005). Epidemiologic evidence also demonstrates that situations which suppress gonadotropin secretion, such as pregnancy and oral contraceptive use, decrease ovarian cancer risk (Risch, 1998) and women with polycystic ovarian syndrome, who have high levels of circulating LH, are at increased risk (Schildkraut, et. al., 1996). Experimental evidence also supports the gonadotropin theory to a certain extent. Transgenic mouse models with elevated gonadotropin levels do display ovarian tumourigenesis, though they tend not to be of epithelial origin (Risma, et. al., 1995; Keri, et. al., 2000). It has also been demonstrated that exogenous gonadotropin-induced ovulations lead to an increase in OSE stratification in rats (Celik, et. al., 2004) and to increased OSE cell proliferation in mice .

1.3.3 Environmental Factors

Few environmental factors directly related to an increase in risk for EOC have been identified. Results from epidemiologic studies indicate possible correlations between the use of talc, exposure to tobacco smoke or radiation, use of psychotropic medications, infection with the virus that causes mumps, high levels of physical activity, high body mass index, high caffeine consumption and increased risk for EOC, though the correlations were often modest at best (Holschneider and Berek, 2000).

The link between heavy use of talc in the genital area and ovarian cancer risk has been one of the well-studied environmental risk factors with supporting experimental evidence. The link initially stemmed from the discovery of talc in normal and malignant ovarian tissue (Henderson, et. al., 1979). Epidemiologic studies also supported a connection with perineal talc use and an increased risk of ovarian cancer (Harlow, et. al., 1992; Cramer, et. al., 1999; Gertig, et. al., 2000). Experimental evidence in a rat model then showed that talc could in fact travel from the vagina to the ovaries, and that exposure of the ovarian surface to talc led to an increase in focal areas of papillary change (Hamilton, et. al., 1984; Henderson, et. al., 1986).

1.3.4 Genetics

Ovarian cancer most often develops sporadically, in that a series of somatic genetic alterations take place in the normal OSE that eventually leads to transformation and tumourigenesis. While there is currently no clear picture of what this series of genetic events comprises, research to date has revealed multiple possibilities. A much smaller number of EOCs appears to be due to inherited germline mutations in tumour suppressor genes, in that a disease-causing genetic alteration is already present at birth, predisposing the individual to disease with a potentially earlier onset. Both of these situations will be discussed in greater detail here.

1.3.4.1 Germline Mutations

Five to fifteen percent of EOCs are thought to have a hereditary component, caused by germline mutations in the tumour suppressor genes *BRCA1* and *BRCA2*,

though predominantly *BRCA1* (Pal, et. al., 2005). As *BRCA1* is the main focus of this work, it will be discussed in greater detail further on.

EOC has also been seen occasionally as part of the tumour spectrum associated with Li-Fraumeni syndrome, a rare condition that is due to germline mutations in the *p53* tumour suppressor gene and confers up to a 90% lifetime risk of developing cancer (Birch, et. al., 2001).

EOCs with endometrioid pathology have been associated with germline mutations in the hereditary non-polyposis colorectal cancer (HNPCC) DNA mismatch repair genes *MSH2* and *MLH1* (Watson and Riley, 2005). Approximately 10-12% of women with HNPCC will develop ovarian cancer in their lifetime (Aarnio, et. al., 1995; Prat, et. al., 2005), though they are at greatest risk for developing colorectal cancer. Between 2 to 4% of colorectal cancer cases are thought to be due to HNPCC (Ponz de, et. al., 1999).

Other less common genetic syndromes that carry an increased risk for ovarian cancer (though not necessarily epithelial) include; Peutz-Jeghers syndrome, which is due to germline mutations in the STK11 tumour suppressor gene and confers a 20% lifetime risk of ovarian cancer (Papageorgiou and Stratakis, 2002); Carney complex, caused by mutations in a protein-kinase A regulatory subunit gene, where more than half of female patients develop ovarian tumours (Stratakis, et. al., 2000); ataxia telangiectasia, a neurodegenerative disease caused by mutations in the *ATM* gene (Smith and Ponder, 1993), as well as Cowden disease, caused by germline mutations in the *PTEN* tumour suppressor gene, a rare disease characterized by multiple hamartomas (Lynch, et. al., 1997).

1.3.4.2 Somatic Mutations

Somatic mutations in other tumour suppressor genes and oncogenes have been found to be associated with sporadic ovarian cancer. These alterations appear to influence pathology, prognosis, as well as chemosensitivity.

Somatic mutations and/or overexpression of *p53* have been found in 40-80% of EOCs (Feki and Irminger-Finger, 2004), making it perhaps the most common alteration seen in these tumours, as well as most other cancers. *p53* mutations and/or overexpression have been shown to be correlated with poor prognosis (Hartmann, et. al., 1994; Klemi, et. al., 1995; Buttitta, et. al., 1997), metastasis (Sood, et. al., 1999), as well as resistance to chemotherapy (; Kigawa, et. al., 2001).

Another tumour suppressor gene that has been associated with sporadic ovarian cancer is *PTEN*. Though predominantly associated with the tumours spectrum seen in Cowden's syndrome, *PTEN* mutations are often detected in EOCs, but most specifically those with endometrioid histology (Li and Karlan, 2001; Kolasa, et. al., 2006). Approximately 30% of endometrioid ovarian tumours display somatic mutations in *PTEN* (Obata and Hoshiai, 2000), while only 5% of serous adenocarcinomas display mutations (Kolasa, et. al., 2006). Epigenetic silencing has been shown to play a significant role in loss of PTEN expressin in EOC (Kurose, et. al., 2001).

While the retinoblastoma (*RB*) tumour suppressor gene does not appear to have a strong association with the development of EOC, there is some evidence for its involvement. Loss of heterozygosity (LOH) of *RB* appears to be a common event in EOC, found in up to 60% of tumours, however whether or not there is a corresponding increase in loss of protein expression continues to be debated (Liu, et. al., 1994; Taylor,

et. al., 1995; Niemann, et. al., 1998; Gras, et. al., 2001). EOC patients with an altered *RB* signaling pathway have been shown to have poorer survival outcomes than those with normal *Rb* signaling (Hashiguchi, et. al., 2004).

Mutations in the oncogene *K-ras* are seen frequently in EOC (Enomoto, et. al., 1991). K-ras is a member of the *ras* family of GTPases and mutations generally result in constitutive activation (Ellis and Clark, 2000). These mutations are predominantly associated with tumours with mucinous histology and are thought to be an early event in ovarian tumourigenesis. Up to 75% of mucinous EOCs demonstrate *K-ras* mutations (Aunoble, et. al., 2000). The hypothesis that *K-ras* mutations may represent an early event in this disease progression is due to the fact that the mutations are more often seen in borderline tumours, which may represent the precursors to malignant mucinous tumours (Caduff, et. al., 1999). To date, no real correlation has been reported between *K-ras* status and prognosis in EOC.

Another oncogene that has been shown to have a possible role in ovarian tumourigenesis is *HER-2/neu*. A member of the family of growth factors that includes EGF-R, HER-2/neu is amplified or overexpressed in up to 60% of EOCs . Higher expression of HER-2/neu message has been shown to be associated with poorer prognosis and chemotherapy resistance (Hengstler, et. al., 1999).

Finally, the *c-myc* oncogene has also been implicated in ovarian tumourigenesis. The gene produces a DNA-binding protein that is involved in the regulation of cellular proliferation (Garte, 1993). Amplification and/or overexpression of the c-myc gene has been found in close to 40% of malignant epithelial ovarian tumours , though most predominantly in adenocarcinomas of the serous subtype (Tashiro, et. al., 1992). There is

some association with alterations in *c-myc* and poor survival outcomes, but generally only when overexpressed in conjunction with *HER-2/neu* (Katsaros, et. al., 1995). *C-myc* amplification is most frequently seen in later stage tumours, thus it is thought that it may have more of a role in disease progression as opposed to initiation (Baker, et. al., 1990).

1.4 Ovarian Cancer Symptoms and Screening

Ovarian cancer is often referred to as "the disease that whispers" due to the rather vague nature of the symptoms of this disease, which often results in late-stage diagnosis. According to the National Ovarian Cancer Association (www.ovariancanada.org), ovarian cancer symptoms include any or all of the following that persist for longer than three weeks: abdominal bloating and discomfort, changes in bowel function, unexplained weight gain, nausea, and changes in menstrual patterns. Because these symptoms can easily be overlooked or attributed to other causes, diagnosis is often not made until the disease is in an advanced state and the symptoms are severe.

The physical inaccessibility of the ovaries renders screening for malignancy in the general population difficult. To date, routine screening is generally only considered cost-effective in those at high risk because of a strong family history of the disease or because of a known *BRCA1* or *BRCA2* germline mutation. In this cohort, screening may generally include a blood test for the tumour-associated antigen CA-125 along with a transvaginal ultrasound (Laframboise, et. al., 2002). The CA-125 tumour marker is an antigenic determinant of a high molecular weight glycoprotein that is recognized by an antibody raised using an ovarian cancer cell line as an immunogen (Jacobs, et. al., 1990). It has been found that CA-125 levels correlate with disease progression and regression in

ovarian cancer (Shimizu, et. al., 1985; Shimizu, et. al., 1986). The measurement of serum CA-125 levels is not, unfortunately, a sufficiently effective screening procedure. Quite a wide range of benign conditions, such as menstruation, pregnancy, benign pelvic masses, pelvic inflammatory disease, ovarian hyperstimulation syndrome, and peritonitis can also cause an increase in serum CA-125 levels (Daoud and Bodor, 1991). As well, it has been found that up to 20% of all malignant ovarian tumours do not secrete CA-125 (Bast, Jr., et. al., 2005) and a significant proportion of women with early stage EOC do not demonstrate elevated CA-125 levels (Woolas, et. al., 1993). Even the combined use of the CA-125 blood test along with transvaginal ultrasound has not proven entirely effective for screening even in high risk groups, however the use of colour Doppler flow ultrasonography is improving the effectiveness of this mode of screening (Cohen and Jennings, 1994). Another step forward has been the use of screening for other tumour-associated antigens in conjunction with CA-125, which include macrophage colony stimulating factor (M-CSF) and OVX1, an endometrial cancer marker (Bast and Woolas, 1993; Woolas, et. al., 1995). Magnetic resonance imaging has not proven accurate or cost-effective in screening even high risk groups to date (Bohm-Velez, et. al., 2000).

The field of bioinformatics is proving useful in the development of new screening tools for the detection of ovarian cancer. Recently proteomic patterns in serum samples were used to distinguish ovarian cancer patients from unaffected controls with a resulting positive predictive value of 94% (Petricoin, et. al., 2002), indicating that the disease may carry a distinct molecular signature that may be exploited for early detection screening purposes. The identification of proteomic signatures by mass spectroscopy have shown differences in expression of certain biomarkers between ovarian tumours of different

histological subtypes (An, et. al., 2006), and may be able to aid in predicting whether tumours are likely to be chemoresistant (Stewart, et. al., 2006). Proteomic analysis has even revealed unique patterns between OSE cells from oophorectomy specimens of women with and without a significant family history of ovarian cancer, which may aid in the further definition of the preneoplastic phenotype of EOC (He, et. al., 2005).

1.5 Treatment of Ovarian Cancer

The current standard treatment plan for advanced ovarian carcinoma generally includes cytoreductive surgery, followed by intravenous (i.v.) chemotherapeutic treatment with a combination of taxane and platinum-based agents. The initial response rate is generally quite high, 60-80%, however the majority of patients go on to develop multi-drug resistance (Qazi and McGuire, 1995). If there is a response-failure to the taxane/platinum combination, patients may also be treated with other common chemotherapeutic agents such as doxorubicin, topotecan, gemcitabine, or etoposide (Berkenblit and Cannistra, 2005).

More recent advances in the treatment of EOC that, while they are not yet necessarily considered the standard of care, have proven quite effective include neoadjuvant chemotherapy as well as intraperitoneal (i.p.) chemotherapy. Improvement in patient outcomes has been seen in those who were treated with chemotherapy prior to debulking surgery and it is quickly becoming a first-line approach in many centres (Park and Kuhn, 2004). This approach appears to be warranted when the tumour(s) is (are) not thought to be initially resectable. Another new strategy in EOC treatment is the delivery of chemotherapeutic agents intraperitoneally rather than intravenously. Significant

improvements in progression-free survival of 6 months and overall survival of a year or more have been demonstrated with this method (Markman, et. al., 2001; Armstrong, et. al., 2006), and it has also been shown in some studies to result in lower toxicity-related side effects, however it has not yet been accepted as a standard of care as other studies have demonstrated an increase in such side effects (Fujiwara, et. al., 2005; Singhal and Lele, 2006).

1.6 The Normal Ovarian Surface Epithelium

The ovarian surface epithelium is a single layer of squamous to cuboidal epithelial cells that covers the outer surface of the ovary (**Figure 1**). It is separated from the ovarian stroma by a basement membrane. Held together laterally by gap junctions and desmosomes, the OSE is continuous, at the ovarian hilum, with the mesothelium of the ovarian ligaments and the lining of the peritoneum (Murdoch, 1996). These cells also share a common embryonic origin, the mesoderm, with the epithelial cells of the urogenital system. They ultimately differentiate from the coelomic epithelium after it invaginates to cover the gonadal ridges during gonadogenesis (Auersperg, et. al., 1997).

The OSE appears to play an active role in the ovulatory cycle, and it has in fact been demonstrated that removal of the OSE can block ovulation in species such as the sheep, pig, and frog (Schuetz and Lessman, 1982; Hall, et. al., 1993; Colgin and Murdoch, 1997). Prior to ovulation, mature or dominant follicles can be found close to the ovarian surface, adjacent to the OSE. In response to stimulation by LH, for which OSE cells have receptors, the epithelial cells secrete proteolytic enzymes such as plasminogen activator, which will break down the underlying basement membrane and

Figure 1: Schematic diagram of the ovarian surface epithelium in relation to other ovarian structures such as the ovarian stroma and follicles composed of granulosa cells and the oocyte.

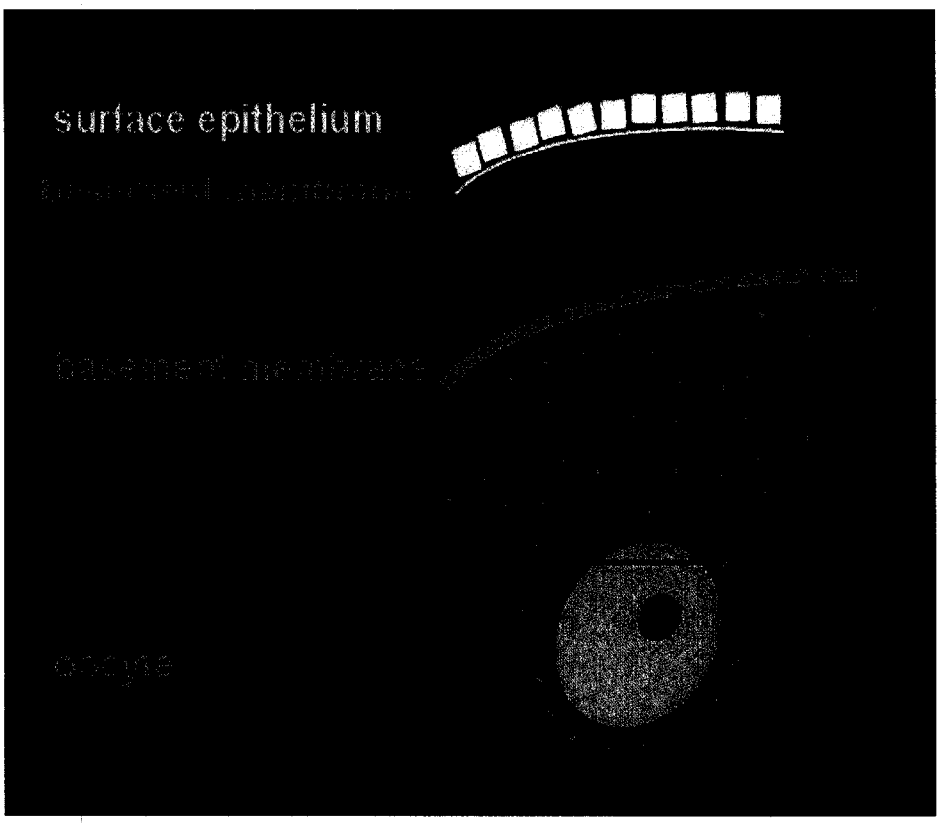
surface epithelium
basement membrane
ovary

weaken the follicular wall with a signal transduction cascade involving matrix metalloproteinases (MMPs) and tumour necrosis factor alpha (Murdoch and McDonnel, 2002). In culture, it has been shown that OSE cells from sheep secrete urokinase plasminogen activator in a basal direction in response to LH (Murdoch, et. al., 1999). This is followed by localized apoptosis and necrosis of the OSE cells immediately overlying the ovulatory follicle. Following ovulation, it is thought that proliferation and migration of OSE cells adjacent to the wound is the mechanism by which the ovulatory wound is repaired and cultured OSE cells have been shown to be capable of producing extracellular matrix (ECM) components such as collagen types I and III necessary for the formation of a basement membrane (Auersperg, et. al., 1991; Kruk and Auersperg, 1992; Kruk and Auersperg, 1994). The OSE appears to have its own cycle, at least in rats, which parallels the estrous cycle, including a proliferative phase just prior to and immediately following ovulation, and a quiescent phase the remainder of the time (Gaytan, et. al., 2005). In general though, the OSE has a very low proliferative index (Heller, et. al., 2003).

Though not without difficulty, OSE cells from various species can be cultured. Human OSE cultures can generally undergo 7-8 passages prior to undergoing senescence, though spontaneous immortalization is sometimes observed (Auersperg, et. al., 2001). In culture these cells retain the homogeneous cobblestone morphology typical of epithelial cells, but display a phenotypic plasticity in that they are capable of undergoing epithelial-to-mesenchymal transition, a process characterized by a switch from apical-basal to anterior-posterior polarity, loss of intercellular contacts, loss of epithelial markers, and acquisition of mesenchymal markers .

1.7 Transformation of the Ovarian Surface Epithelium

As mentioned previously, the vast majority of malignant ovarian tumours are epithelial in nature and thought to arise from the OSE. The main rationale behind the theory that the OSE is the tissue of origin of EOCs originates from observations of epithelial inclusion cysts found within the ovarian stroma. These epithelium-lined cysts are thought to form when invaginations of the OSE into the ovarian stroma, which may result following ovulatory wound repair, pinch off and become surrounded by stroma (Ghahremani, et. al., 1999). Mullerian metaplasia of serous subtype can been seen in some of these cysts, and intraepithelial neoplasia has also been observed, raising the possibility that these structures are the putative precursor lesions for EOC (Okamura and Katabuchi, 2001). To add to this evidence, it has been shown that ovaries removed prophylactically from women with *BRCA1* germline mutations or those with a significant family history of EOC demonstrate more epithelial changes in their ovaries, particularly more inclusion cysts, and occasionally occult neoplasia (Salazar, et. al., 1996; Werness, et. al., 1999; Colgan, et. al., 2001; Finch, et. al., 2005). As well, more of these structures have been found in the contralateral "normal" ovary of women with unilateral EOC (Mittal, et. al., 1993).

In vitro studies with cultured OSE cells have helped to shed some light on the possible molecular chain of events that may need to take place in order to achieve transformation in these cells. Several studies have shown that the co-expression of the SV40 Large T antigen (SV40-TAg) along with the cell adhesion molecule E-cadherin, which is not expressed in the normal OSE but is expressed in EOCs, has the ability to

result in transformation of human OSE cells (Maines-Bandiera, et. al., 1992; Auersperg, et. al., 1999; Ong, et. al., 1999). Introduction of SV40-TAg, which impedes both the *Rb* and *p53* tumour suppressor pathways, into murine OSE (MOSE) cells also resulted in transformation, whereas *p53*-deficiency alone did not (Kido and Shibuya, 1998). Studies of OSE cells collected from oophorectomy specimens from women with or without a significant family history of ovarian cancer (though not necessarily a confirmed *BRCA1* mutation) have also yielded interesting results. OSE cells collected from "high risk" ovaries show greater telomeric instability (Kruk, et. al., 1999), cytogenetic instability (Pejovic, et. al., 2006), retention of expression of both CA-125 and keratins (Auersperg, et. al., 1995; Dyck, et. al., 1996), as well as altered expression of E-cadherin (Wong, et. al., 1999).

1.8 The *BRCA1* Tumour Suppressor Gene

1.8.1 Structure

The *BRCA1* tumour suppressor gene is composed of 24 exons and yields a large 220 kD protein. It contains 1863 amino acids in humans (Miki, et. al., 1994), and 1812 in mice. In humans this gene maps to chromosome 17q21 (Chamberlain, et. al., 1993) and in mice it is found on chromosome 11D (Schrock, et. al., 1996). The mouse and human proteins display 60% identity and 72% similarity, with the greatest homology seen in the amino and carboxy termini (Sharan, et. al., 1995). The N-terminus of BRCA1 contains a zinc RING finger domain with E3 ubiquitin ligase activity similar to that seen in other DNA-interacting proteins (Wu, et. al., 1996). The C-terminus contains two BRCA1 C-

terminal (BRCT) domains, which bind proteins such as p53, RNA Polymerase II, BRCA2, and RB, either directly or indirectly. Two nuclear localization signals can be found within exon 11, which encodes over 60% of the protein. BRCA1-interacting proteins which bind in this region include, RAD50, RAD51, RB, and c-Myc (Deng and Brodie, 2000) (**Figure 2**).

1.8.2 Function

BRCA1 has been identified as a transcription factor with many diverse functions within the cell. It is perhaps best known for its tumour suppressor activity; however *BRCA1* has also been shown to be involved in DNA damage recognition and repair, cell cycle control, regulation of apoptosis, as well as development. While the list of functional roles for *BRCA1* continues to grow, only these five main roles will be discussed here.

1.8.2.1 Tumour Suppressor

BRCA1 has been qualified as a tumour suppressor gene as it fits the criteria for Knudson's two-hit hypothesis (Knudson, Jr., 1984), which states that, in the case of tumour suppressor genes, two genetic "hits" are needed for cancer formation, affecting each of the two copies of the gene. In the case of sporadic disease, both hits are acquired in the adult over their lifetime, in the case of hereditary disease, an individual is born with one "hit", and then acquires the second. Germline *BRCA1* mutations are inherited in an autosomal dominant fashion (Gallion and Smith, 1994) and LOH is seen in the resulting breast and ovarian tumours (Neuhausen and Marshall, 1994). *In vitro* studies have shown that overexpression of *BRCA1* in cancer cell lines leads to growth suppression (Holt, et.

Figure 2: Schematic diagram of the structure of the human BRCA1 protein. Functional domains and interacting sites with various proteins are demonstrated. Adapted from (Deng, et. al., 2006) and (Lee, et. al., 2001).

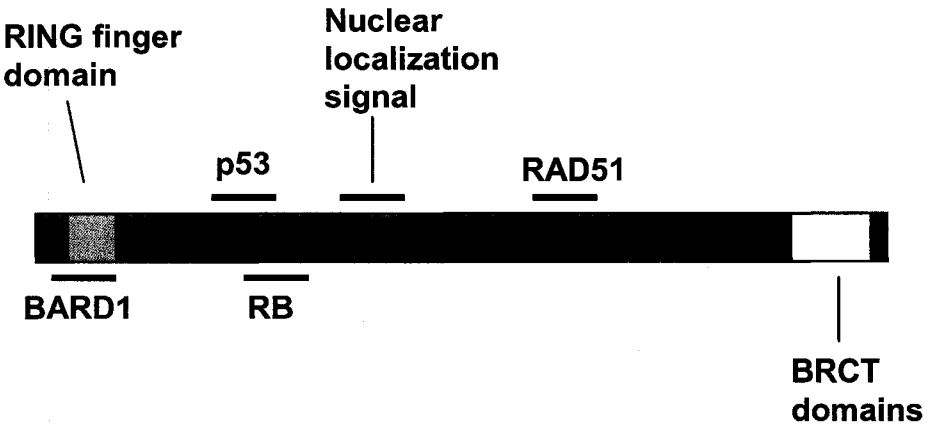
RING finger domain
Nuclear localization signal
p53
RAD51
BARD1
RB
BRCT domains

al., 1996) and that loss of *BRCA1* expression in cultured tumour cells results in a loss of growth control characterized by an increase in proliferation (Thompson, et. al., 1995).

1.8.2.2 DNA Damage Repair

BRCA1 has been shown to be an integral component of the cell's DNA damage recognition and repair mechanism. BRCA1 associates with a variety of other molecules also involved in DNA damage recognition and repair, such as BRCA2, BARD1, Rad50, Rad51, Mre11, and Nbs1 (Lee and Chung, 2001). It has also been shown to form a complex, known as the *BRCA1*-associated genome surveillance complex, or BASC, with other tumour suppressors and repair genes among them *MSH2 & 6*, *MLH1*, *ATM*, *BLM*, and the hRad50-hMRE11-p95 complex, which functions as a sensor of damaged DNA (Wang, et. al., 2000b). It is thought, in this model, that *BRCA1* serves a central role as both a scaffold for the other members and a coordinator of the repair process.

Hyperphosphorylation of BRCA1 is seen following exposure to a variety of DNA-damaging agents and it appears that it can be phosphorylated by the ataxia telangiectasia related proteins ATM and ATR, as well as by the checkpoint kinase 2 protein Chk2 (Cortez, et. al., 1999; Tibbetts, et. al., 2000; Lee, et. al., 2000). It is thought that following this phosphorylation signal, the complex moves to the damage site and the cell cycle is arrested while repair is initiated (**Figure 3**). If repair is not possible, the result is often commitment to cell death.

Functional *BRCA1* has been implicated in several different types of DNA-damage repair, such as homologous recombination, non-homologous end-joining repair, transcription-coupled repair, as well as nucleotide excision repair (Ting and Lee, 2004).

Figure 3: **A simplified schematic diagram of the role of BRCA1 in DNA damage detection and repair**. For simplicity only a few of the binding partners involved in this process are depicted. Adapated from (Welsch, et. al., 2000).

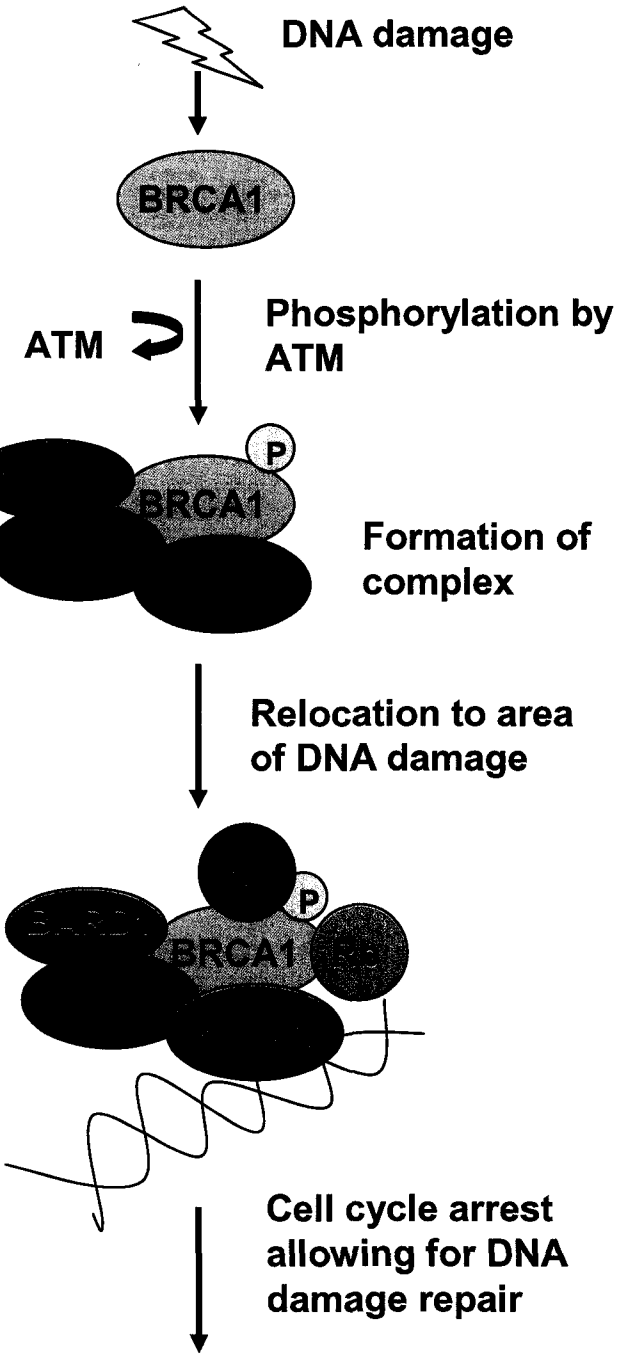

Normal Cell Cycle

Cells with mutated or deficient *BRCA1* display defects in these various types of repair, depending on how the damage is incurred. A hallmark of *BRCA1*-deficient tissues is an increase in genomic instability, resulting from the inability to effectively detect and repair damage, leading to an accumulation of defects rendering the cells more susceptible to transformation (Shen, et. al., 1998; Deng, 2001; Weaver, et. al., 2002). Also, in its role as a transcription factor, *BRCA1* has the ability to transcriptionally regulate various genes involved in DNA-damage repair. It can induce damage recognition factors involved in the global genomic repair pathway, such as *GADD45*, *DDB2*, and *XPC* (Hartman and Ford, 2002).

1.8.2.3 Cell Cycle

One of the ways in which *BRCA1* is involved in dealing with damaged DNA is via its role in cell cycle control. Tumour suppressor genes are labeled "caretakers" or "gatekeepers" based on whether they can activate cell cycle checkpoints in order to maintain genomic integrity or mainly to control proliferation, and *BRCA1* has been identified as a caretaker (Kinzler and Vogelstein, 1997). *BRCA1* has been shown to exert control on the G1/S, S, G2/M, and the mitotic spindle checkpoints. Its ability to regulate expression of p21 plays a large role in control of the G1/S checkpoint. *In vitro* experiments have demonstrated that, without functional *BRCA1*, there is no transactivation of p21, and a failure to arrest in G1/S (Somasundaram, et. al., 1997).

Intra-S-phase arrest, which prevents cells from undergoing replication after DNA damage, also appears to require functional *BRCA1*. HCC1937 cells, which have a defective *BRCA1*, display a defective S-phase checkpoint, as well as a defective G2/M checkpoint when challenged with ionizing radiation (Xu, et. al., 2001a). Reconstitution of

BRCA1 in these cells rescues this defect. Phosphorylation of BRCA1 by ATM also appears to be required for proper S-phase arrest in the face of DNA damage (Lou, et. al., 2003).

The G2/M checkpoint allows for the repair of DNA prior to mitosis so that damage will not be passed on to the resulting daughter cells, and *BRCA1* also plays a critical role here. *BRCA1* null mouse embryonic fibroblasts display a defective G2/M arrest (Xu, et. al., 1999b). Again, without phosphorylation of BRCA1 by ATM, there is failure to arrest in G2/M following ionizing radiation (Aprelikova, et. al., 2001). It is thought that *BRCA1* may activate this checkpoint via transcriptional control of *GADD45* (Mullan, et. al., 2001; Yoshida and Miki, 2004) and by its ability to repress Cyclin B (MacLachlan, et. al., 2000).

The final point at which *BRCA1* can exert control in the cell cycle is the mitotic spindle checkpoint. This checkpoint serves to ensure the proper attachment of the chromosomes to the mitotic spindle as well as microtubule tension in order to prevent premature separation of the sister-chromatids. BRCA1 has been shown to associate with and activate MEKK3, which is an upstream regulator of the c-Jun/stress-activated protein kinase and p38/MAPK pathways, following microtubule damage (Gilmore, et. al., 2004). Another study demonstrated that downregulation of *BRCA1* in the MCF-7 breast carcinoma cell line led to a premature degradation of cyclin B1 which precipitated an early inactivation of the spindle checkpoint and that this rendered the cells resistant to the mitotic spindle poison paclitaxel (Chabalier, et. al., 2006).

1.8.2.4 Apoptosis

When the repair of damaged DNA fails, the normal result is that the cell is committed to programmed cell death, or apoptosis. While the main role of *BRCA1* is in the recognition and coordination of this repair, it has also been shown to be involved in the apoptotic death pathway, though perhaps more indirectly than directly. Exogenous expression of *BRCA1* can induce apoptosis, and requires JNK activation (Harkin, et. al., 1999). In contrast, antisense inhibition of *BRCA1* has been shown to increase levels of apoptosis (Husain, et. al., 1998). *BRCA1* has been shown to modulate stress-induced apoptosis in breast and ovarian cancer cell lines and did so through a p53-independent pathway involving H-Ras, MEKK4, JNK, Fas ligand/Fas interactions, and caspase-9 activation (Thangaraju, et. al., 2000). This study employed several different types of apoptotic stimuli, indicating that *BRCA1* could influence apoptosis in response to a variety of stress signals. This list was expanded when it was shown that *BRCA1* could also sensitize cells to interferon-gamma-mediated apoptosis (Andrews, et. al., 2002).

1.8.2.5 Development and Differentiation

The major implications of the role of *BRCA1* in the above processes are never more evident than when you examine the involvement of *BRCA1* in development. *BRCA1* is expressed in all developing tissues in the mouse, particularly those that are rapidly proliferating and differentiating (Lane, et. al., 1995; Marquis, et. al., 1995). *BRCA1* null mouse embryos die in utero prior to embryonic day eight, mainly due to a massive proliferation defect and substantial increase in cellular apoptosis, a phenotype that can be partially rescued by the concomitant inactivation of either p53 or p21 (Hakem, et. al., 1997). This molecular defect ultimately results physiologically in neural

tube closure defects such as anencephaly and spina bifida (Gowen, et. al., 1996; Hakem, et. al., 1996). Transgenic embryos in which only splice variants of exon 11 of the *BRCA1* gene are left intact, while still embryonic lethal, survive approximately ten days longer than the completely null animals, indicating that this large exon can partially compensate for the full length transcript .

The embryonic lethality of the *BRCA1* null phenotype has made it difficult to study the role of this gene in the development of various tissues; however the advent of mammary tissue-specific promoters has made this possible in the mammary gland. *BRCA1* has been shown to be quite critical for normal development of the mammary gland. The first hint for a possible role for *BRCA1* in mammary gland development and differentiation was that *Brca1* mRNA is upregulated during puberty and pregnancy in the mouse . It has since been shown that downregulation of *BRCA1* in mammary epithelial cells *in vitro* attenuates their differentiation and overexpression accelerates it, whereas the same conditions had no effect on muscle or neuronal cell differentiation (Kubista, et. al., 2002). In transgenic mouse models, tissue-specific deletion of *Brca1* in the mammary epithelium results in blunted ductal morphogenesis (Xu, et. al., 1999a).

1.8.3 Role of *BRCA1* In Ovarian Cancer

As mentioned previously, as many as 15% of EOCs are thought to be the result of hereditary germline mutations in *BRCA1* or *BRCA2* . While somatic mutations in sporadic EOCs appear to be relatively rare, *BRCA1* dysfunction as the result of epigenetic factors is quite common in sporadic EOCs.

1.8.3.1 Hereditary Ovarian Cancer

A significant family history of breast/ovarian cancer, which can be defined as an individual with breast cancer diagnosed before the age of 45, bilateral breast cancer at any age, diagnosis of breast and ovarian cancer in the same individual, two or more first degree relatives with breast and/or ovarian cancer, particularly if diagnosed before the age of 50, may be indicative of a hereditary germline mutation in *BRCA1* or *BRCA2* (Nelson, et. al., 2005)(**Figure 4**). The lifetime risk for developing EOC for a *BRCA1* germline mutation carrier is estimated to be between 40 and 65% (Ford, et. al., 1994; Easton, et. al., 1995; Antoniou, et. al., 2003).

While the rate of *BRCA1* mutations is between 5-15% in the general ovarian cancer population, i.e. not selected for significant family history, the rates are much higher when family history is considered, and varies based on population genetics. For example, 79% of Russian families with a history of breast/ovarian cancer have been found to have a specific *BRCA1* mutation, 5832insC. This mutation is seen at a rate of 47% in Israeli breast/ovarian cancer families, in 29% of Italian breast/ovarian cancer families, and in 20-25% of these families of British, French, Scandinavian, or Hungarian descent (Szabo and King, 1997).

Certain countries and ethnic groups also display *BRCA* mutations unique to them, known as founder mutations, and this is best exemplified in the Ashkenazi Jewish population. There are two founder mutations for *BRCA1* seen in this group, 185delAG and 5832insC. The first is seen in the general Ashkenazi Jewish population at a rate of 1%, the latter about 0.11% (Tonin, et. al., 1996). The 185delAG mutation is estimated to have originated over 2000 years ago . The founder mutation rate for Ashkenazi Jewish

Figure 4: Pedigree of a family with a *BRCA1* germline mutation. Circles indicate females and squares indicate males. Darkened circles are affected individuals. Breast indicates a breast cancer diagnosis followed by the age at diagnosis, while ovarian indicates an ovarian cancer diagnosis. A diagonal line through the circle or square indicates the individual is deceased.

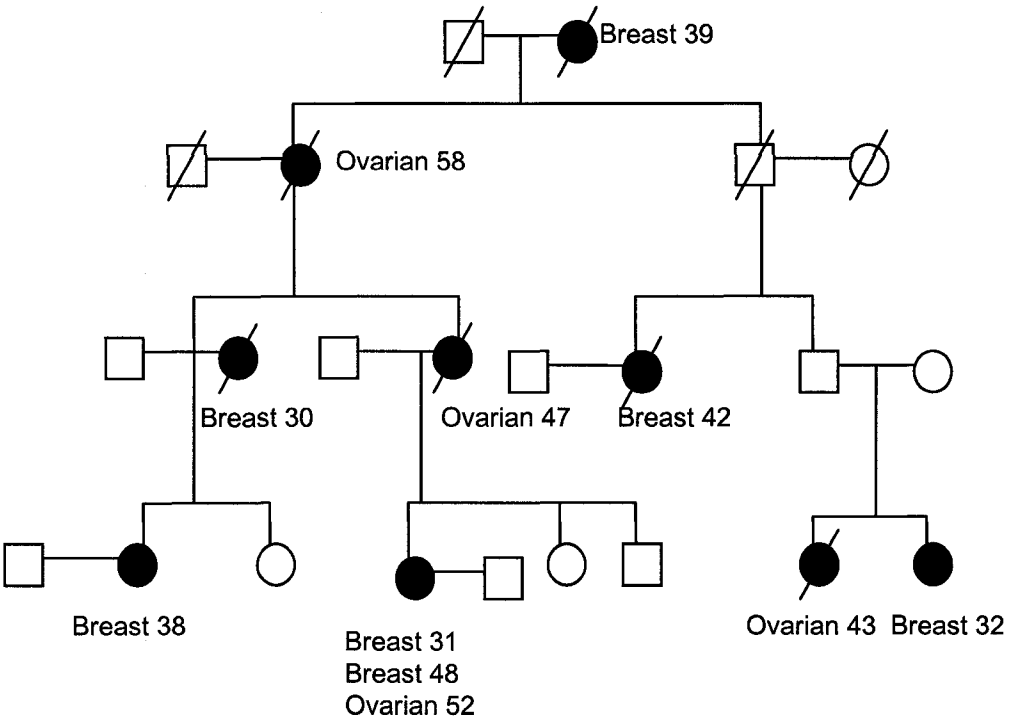
Breast 39
Ovarian 58
Breast 30
Ovarian 47
Breast 42
Breast 38
Breast 31
Breast 48
Ovarian 52
Ovarian 43
Breast 32

women with ovarian cancer is about 40% (Moslehi, et. al., 2000). Founder mutations have also been identified in families of Dutch, Lithuanian, Russian, Germanic, French, Italian, British, French-Canadian, African-American, Norwegian, Swedish, Icelandic, Belgian, and Finnish descent (Neuhausen, 2000). There is little evidence for clustering of mutations into "hotspots" on the *BRCA1* gene, however mutations located in the N-terminal region appear more likely to be associated with ovarian cancer and C-terminal mutations with breast cancer (Gayther, et. al., 1995).

The types of germline *BRCA1* mutations seen include frameshift and nonsense mutations, which result in a truncated protein product, splice site alterations which result in a smaller or less stable message, missense mutations, as well as alterations in the promoter region, which give rise to decreased or absent protein expression (Szabo, et. al., 2004). Nonsense mutations or frameshift mutations consisting of insertions or deletions comprise the majority of *BRCA1* mutations that have been documented and are generally accepted as disease causing (Szabo, et. al., 2004). Splice site and missense mutations that include insertions and in-frame deletions are the most difficult to detect by current screening strategies, and are thus less likely to have been clearly designated as deleterious (Liu, et. al., 2001; Mirkovic, et. al., 2004).

Screening for *BRCA1* mutations can be done several ways, all of which require only a blood sample. The single-stranded conformation analysis (SSCA) looks for differences in single-stranded DNA structure, mainly folding, between a control and a mutated sample. It is sensitive enough to detect single base pair changes (Lessa and Applebaum, 1993). The protein truncation test (PTT) is more sensitive than SSCA and quite widely used (Geisler, et. al., 2001). This test detects mutations based on mutations

producing truncated proteins that will migrate at different rates than controls on a polyacrylamide gel (Hogervorst, et. al., 1995). LOH analysis prior to the PTT has been shown to improve sensitivity (Sorlie, et. al., 1998). These tests are unable to detect missense mutations. Complete gene sequencing is also possible, though the results are difficult to interpret, as this will also detect non-deleterious or unclassified polymorphisms (Abkevich, et. al., 2004).

BRCA1 mutation-associated EOCs also have a distinct pathological phenotype. These tumours are more likely to be invasive serous adenocarcinomas that are poorly differentiated (Narod and Boyd, 2002). They are more likely to be high grade, have increased solid component, as well as increased p53 immunoreactivity (Lakhani, et. al., 2004). *BRCA1* mutations have been associated with other pathologies, but serous is by far the most common, with clear cell being the least likely tumour type to be associated with a mutation (Lakhani, et. al., 2004). *BRCA1* mutations carriers are at increased risk for pancreatic, colorectal, and prostate cancer (Rosen, et. al., 2001; Kirchhoff, et. al., 2004; Lynch, et. al., 2005).

1.8.3.2 Sporadic Ovarian Cancer

While somatic mutations in sporadic EOCs appear relatively rare, *BRCA1* dysfunction of some sort is still a relatively common occurrence in sporadic tumours. Reduced mRNA levels and decreased BRCA1 protein levels are seen in a large proportion of sporadic ovarian cancers (Russell, et. al., 2000). Epigenetic alterations, such as hypermethylation, are almost always associated with LOH, and are thought to provide an epigenetic "second hit" that will lead to disease formation (Esteller, et. al., 2001). Another study demonstrated that LOH or hypermethylation were never seen in

benign ovarian tumours, hypermethylation was not seen in borderline tumours and LOH was only seen in 15% of these, while 66% of ovarian carcinomas displayed LOH and 31% hypermethylation (Wang, et. al., 2004). As with ovarian tumours associated with germline *BRCA1* mutations, *BRCA1*-dysfunction in sporadic tumours is also associated with a serous pathology as well as high grade and poor differentiation (Boyd, et. al., 2000).

1.8.4 *BRCA1* in Association with *p53*

Up to 60% of *BRCA1* mutation-associated ovarian tumours also display mutations in the *p53* tumour suppressor gene (Ramus, et. al., 1999; Zweemer, et. al., 1999). This data, coupled with evidence from both *in vivo* and *in vitro* studies demonstrate a strong association between these two genes and their pathways as related to ovarian carcinogenesis as well as tumourigenesis in general and there is considerable experimental evidence that indicates that loss of *p53* expression may also be at least a partial requirement for *BRCA1*-associated tumourigenesis.

Firstly, BRCA1 and p53 are capable of physical association and regulation of each other's activity. BRCA1 is capable of binding p53 and activating its transcriptional activity (Ouchi, et. al., 1998). Conversely, addition of exogenous *BRCA1* results in the downregulation of p53 in response to DNA damage (Arizti, et. al., 2000). As mentioned previously, concomitant loss of *p53* expression partially rescues the embryonic lethality of the *Brca1* knockout mouse phenotype . It is thought that this is accomplished by the fact that the loss of *BRCA1* alone triggers *p53*-dependent checkpoint controls, and without this measure, the cells are able to continue to proliferate. Antisense inhibition of

BRCA1 results in a rise in p53 and p21 expression levels, and the same study found that somatic mutations in the *p53* gene were present in half of the *BRCA1*-associated ovarian tumours they examined, from which they concluded that loss of *BRCA1* activates the *p53*-dependent DNA-damage repair pathway and thus deleterious *p53* mutations would be a major contributing factor to *BRCA1*-related carcinogenesis (Reedy, et. al., 2001). Lastly, as will be discussed in detail later, inactivation of p53 appears to accelerate *Brca1*-associated mammary tumourigenesis (; Brodie, et. al., 2001).

1.8.4 *BRCA1* in Association with *RB*

As with *p53*, it has been demonstrated that *BRCA1* and *RB* are capable of physical interaction. The hypophosphorylated form of RB has been shown to preferentially bind to the exon 11 region of *BRCA1*, and this same study found that the ability of *BRCA1* to suppress cellular proliferation depended on the presence of wildtype *RB* (Aprelikova, et. al., 1999). *RB* has been shown to modify *BRCA1* expression via its ability to modulate *E2F* transcriptional activity, with *BRCA1* being an *in vivo* target of *E2F1* (Wang, et. al., 2000a). It has also been shown that overexpression of *BRCA1* inhibits the expression of *RB* and the *RB* family members *p107* and *p130* (Fan, et. al., 2001). No association has been made to date between *RB* and *BRCA1* dysfunction in ovarian cancer specifically.

1.9 Mouse Models of Cancer

The ability to accurately recapitulate cancer in a mouse model system provides an extremely powerful tool to researchers. Xenograft models, in which human tumour cells are injected into immune-compromised mice, have allowed for the preliminary testing of

many potential therapeutic options, as well as the study of the effect of genetic alterations on tumourigenesis. However, this method has several drawbacks. There is the species difference between the host and the graft, the fact that the mice lack an immune system that would normally be present in the human condition, the limited injection sites that do not necessarily properly mimic the natural tumour environment, and the fact that one must use cells that are already transformed. Thus, the ability to develop a mouse model in which tumourigenesis "spontaneously" occurs in its natural environment as the result of specific molecular alterations is of utmost importance when studying disease initiation and progression. A defined model also provides the opportunity to test not only potential therapeutics, but also early detection and prevention strategies.

1.9.1 General

The first generation of mouse models of cancer sought to generally either constitutively express oncogenes or to inactivate expression of tumour suppressor genes, either in the whole organism or in specific tissues. The overexpression of c-Myc in mouse mammary epithelium, which led to mammary tumourigenesis (Stewart, et. al., 1984), and the expression of TAg in the brain, which led to the development of glioblastomas, were some of the first experiments to show that specific genetic alterations could induce tumour formation in mice (Adams and Cory, 1991). Conversely, knocking out expression of the tumour suppressor *Rb* led to the formation of pituitary adenomas, and knocking out *p53* expression resulted in the formation of sarcomas and lymphomas in the mice (Kumar, et. al., 1995; Macleod, et. al., 1996). Creating a transgenic mouse in which a gene is constitutively expressed in the germline involves incorporating the DNA

of interest into the germline of the mice. In order to accomplish this, the DNA must be microinjected into the nucleus of fertilized eggs of a donor mouse. These eggs are then transferred to the oviduct of a pseudopregnant surrogate mother mouse. The resulting pups are then screened for the presence and expression of the transgene. Creating a mouse in which a gene is knocked out follows a similar though slightly more complicated protocol. The "new" DNA that will replace the DNA of interest is transfected into embryonic stem (ES) cells, in which homologous recombination will take place, incorporating the new DNA. The cells carrying the transgene are selected and then injected into mouse blastocysts, which are then transferred to a pseudopregnant surrogate. The resulting pups will be chimeras of cells carrying DNA from the ES cells and cells from the donor blastocyst. When these animals are bred to animals of the same strain as the donor blastocyst, resulting pups with the coat colour of the ES cell donor are the knockout mice (Nagy, et. al., 2003).

While traditional transgenic mouse models have proven extremely useful in modeling carcinogenesis, these models have some distinct limitations. The genetic alterations are made in the germline, and it often results, in the case of knockouts, that the gene is indispensable for proper development and hence the result is embryonic lethality. Even without lethality, developmental defects and other non-specific effects can interfere with the analysis of any tumourigenic phenotype. As a result, several methods have been developed to allow for spatial and temporal regulation of transgene expression. One manner in which spatial regulation can be accomplished is via the use of a tissue specific promoter to drive transgene expression specifically to the tissue of interest. A primary example is the use of the mouse mammary tumour virus (MMTV) promoter to drive gene

expression in the mammary epithelium specifically, which has proven highly efficient in the development of mouse models of breast carcinogenesis (Callahan and Smith, 2000).

Temporal or inducible regulation of transgene expression can be critical if expression in the germline during embryonic development proves deleterious. Temporal regulation can be accomplished by using an inducible promoter, an example of which is the tetracycline (Tet)-dependent system. This system can be either Tet-Off or Tet-On. In the Tet-Off system, expression of the transgene, which is under transcriptional control of a Tet-responsive element (TRE), is regulated by the Tet-controlled transactivator protein (rTA) (Baron and Bujard, 2000). The transgene cannot be activated in the presence of doxycycline (Dox), which can be delivered to transgenic mice via their drinking water. In the Tet-On system, the reverse rTA (rtTA) protein is used. In this case, the transgene can only be activated in the presence of Dox, although some degree of leakiness of the system is not uncommon. Another manner in which transgene expression can be induced in a temporally regulated manner is via the Cre-loxP system. Cre is the 38 kD product of the cre (cyclization recombination) gene of bacteriophage P1 and is a site-specific recombinase. It recognizes a 34 bp site on the P1 genome called loxP (locus of X-over P1). LoxP sites are composed of two 13 bp inverted repeats that flank an 8 bp non-palindromic core. Cre catalyzes recombination between loxP sites and the intervening DNA is excised as a covalent closed circle (Sauer, 1998) (**Figure 5**). This system can be used in the transgenic mouse setting by creating a mouse in which the gene of interest is flanked by loxP sites (a conditional knockout) or the gene of interest is preceded by loxP sites flanking a stop-sequence (a conditional knockin). This mouse is then bred to a transgenic mouse that expresses Cre under the control of a tissue-specific promoter and a

Figure 5: Schematic diagram of Cre recombinase-mediated recombination at loxP sites. LoxP sites are inserted into the gene of interest flanking the region to be excised. Upon exposure to Cre recombinase, the DNA is cut at these sites and recombination occurs between the sticky ends. The circular fragment is degraded.

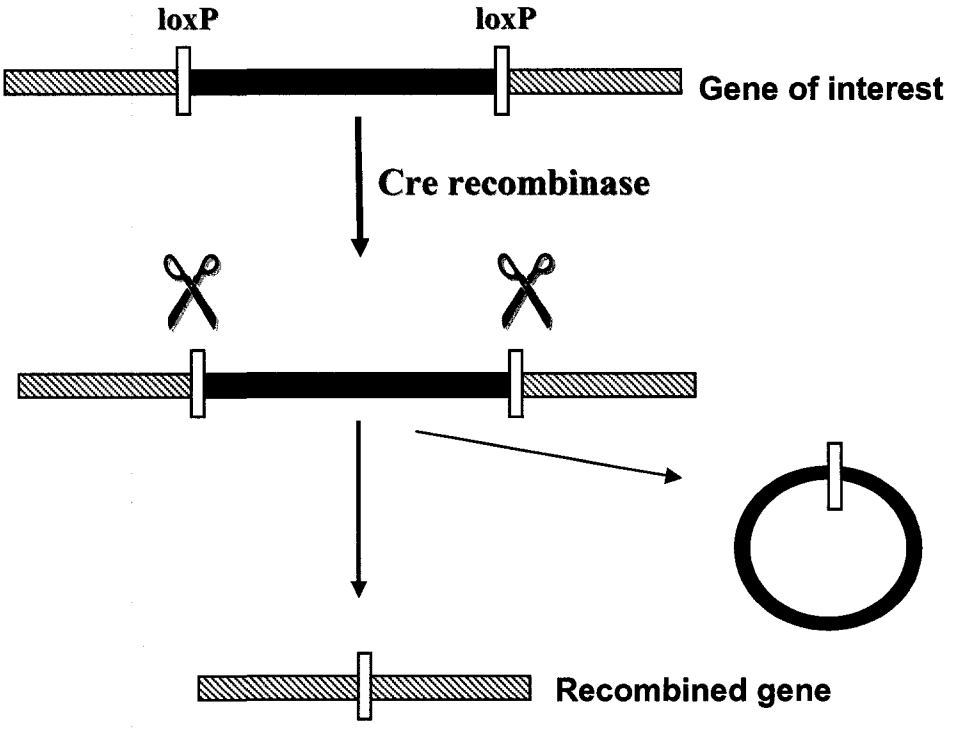
loxP
loxP
Gene of interest
Cre recombinase
Recombined gene

percentage of the resulting offspring will have the gene of interest removed or expressed. In order to make this system temporally regulated, or in the absence of a tissue specific promoter, the Cre-loxP system can be joined with the Tet-dependent system (St-Onge, et. al., 1996) or Cre recombinase can be delivered via a viral vector, such as an adeno- or retrovirus (Wang, et. al., 1996).

1.9.2 *Brca1*-deficient Mouse Models of Cancer

Because of the early embryonic lethality of traditional *Brca1* knockout mice, studies of *Brca1*-related tumourigenesis in mice have generally employed the Cre-loxP system in order to circumvent this issue, though a small number of studies have used *Brca1* heterozygotes or viable truncation mutants. As *BRCA1* mutations in humans are associated predominantly with cancers of the breast, the majority of conditional models developed have focused on tumourigenesis in the mammary epithelium. Despite the very strong association of *BRCA1* mutations with ovarian cancer, little work has been done with respect to mouse models in this area.

One of the first transgenic models of *Brca1*-associated tumourigenesis examined mice which were heterozygous for *Brca1* and *p53*-null (Cressman, et. al., 1999). The mice predominantly developed lymphomas, though a small number did form mammary carcinomas. Another study using mice with a truncation mutation that eliminated the C-terminal portion of the protein product found that these mice were also predisposed to tumour development, however the majority of the tumours were lymphomas or sarcomas, with less than 15% developing mammary tumours (Ludwig, et. al., 2001).

The first model to examine *Brca1*-associated tumourigenesis specifically in the mammary epithelium utilized either the MMTV or the whey acidic protein (WAP) promoters to drive expression of Cre recombinase specifically to this tissue and crossed these mice with transgenic mice with loxP sites flanking exon 11 of *Brca1* . The offspring of these mice displayed defects in mammary gland development in the form of blunted ductal morphogenesis and developed epithelial mammary tumours after a long latency. They found that these tumours displayed various hallmarks of genetic instability, such as chromosomal abnormalities and aneuploidy. They also found that creating these same mice on a *p53*-null background accelerated tumour development. A later study used the same model, but the mice were created on a p53-wildtype or p53-heterozygous background . They found that even p53-heterozygosity was sufficient to accelerate mammary tumour development.

Work by Berton, et al, utilized the keratin 5 promoter to drive expression of Cre to a wider range of epithelial tissues besides (but including) the mammary epithelium, such as the epithelium of the epidermis, the oral/sinus cavity, esophagus, bladder, and vagina (Berton, et. al., 2003). In this case, the mice were more prone to the development of tumours of the skin, inner ear, and oral epithelium, but did not develop mammary or ovarian tumours.

1.9.3 Models of Ovarian Cancer

One of the major stumbling blocks in ovarian cancer research has been the lack of a mouse model that accurately mimics the human disease. Until quite recently, researchers relied on xenograft models using human cancer cell lines which, while

generating plenty of critical data, have several major limitations. The recent development of several transgenic models, utilizing either Cre-loxP technology or specific promoters has proven quite successful and has opened many research avenues which could not be explored until now.

The first transgenic mouse model of EOC was published in 2003 and was based on expression of SV40 TAg driven by the Mullerian Inhibiting Substance Type II Receptor (MISIIR) promoter (Connolly, et. al., 2003). MISIIR is expressed in the OSE, as well as other ovarian tissues such as the granulosa cells, and in the remainder of the reproductive tract. Approximately fifty percent of the transgenic females developed bilateral epithelial ovarian tumours by six to thirteen weeks of age. The disease progression in these mice mimicked that of humans, in that metastatic spread and ascites production within the peritoneal cavity was a common occurrence.

Because there still lacks an adequate OSE-specific promoter (as mentioned, MISIIR is expressed in multiple ovarian tissues), researchers have turned to using the Cre-loxP recombination system to control gene expression. Several studies have employed this system in conjunction with a technique known as intrabursal injection. This involves performing microsurgeries to inject substances, in this case adenoviral Cre recombinase, under the bursal membrane, which surrounds the ovary of rodents. In this manner, the OSE is bathed in adenovirus expressing Cre recombinase, targeting recombination to this tissue. This methodology was employed by Flesken-Nikitin, *et al* to conditionally inactivate the tumour suppressor genes *p53* and *Rb* in transgenic mice bearing loxP sites flanking segments of one or both genes (Flesken-Nikitin, et. al., 2003). The result was that while inactivation of either tumour suppressor alone was not

sufficient to drive tumourigenesis in the OSE, or only in a very small number of animals, inactivation of both genes resulted in the development of poorly differentiated adenocarcinomas by a median time of 227 days following intrabursal injection. Dinulescu, *et al* also utilized this technique to inactivate the tumour suppressor *Pten* and activate the oncogene *K-ras* in the OSE of mice (Dinulescu, et. al., 2005). Activation of *K-ras* or inactivation of *Pten* alone led to the development of lesions with endometrial glandular morphology, whereas manipulation of both of the genes in tandem resulted in the development of endometrioid ovarian adenocarcinomas within seven weeks of intrabursal injection.

To date, only one study has sought to examine inactivation of the *Brca1* tumour suppressor gene in the mouse ovary, and in this case they targeted inactivation to the granulosa cells using the Cre-loxP system and the FSH receptor promoter to drive Cre expression (Chodankar, et. al., 2005). More than half of the mice developed benign uterine and ovarian cystadenomas, but no carcinomas were observed. At this time, no studies have examined targeted inactivation of *Brca1* in the murine OSE.

1.10 Project Rationale

The molecular events that take place in the normal OSE that ultimately result in transformation and epithelial ovarian tumourigenesis are not currently well understood. Germline mutations in the *BRCA1* tumour suppressor gene are linked to a significantly increased risk for the development of ovarian cancer; however the impact of loss of function of this gene in normal OSE cells and its relation to ovarian carcinogenesis has not been studied in any great depth to date.

As well, a study recently demonstrated that tandem inactivation of both the *p53* and *Rb* tumour suppressor genes in the mouse OSE led to the development of malignant epithelial ovarian tumours . As *BRCA1*-related ovarian cancers have an earlier onset and a specific pathology, but also frequently demonstrate aberrant expression of p53, it is of interest to examine the influence of loss of *Brca1* in conjunction with that of *p53* and/or *Rb* on latency of tumour development as well as tumour pathology.

1.11 Project Objectives

The first objective of this project was to inactivate *Brca1* in the murine OSE, both *in vivo* and *in vitro* using the Cre-loxP system, and to examine the cellular consequences of *Brca1* deficiency in these cells in terms of effects on proliferation, apoptosis, sensitivity to chemotherapeutic agents, capability for anchorage-independent growth, as well as physiological effects on OSE morphology and tumour development.

The second objective of this work was to inactivate *Brca1* in conjunction with the tumour suppressors *p53* and/or *Rb* in the murine OSE both *in vitro* and *in vivo* in order to assess the effect of combined inactivation of these three genes in these cells, in terms of effects on proliferation, sensitivity to chemotherapeutic agents, capability for anchorage-independent growth, as well as physiological effects on OSE morphology and tumour development, given that combined inactivation of *p53* and *Rb* in the mouse OSE has been shown to result in the development of epithelial ovarian tumours.

1.12 Hypotheses

It is hypothesized that inactivation of the *Brca1* gene in the mouse ovarian surface epithelium, either *in vitro* or *in vivo*, will cause these cells to assume a preneoplastic phenotype that sensitizes the cells to transformation, manifested as loss of growth control *in vitro* and the development of putative premalignant lesions such as epithelial inclusion cysts and possibly epithelial ovarian tumours *in vivo*. Further, *Brca1* inactivation in OSE cells with a combined deficiency for *p53* and *Rb* will decrease the latency and increase the growth rate of tumour development, as well as influencing the pathology of these tumours.

Chapter 2 – Materials and Methods

2.1 Experimental Animals

Brca1$^{loxP/loxP}$ [FVB;129-*Brca1*^{tm2Brn}] conditional knockout mice, bearing loxP sites in introns 4 and 13 of the *Brca1* gene, and *p53* $^{loxP/loxP}$ [FVB;129-*Trp53*^{tm1Brn}] (Jonkers, et. al., 2001) mice bearing loxP in introns 1 and 10 of the *p53* gene, were obtained from the Mouse Models of Human Cancers Consortium Mouse Repository (National Cancer Institute, Rockville, MD, USA). Rb$^{loxP/loxP}$ mice [129sv-*Rb1*^{tm2Brn}] (Vooijs, et. al., 1998), bearing loxP sites flanking exon 19 of the *Rb* gene, were obtained from Dr. Ruth Slack at the University of Ottawa (Ottawa, Ontario, Canada). The mice were intercrossed through multiple generations to create colonies of homozygous *Brca1*$^{loxP/loxP}$/ *p53* $^{loxP/loxP}$, *Rb*$^{loxP/loxP}$/*p53*$^{loxP/loxP}$, and *Rb*$^{loxP/loxP}$/*Brca1*$^{loxP/loxP}$ double conditional knockout mice. These mice were then intercrossed through successive generations in order to obtain *Brca1*$^{loxP/loxP}$/*Rb*$^{loxP/loxP}$/*p53*$^{loxP/loxP}$ triple conditional knockout mice (**Figure 6**). It took approximately two years to achieve the triple conditional knockout mice. All animal experiments described in this study were performed according to the *Guidelines for the Care and Use of Animals* established by the Canadian Council on Animal Care.

2.2 Genomic DNA extraction

DNA extraction buffer (50mM KCl, 10mM Tris-HCl, 2mM $MgCl_2$, 0.1mg/ml gelatin, 0.45% Nonidet, and 0.45% Tween-20) containing 40µg/ml proteinase K (Roche, Mississauga, ON, Canada) was added to cell pellets from cultured cells, tumour

Figure 6: Breeding scheme used to create double and triple conditional knockout mice. LoxP/loxP indicates the presence of loxP sites on both alleles of the gene. LoxP/wt indicates that one allele contains a loxP site, while the other has the wildtype sequence. Only the desired resulting genotypes are listed.

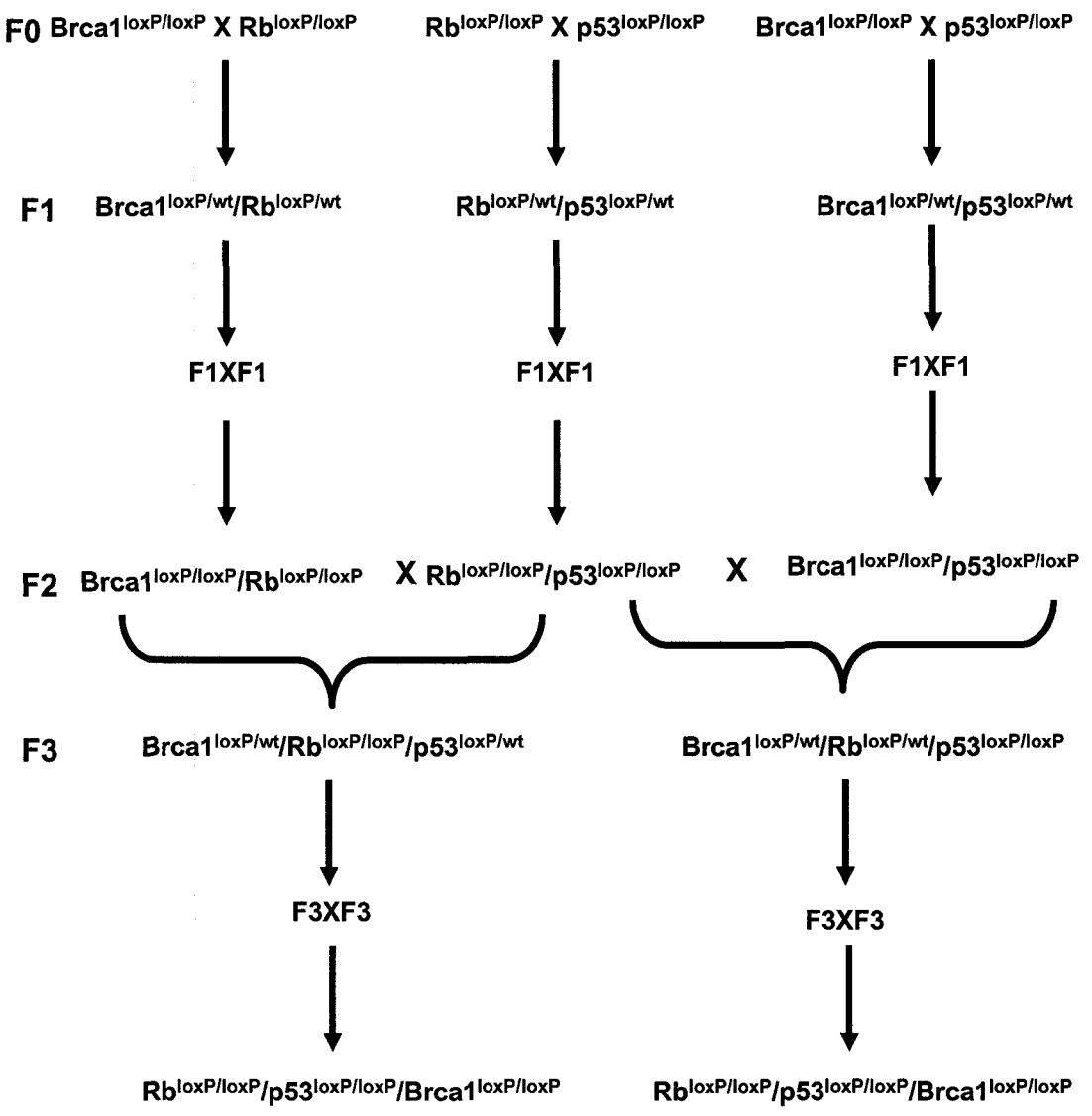
F0 Brca1loxP/loxP X RbloxP/loxP
RbloxP/loxP X p53loxP/loxP
Brca1loxP/loxP X p53loxP/loxP
F1 Brca1loxP/wt/RbloxP/wt
RbloxP/wt/p53loxP/wt
Brca1loxP/wt/p53loxP/wt
F1XF1
F1XF1
F1XF1
F2 Brca1loxP/loxP/RbloxP/loxP
X RbloxP/loxP/p53loxP/loxP
X
Brca1loxP/loxP/p53loxP/loxP
F3 Brca1loxP/wt/RbloxP/loxP/p53loxP/wt
Brca1loxP/wt/RbloxP/wt/p53loxP/loxP
F3XF3
F3XF3
RbloxP/loxP/p53loxP/loxP/Brca1loxP/loxP
RbloxP/loxP/p53loxP/loxP/Brca1loxP/loxP

fragments, OSE cells stripped from the ovary, or ear punches or tail snips from mice and incubated at 58°C overnight. The volume of extraction buffer (250-500µl) varied depending on the size of the sample. Following incubation, 70-140 µl of NaCl was added and the samples were briefly vortexed. Samples were then centrifuged at 5000 rpm for 10 min and the supernatant was transferred to a new tube and the pellet was discarded. Isopropanol (320-640µl) was added to the supernatant and the sample was mixed by inverting the tube several times. Samples were then centrifuged for 5 min at 14,000 rpm. The supernatant was discarded and 250-500µl of 70% ethanol was added to the remaining pellet. The sample was vortexed briefly and then centrifuged at 14,000 rpm for 5 min. The supernatant was discarded and the pellet was allowed to air dry at room temperature. The DNA pellet then resuspended in Tris-EDTA (TE, 50mM, pH 6.8) buffer. DNA content was measured using an Eppendorf Biophotometer (Eppendorf, Mississauga, ON, Canada) with TE buffer as the blank.

2.3 Genotyping

Genomic DNA extracted from ear punches or tails snips collected at weaning were subjected to PCR in order to identify the mice as wildtype or floxed (bearing loxP sites). Primers were obtained from Sigma Genosys (Oakville, ON, Canada) and are desalted. All PCR amplification was carried out in an Eppendorf Mastercycler (Eppendorf) and PCR samples were separated on agarose gels (1-1.2% in Tris acetate-EDTA (TAE) buffer).

2.3.1 *Brca1*$^{loxP/loxP}$ mice

Brca1$^{loxP/loxP}$ mice were genotyped using primers Brca1int4fwd (5' TAT CAC CAC TGA ATC TCT ACC G 3') and Brca1int4rev (5' GAC CTC AAA CTC TGA GAT CCA C 3') or Brca1int13fwd (5' TAT TCT TAC TTC GTG GCA CAT C 3') and Brca1int13rev (5' TCC ATA GCA TCT CCT TCT AAA C 3'). Amplification of genomic DNA with primers Brca1int4fwd and Brca1int4rev yields a 461bp and 391bp fragment for floxed and wildtype sequences respectively (**Figure 7A**), while primers Brca1int13fwd and Brca1int13rev yield a 562bp fragment for the floxed sequence and a 492bp fragment for the wildtype sequence. PCR reactions were prepared in 20 µl volumes with ddH_2O to contain a final volume of 1/20 genomic DNA, 1X PCR buffer (10X stock containing 200 mM Tris HCl (pH 8.4) and 500 mM KCl, Invitrogen, Burlington, ON, Canada), 2.5 mM $MgCl_2$ (50 mM stock, Invitrogen), 0.1 mM deoxynucleoside triphosphates (dNTPs, 10mM stock, Invitrogen), 0.5 µM of each primer (100 µM stock), and 0.05 U/µl thermophilic DNA polymerase (Taq, 5 U/µl stock, Invitrogen). PCR conditions were as follows: 94°C for 5 min; 30 cycles of 94°C for 30 sec, 60°C for 30 sec, and 72°C for 60 sec, followed by 72°C for 10 min. Samples were then stored at 4°C.

2.3.2 *p53*$^{loxP/loxP}$ mice

p53$^{loxP/loxP}$ mice were genotyped using primers p53int1fwd (5' CAC AAA AAC AGG TTA AAC CCA G 3') and p53int1rev (5' AGC ACA TAG GAG GCA GAG AC 3') to yield a 288 bp band for wildtype or a 370 bp band for floxed sequences (**Figure 7B**) or primers p53int10fwd (5' CAC AAA AAC AGG TTA AAC CCA G 3') and

Figure 7: Genoptyping of the conditional knockout mice. A) LoxP sites flank exons 5-13 of the Brca1 gene (left). Primers Brca1int4fwd (a) and Brca1int4rev (b) or primers Brca1int13fwd (c) and Brca1int13rev (d) are used to detect the presence of loxP sites. Wildtype (wt) animals do not have any loxP sites and yield a 461bp band on an agarose gel when using primers a & b (right), while animals with loxP sites on both alleles yield a 562bp band. Heterozygous animals yield both bands. **B)** LoxP sites flank exon 19 of the Rb gene (left). Primers Rb18 (a) and Rb19 (b) are used to detect the presence of loxP sites, yielding a 650bp band in wildtype animals and a 750bp band in those with loxP sites on both alleles of the Rb gene, while heterozygous animals produce both bands (right). **C)** LoxP sites flank exons 2-10 of the p53 gene (left). Primers p53int1fwd (a) and p53int1rev (b) or primers p53int10fwd (c) and p53int10rev (d) can be utilized to detect the presence of loxP sites in genomic DNA. Wildtype (wt) animals do not have any loxP sites and yield a 288bp band when using primers a & b (right), while animals with loxP sites on both alleles yield a 370bp band. Heterozygous animals yield both bands.

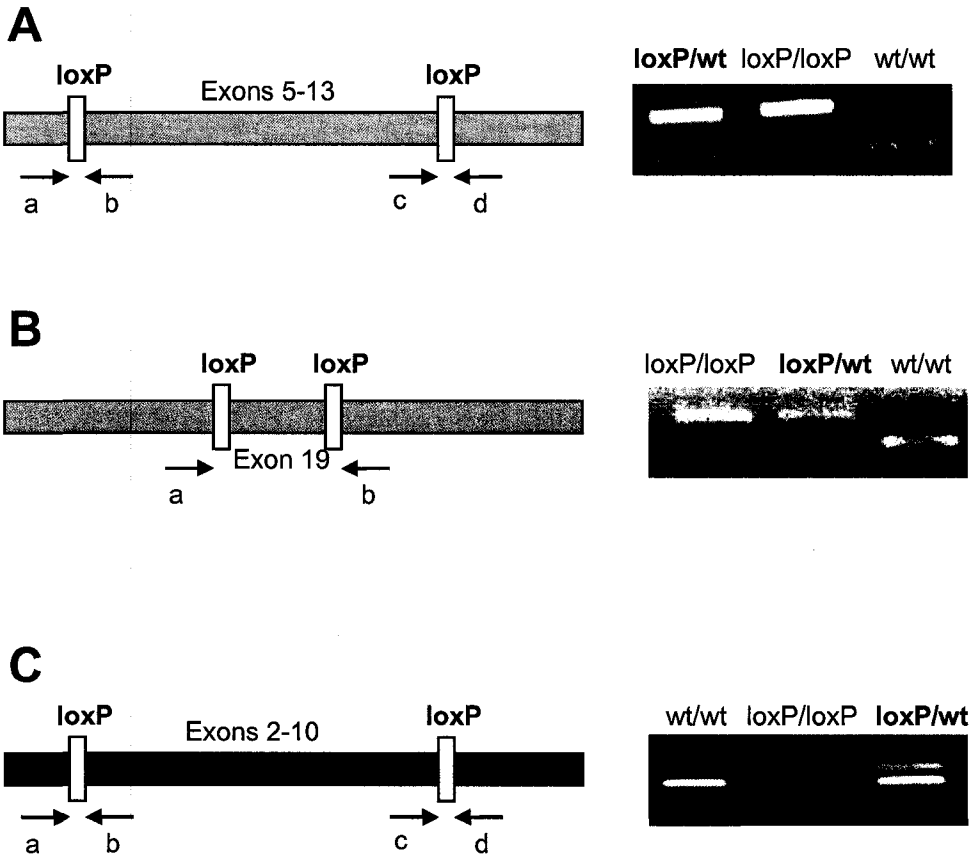
A
loxP
Exons 5-13
loxP
a
b
c
d
loxP/wt loxP/loxP wt/wt
B
loxP
loxP
Exon 19
a
b
loxP/loxP loxP/wt wt/wt
C
loxP
Exons 2-10
loxP
a
b
c
d
wt/wt loxP/loxP loxP/wt

p53int10rev (5' GAA GAC AGA AAA GGG GAG GG 3'), which yield a 431 bp or a 584 bp fragment for wildtype and floxed sequences respectively. PCR reactions were prepared in 20 µl volumes with ddH_2O to contain a final volume of 1/20 genomic DNA, 1X PCR buffer, 2.5 mM $MgCl_2$, 0.1 mM dNTPs, 0.5 µM of each primer (100 µM stock), and 0.05 U/µl Taq. PCR conditions were as follows: 94°C for 5 min; 30 cycles of 94°C for 30 sec, 60°C for 30 sec, and 72°C for 60 sec, followed by 72°C for 10 min. Samples were then stored at 4°C.

2.3.3 *Rb*$^{loxP/loxP}$ mice

Rb$^{loxP/loxP}$ mice were genotyped using primers Rb18 (5' GGC GTG TGC CAT CAA TG 3') and Rb19 (5' AAC TCA AGG GAG ACC TG 3'). DNA from wildtype mice yielded a 750bp band, while floxed mice were identified by the presence of a 650bp band (**Figure 7C**). PCR reactions were prepared in 25 µl volumes with ddH_2O containing a final volume of 1/20 genomic DNA, 1X PCR buffer, 2.5 mM $MgCl_2$, 0.08 mM dNTPs, 1 µM of each primer (100 µM stock), and 0.05 U/µl Taq. PCR conditions were as follows: 94°C for 5 min; 30 cycles of 94°C for 30 sec, 58°C for 30 sec, and 72°C for 50 sec, followed by 72°C for 10 min. Samples were then stored at 4°C.

2.4 Detection of recombination at loxP sites

Genomic DNA was extracted from cultured cells, tumour fragments, OSE cells stripped from the ovary, or ear punches or tail snips from mice as described above.

2.4.1 Excision of exons 5-13 of *Brca1*

For detection of Cre-mediated excision of exons 5-13 of *Brca1* (hereafter designated *Brca1*$^{\Delta 5\text{-}13}$), PCR amplification was performed using primers Brca1int4fwd

and Brca1int13rev to yield a 600bp product. When no recombination has occurred in a sample the primers are too far apart and thus no product can be detected. Detection of any remaining wildtype sequence following Cre exposure was performed in a separate amplification utilizing primers for exon 11 of *Brca1*, Brca1exon11fwd (5') and Brca1exon11rev (5') yielding a 592bp product (Sgagias, et. al., 2004). PCR conditions were the same as described in section 2.3.1.

2.4.2 Excision of exons 2-10 of *p53*

For detection of Cre-mediated excision of exons 2-10 of *p53* (hereafter designated $Trp53^{\Delta 2\text{-}10}$), primers p53int1fwd and p53int10rev were used, yielding a 612 bp product. When no recombination has occurred in a sample the primers are too far apart and thus no product can be detected. Remaining wildtype sequence following Cre exposure was detected using primers p53int1fwd and p53int1rev or primers p53int10fwd and p53int10rev in a separate amplification. PCR conditions were the same as described in section 2.3.2.

2.4.3 Excision of exon 19 of *Rb*

For detection of Cre-mediated excision of exon 19 of the *Rb* gene (hereafter designated $Rb^{\Delta 19}$), primers Rb18 and Rb212 (5' GAA AGG AAA GTC AGG GAC ATT GGG 3") were used, yielding a 260bp product when recombination has occurred and a 750 bp product for the wildtype fraction. Twenty µl PCR reactions were set up containing 1/20 genomic DNA, 1X PCR buffer, 1.8 mM $MgCl_2$, 0.1 mM dNTPs, 0.5 µM of each primer (100 µM stock), and 0.125 U/µl Taq. The PCR conditions used for amplification were as follows: 94°C for 5 min prior to the addition of Taq, followed by 30 cycles of

94°C for 30 sec, 58°C for 30 sec, and 72°C for 50 sec, followed by 72°C for 10 min. Samples were then stored at 4°C.

2.5 Primary Culture of Mouse OSE (MOSE) Cells

Prior to MOSE cell collection, 6- to 8-week old mice from the genotypes described above were superovulated by intraperitoneal (IP) administration of 5 I.U. pregnant mares' serum gonadotropin (PMSG; Intervet, Whitby, ON, Canada), followed 46-48 hrs later by IP injection of 5 I.U. human chorionic gonadotropin (hCG; Sigma-Aldrich, Oakville, ON, Canada). Ovaries were individually dissected 72 hrs following hCG administration. Five to ten mice were used for each collection and both ovaries were collected from each mouse. The ovaries were washed twice with phosphate-buffered saline (PBS, Hyclone, Logan, UT, USA), incubated in 0.25% Trypsin/PBS (1 ml/ovary; Invitrogen) in a 15 ml Falcon tube at 37°C for 1 hr. Alpha minimum essential medium (α-MEM; Gibco BRL, Burlington, ON, Canada) containing 4% heat-inactivated fetal bovine serum (HI-FBS, Cansera, Etobicoke, ON, Canada), 5 U/ml penicillin/ 0.005mg/ml streptomycin solution (Sigma-Aldrich), 0.1μg/ml gentamicin (Gibco-BRL), and 1μg/ml insulin-transferrin-sodium-selenite solution (ITSS; Roche) was added to inactivate the trypsin and the tube was agitated gently by hand to remove the OSE cells from the ovary. The supernatant containing the OSE cells was centrifuged at 1000 rpm for 10 min. The cells were resuspended in the above medium and plated in 24-well tissue culture plates (Becton-Dickinson, Oakville, ON, Canada) and passaged upon reaching confluence. Following the first passage the cells were grown in the same medium with the exception that the concentration of HI-FBS was increased to 10% (hereafter referred to as MOSE

medium). It took approximately two months for each culture to reach a sufficient number and stability of cells to be able to survive adenoviral infection.

2.6 *In Vivo* Intrabursal Adenovirus Administration

Recombinant adenoviruses Ad5CMVeGFP (AdGFP), Ad5CMVLacZ (AdLacZ), or Ad5CMVCre (AdCre) (Vector Development Laboratory, Houston, TX, USA) were delivered to the OSE *in vivo* via intrabursal injection. Six to eight week-old virgin animals from the various genotypes described above were anesthetized via IP injection of Avertin (2.5% v/v in 0.85% NaCl, 0.015-0.017 ml/g body weight; Sigma-Aldrich) and the ovaries were individually accessed via dorsal incision. While viewed under a microscope, approximately 10 µl of adenovirus (4 X 10^7 pfu/µl in PBS) was delivered into the bursal space using a 1cc syringe and a 30-gauge beveled needle at the oviductal-bursal junction. The ovary was then placed back into the peritoneal cavity and a single suture was used to close the incision in the body wall. Both the left and right ovaries were injected in each animal. The animals were not bred over the course of the experiment.

2.7 *In Vitro* Adenovirus Infection

For *in vitro* infections, MOSE cells were infected with an MOI of 200 pfu/cell. Cells were allowed to plate overnight and were then washed twice with PBS. A thin layer of serum-free α-MEM containing the appropriate concentration of adenovirus was added and cells were incubated at 37°C for 2 hours. The adenovirus-containing media was then removed and the cells were washed twice with PBS and normal growth medium was added. All experiments were initiated following replating of the cells 72 hrs after

adenoviral infection. In order to examine LacZ expression in whole ovaries or plated cells, the ovaries or cells were washed twice with PBS, fixed in 0.2% gluteraldehyde in 0.1M PBS for at least 20 min at 4°C, washed twice with PBS and stained overnight with X-Gal (Bio-WORLD, Dublin, OH, USA) at 37°C in the dark. eGFP expression was visualized with a Leica MZFLIII fluorescence stereomicroscope (Leica Microsystems, Wetzlar, Germany).

2.8 Tissue Collection

Animals were sacrificed via CO_2 asphyxiation at 60, 120, 180, or 240 days post-injection of adenovirus for time point experiments or when they had reached a survival endpoint due to tumour burden for survival experiments. The criteria used to determine survival endpoint were defined as any or all of the following; complete anorexia lasting longer than 24 hours, dehydration lasting longer than 24 hours despite fluid therapy, presence of respiratory distress, abnormal neurologic activity (seizures or the inability to walk), diarrhea, rapid weight loss greater than 5 g from the average body weight of control mice of the same age, rapid weight gain exceeding 5 g from the average body weight, presence of abdominal distention that impairs mobility, presence of a palpable mass that impairs mobility .

When animals were sacrificed at a predetermined time point, the ovaries (with the ovarian fat pad and bursal membrane intact) were removed individually along with the attached oviduct and a portion of the uterus, fixed in formalin and paraffin-embedded. Serial sections with a thickness of 5 μm were cut either for hematoxylin and eosin (H&E) staining or immunohistochemistry (IHC).

When animals were sacrificed because they had reached loss-of-wellness endpoint, tumour(s), if present, were removed along with any attached anatomical structures (e.g. uterus) and fixed in formalin and paraffin embedded. Prior to fixation, a small piece of tumour tissue was removed and processed for genomic DNA isolation. The ovaries were removed and processed as described above, if they were not associated with tumour. Serial sections of tumour tissue with a thickness of 5 μm were cut either for H&E staining or IHC.

When present, peritoneal ascites fluid was collected and processed as follows: collected fluid was centrifuged at 5000 rpm for 10 min at room temperature to allow the cellular fraction to pellet. The plasma-containing supernatant was removed via vacuum aspiration along with as much of the red blood cells, if present, as possible. The remaining cell pellet was resuspended in MOSE medium and the cells were plated in a tissue-culture vessel. The following day the cells were washed with PBS to remove any remaining contaminating red blood cells and fresh MOSE medium was added.

2.9 Histological Analysis

Morphological changes to the OSE were assessed by examining five non-consecutive, and spaced at 20-25 μm intervals, H&E sections from the middle of each ovary at 200X magnification using an Olympus BX50 microscope (Olympus, Melville, NY, USA). This number and spacing of sections was deemed to be a sufficiently representative sampling of the whole ovary based on previous analysis of a subset of serial sections of whole ovaries. Samples were blinded prior to the histological analysis. Sections were evaluated for the number of areas of columnar cells, areas of hyperplasia,

and invaginations of the OSE, as well as epithelial inclusion cysts. Hyperplasia was defined as cells that had lost apical/basal polarity and exhibited layering with the formation of papillations of the OSE. Areas of columnar cells or hyperplasia were defined as a segment of epithelium that constituted these morphological changes flanked on either side by morphologically normal epithelium. Epithelial invaginations were defined as structures where the OSE distinctly invaginated into the ovarian stroma at or close to a right angle to the normal OSE such that the structure was flanked by ovarian stroma on both sides. Inclusion cysts were defined as a spherical structure (as assessed by examining serial sections, to ensure that these structures were not merely invaginations sectioned tangentially) within the ovarian stroma with a discernible epithelium-lined lumen. The epithelial nature of the lining of inclusion cysts was confirmed via immunohistochemistry for CK19. Proliferation of the OSE *in vivo* was assessed by counting the number of Ki67-positive cells in the OSE in five non-consecutive sections per ovary.

2.10 Immunohistochemistry

Paraffin sections were deparaffinized in xylene and rehydrated in ethanol according to standard protocol. High temperature antigen retrieval was performed using sodium citrate buffer (pH 6.0) and endogenous peroxidase activity was blocked using 3% hydrogen peroxide in Stockholm PBS (S-PBS). All samples were blocked using an avidin/biotin blocking kit (DAKO, Cytomation, Carpentaria, CA, USA). Primary antibodies were diluted in S-PBS at the following concentrations: rat anti-CK19, 1:100 (TROMA-1, Developmental Studies Hybridoma Bank, University of Iowa, USA); rat

anti-Ki67, 1:25 (DAKO); rabbit anti-p53, 1:50 (Santa Cruz Biotechnology; Santa Cruz, CA, USA); E-cadherin, 1:100 (Santa Cruz); and Collagen IV, 1:100 (Novus Biologicals, Littleton, CO, USA); mouse-anti smooth muscle actin (SMA), 1:100 (DAKO); mouse anti-Desmin, 1:100 (DAKO); and rat anti-CD34, 1:50 (Novus Biologicals). For antibodies raised in rat or rabbit, sections were incubated with primary antibody at room temperature for 2 hours or overnight. Following three 5-min washes in S-PBS, sections were stained with an anti-rabbit or rat secondary antibody (1:200, DAKO) for 20 min followed by three 5-min washes and incubation with a streptavidin/horseradish peroxidase solution (1:200, DAKO) for 20 min. For antibodies raised in mice, the Vector® Mouse on Mouse™ immunodetection kit (Vector Laboratories, Burlingame, CA, USA) was used according to manufacturer specifications. Developing was performed with diaminobenzidine (DAB) as a substrate (0.2% DAB, 0.001% H_2O_2; Sigma-Aldrich). Slides were counterstained with hematoxylin, dehydrated, and coverslipped with Permount mounting medium (Fisher Scientific, Ottawa, ON, Canada).

2.11 *In vitro* proliferation assay

MOSE cells that had been infected 72 hours earlier with either AdCre recombinase or AdGFP were plated in 24-well tissue culture plates at a density of 2.0 X 10^4 cells/well. Cells were trypsinized with 0.05% trypsin (Hyclone) and counted using a Coulter Counter (Beckman Coulter, Mississauga, ON, Canada) at 24, 48, 72, or 96-hour time points. Growth medium was replaced every 48 hours. Experiments were performed three times in triplicate, with a separate infection for each replicate. The same experiments were also performed on MOSE cells several passages (greater than three

passages, but less than ten) following infection with AdCre or AdGFP. These experiments were performed three times in triplicate.

2.12 Cisplatin sensitivity assay

MOSE cells that had been infected 72 hours earlier with either AdCre or AdGFP were plated in 12-well plates at a density of 8.0 X 10^4 cells/well. The following day the normal growth medium was replaced with either fresh media or media containing 1μM or 5μM cisplatin (1mg/ml stock, Faulding Pharmaceutical Co, Paramus, NJ, USA). Remaining adherent cells were trypsinized and counted using a Coulter Counter at 24 and 48 hours following the addition of cisplatin. Experiments were performed three times in triplicate, with a separate infection for each replicate.

2.13 Paclitaxel sensitivity assay

MOSE cells that had been infected 72 hours earlier with either AdCre or AdGFP were plated in 12-well plates at a density of 4.0 X 10^4 cells/well. The following day the normal growth medium was replaced with medium containing either 25nM paclitaxel (Taxol®, 6 mg/ml stock, diluted 1 in 1000 in dimethylsulfoxide (Fisher Scientific), Bristol-Myers Squibb, Houston, TX, USA) or an equivalent volume of DMSO alone. Remaining adherent cells were trypsinized and counted using a Coulter Counter at 96 hours following the addition of paclitaxel. Experiments were performed three times in triplicate, with a separate infection for each replicate.

2.14 Flow cytometry

Cultured MOSE cells were trypsinized and washed twice with PBS, followed by fixation in 70% ethanol at -20°C for a minimum of 1 hour. Both floating and adherent cells were collected for analysis. Cells were then washed twice with PBS containing 1% serum and resuspended in propidium iodide (Sigma, 20mg/ml in PBS) containing RNAse A (40mg/ml, MBI Fermentas, Burlington, ON, Canada). Samples were analyzed for the percentage of cells in the sub-G1 fraction using a BD LSR flow cytometer with CellQuest software (BD Biosciences, Mississauga, ON, Canada).

2.15 Western Blotting

Protein samples were collected in RIPA buffer containing 1X protease and phosphatase inhibitors (Halt™ protease inhibitor cocktail kit and Halt™ phosphatase inhibitor cocktail kit, Pierce, Rockford, IL, USA) and protein content was measured using a commercially available protein assay (Bio-Rad Protein Assay Kit, Bio-Rad Laboratories, Mississauga, ON, Canada) and a Beckman DU® 640 Spectrophotometer (Beckman Instruments Inc., Mississauga, ON, Canada). Samples were separated on a 4-12% Bis-Tris pre-cast polyacrylamide gel (Invitrogen) and transferred to a nitrocellulose membrane (Hybond C Extra, Amersham, Oakville, ON, Canada). Blocking was carried out with 5% milk in Tris-buffered saline with Tween-20 (TBS-T). For all subsequent immunoblotting, antibodies were diluted to the appropriate concentration in 5% milk in TBS-T. Blots were incubated for 2 hours at room temperature or overnight at 4°C with the following primary antibodies: rabbit anti-p53, 1:500 (Santa Cruz) and mouse anti-

GAPDH, 1:2000 (AbCam, Cambridge, MA, USA). Visualization of protein bands was performed using the ECL Plus western blotting detection system (Amersham) and GeneSnap image acquisition system (Syngene, Frederick, MD, USA).

2.16 Colony formation in soft agar

For the base agarose, equal parts 2X α-MEM (containing 20% HI-FBS, 10 U/ml penicillin/ 0.010mg/ml streptomycin solution 0.2μg/ml gentamicin and 2μg/ml ITSS) and 1.5% molten low-melting point agarose were mixed and 400μl was added to each well of a 24-well plate. The base layer was allowed to solidify at room temperature. The top layer consisted of equal parts 2X α-MEM as described above and 1% molten low-melting point agarose. Cells were resuspended well, to ensure a single-cell suspension, in the agarose/media mix while it was still liquid to a final dilution of 2.0 X 10^3 cells/700μl. The 700μl suspension was layered on top of the base agarose layer. Solidification was allowed to occur over a few minutes at room temperature, after which the plates were incubated at 37°C and 5% CO_2. Wells were assessed for the presence or absence of colony formation for up to 6 weeks.

2.17 Growth on poly-HEMA-coated plates

Poly-HEMA (poly(2 hydroxyethyl methaxrylate), Sigma-Aldrich) was resuspended to a stock concentration of 120 mg/ml in 95% ethanol and allowed to dissolve O/N at 65°C. The stock solution was diluted 1 in 10 in 95% ethanol to create a working solution of 12mg/ml. The wells of 12-well tissue culture plates were coated with 250μl of this working solution and allowed to dry in a 37°C drying oven O/N. Coating of

the plates with poly-HEMA prevents the attachment of cells to the bottom of the dish. Single cell suspensions were plated at a density of 2.0 X 10^4 cells/well in MOSE medium and maintained at 37°C and 5% CO_2. Plates were examined daily for anchorage-independent cell growth as assessed by the presence of floating cell aggregates.

2.18 Ascites cell culture

When present in sufficient volume at survival endpoint, peritoneal ascites was aspirated using a 25-gauge needle and a 1-3cc syringe. Cells were pelleted via centrifugation at 1000 rpm for 10 minutes, resuspended in the MOSE medium and then plated in standard tissue culture vessels. The following day, the media was aspirated, the cells were washed 2-3 times with PBS to remove contaminating red blood cells and fresh culture medium was added. Cells were passaged upon confluence and were subsequently used for confirmation of recombination at loxP sites in this cell population.

2.19 Statistical Analyses

Counts of morphological features in the OSE are expressed as the mean ± SEM (standard error of the mean) of the mean number of morphological features per section in five non-consecutive ovarian sections for n ovaries, where n is the number of ovaries examined. *In vitro* cell counts are expressed as the mean ± SEM of three independent experiments performed in triplicate. The probability of significant differences upon comparison of only two groups was determined by Student's *t* test. When multiple groups were analyzed, statistical comparisons where made by analysis of variance (ANOVA). Bonferroni's posttest was used to determine significance between specific groups when

whole group differences where detected by ANOVA. Survival curves were compared using a Log-Rank test. For all analyses, significance was inferred at $P<0.05$ and P values were two-sided. Analyses were performed using Graphpad Prism statistical software (Graphpad Software, San Diego, CA, USA).

Chapter 3 – Results:

Conditional inactivation of Brca1 in the mouse ovarian surface epithelium *in vitro* and *in vivo*

3.1 The OSE can be efficiently infected with adenoviral vectors both *in vivo* and *in vitro.*

To ensure that intrabursal administration of adenoviral vectors resulted in infection confined to the OSE cells, without significant leakage from the bursal space, animals were injected with either AdGFP or AdLacZ and the ovaries and surrounding tissues, including the bursal membrane, ovarian fat pad, oviduct, and uterus, were removed and examined one week post-surgery. Intrabursal administration of adenoviral vectors results in a high rate of infectivity that is confined to the OSE, without penetrating into the ovarian stroma below (**Figure 8B**). Surrounding tissues, such as the ovarian fat pad, oviduct, and uterus, do not demonstrate signs of infection (**Figure 8A**). Administration of adenoviral vectors to MOSE cells *in vitro* also results in the infection of the majority of cells (**Figure 8C**).

3.2 Detection of recombination at loxP sites following adenoviral Cre recombinase infection.

Recombination at loxP sites following infection with AdCre was confirmed by collecting Cre-infected ($Brca1^{\Delta 5\text{-}13}$) and AdGFP-infected ($Brca1^{loxP/loxP}$) ovaries at 180

Figure 8: Infection of OSE cells with adenoviral vectors both *in vivo* and *in vitro*. A) One week following intrabursal injection of AdGFP, eGFP expression (seen in the right panel using a GFP microscope) is confined to the ovary beneath the bursa (arrow), and expression cannot be detected in surrounding tissues such as the ovarian fat pad (fp), oviduct (ov), or uterus (u) (labeled in the left panel). These structures can be seen clearly in the left panel, which is the same tissue shown under white light. The arrowhead in the left panel indicates a photographic lighting artifact. **B)** One week following intrabursal injection of AdLacZ, ovaries were removed, stained with X-Gal, and forceps were used to remove a portion of the OSE (strip between arrows) to demonstrate that infection is confined to the OSE and does not penetrate into the underlying ovarian stroma. **C)** Cultured $Brca1^{loxP/loxP}$ MOSE cells were infected with AdLacZ with an MOI of 200 and stained with X-Gal after 24 hours. Scale bars represent 1.6mm (B) or 50μm (C).

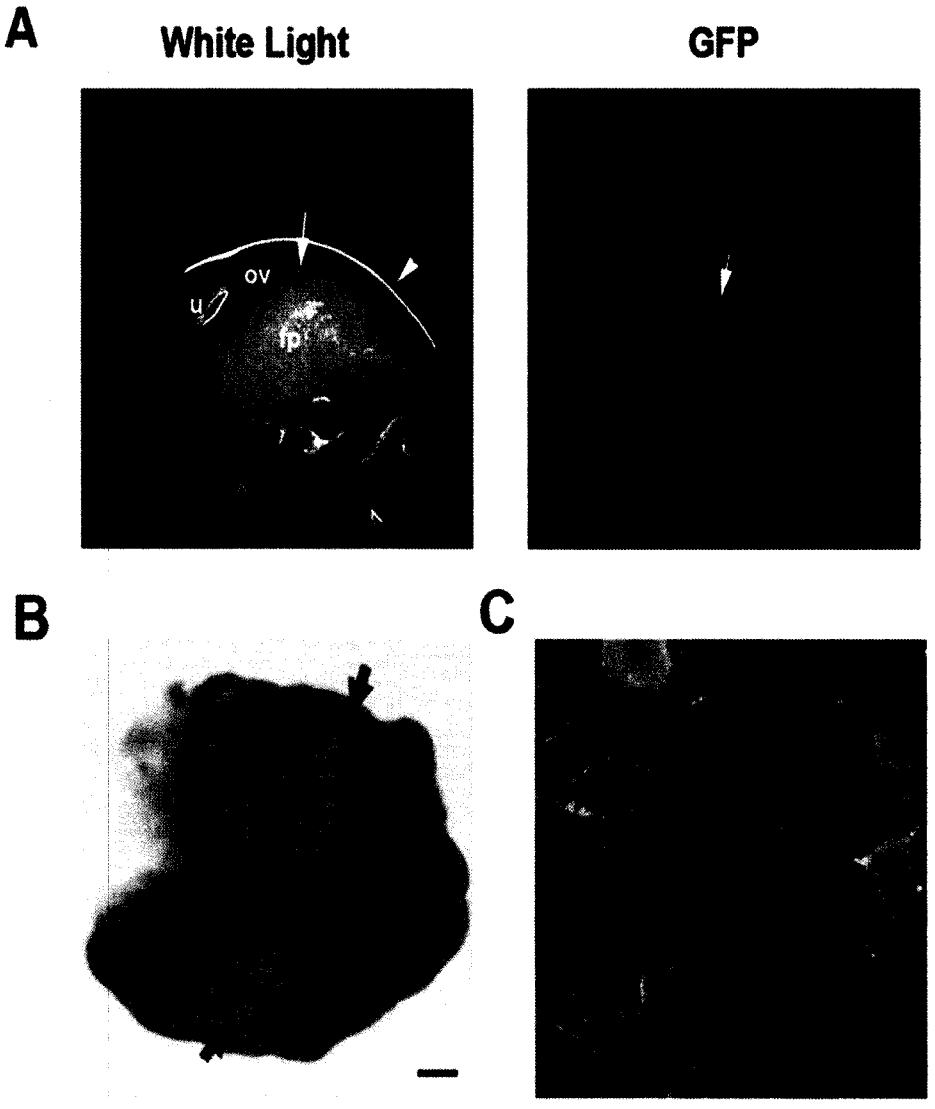
A
White Light
GFP
ov
fp
B
C

days post intrabursal injection and removing the OSE cells as described in Materials and Methods. Recombination at loxP sites is evident only in the AdCre infected cells and not in the AdGFP infected cells (**Figure 9A**). Genomic DNA was also extracted from MOSE cells infected *in vitro* 72 hours after adenoviral infection. Recombination at loxP sites could be detected in all of the samples we analyzed with little if any wildtype fraction remaining (**Figure 9B**).

3.3 Conditional inactivation of *Brca1* in mouse OSE results in an increase in morphological changes.

To assess the consequences of inactivation of the *Brca1* tumour suppressor gene in the OSE, mice bearing loxP sites flanking a segment of their *Brca1* gene were injected under the ovarian bursal membrane with either adenoviral Cre recombinase to inactivate *Brca1* ($Brca1^{\Delta 5\text{-}13}$) or AdGFP as a control adenovirus ($Brca1^{loxP/loxP}$). Five non-consecutive 5μm sections at 20-25μm intervals from each ovary were assessed for morphological changes to the OSE defined as areas of columnar cells, areas of hyperplasia, epithelial invaginations, and epithelial inclusion cysts. Examples of these morphologies are shown in **Figure 10**. There were no significant differences between $Brca1^{loxP/loxP}$ and $Brca1^{\Delta 5\text{-}13}$ ovaries in terms of the dimensions of age-matched ovaries in the sections evaluated.

The number of morphological changes in the OSE increased overall in both the $Brca1^{\Delta 5\text{-}13}$ and $Brca1^{loxP/loxP}$ ovaries over time (**Table 1**). Significant increases in the number of changes were evident after 180 days in the $Brca1^{\Delta 5\text{-}13}$ group ($P<0.001$), whereas a significant difference was not evident until the 240-day time point in the

Figure 9: Detection of recombination at loxP sites following adenoviral Cre recombinase infection *in vivo* and *in vitro*. **A)** PCR of genomic DNA from OSE cells collected from $Brca1^{loxP/loxP}$ mice 180 days following intrabursal injection of AdCre ($Brca1^{\Delta 5\text{-}13}$) or AdGFP ($Brca1^{loxP/loxP}$). **B)** PCR of genomic DNA collected from cultured $Brca1^{loxP/loxP}$ OSE cells 72 hours following *in vitro* infection with AdCre ($Brca1^{\Delta 5\text{-}13}$) or AdGFP ($Brca1^{loxP/loxP}$).

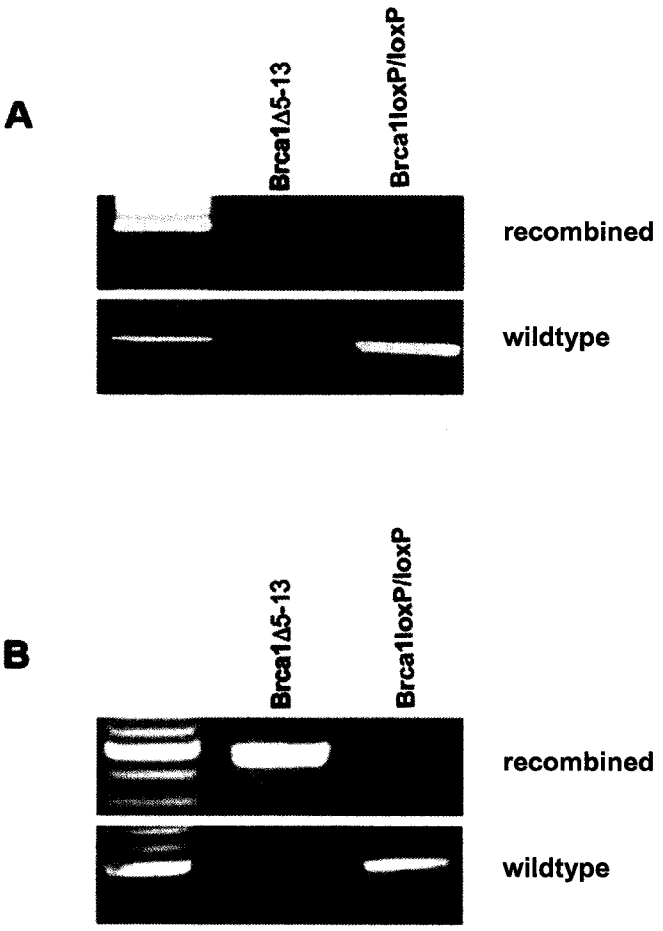
A
Brca1Δ5-13
Brca1loxP/loxP
recombined
wildtype
B
Brca1Δ5-13
Brca1loxP/loxP
recombined
wildtype

Figure 10: Morphological changes observed in the mouse OSE. A) Representative ovary from a *Brca1*$^{loxP/loxP}$ mouse 180 days following intrabursal injection of AdGFP (H&E, 25X) **B)** Representative ovary from a *Brca1*$^{\Delta 5\text{-}13}$ mouse 180 days following intrabursal injection of AdCre (H&E, 25X, arrows indicate areas of hyperplasia) **C)** Normal cuboidal OSE cells (H&E, 200X) **D)** Columnar OSE cells (H&E, 200X) **E)** Hyperplasia (H&E, 200X) **F)** Epithelial invagination (arrowhead, H&E, 100X) **G)** Epithelial inclusion cyst (arrow, H&E, 100X) The arrowhead indicates what is in fact an invagination in tangential section.

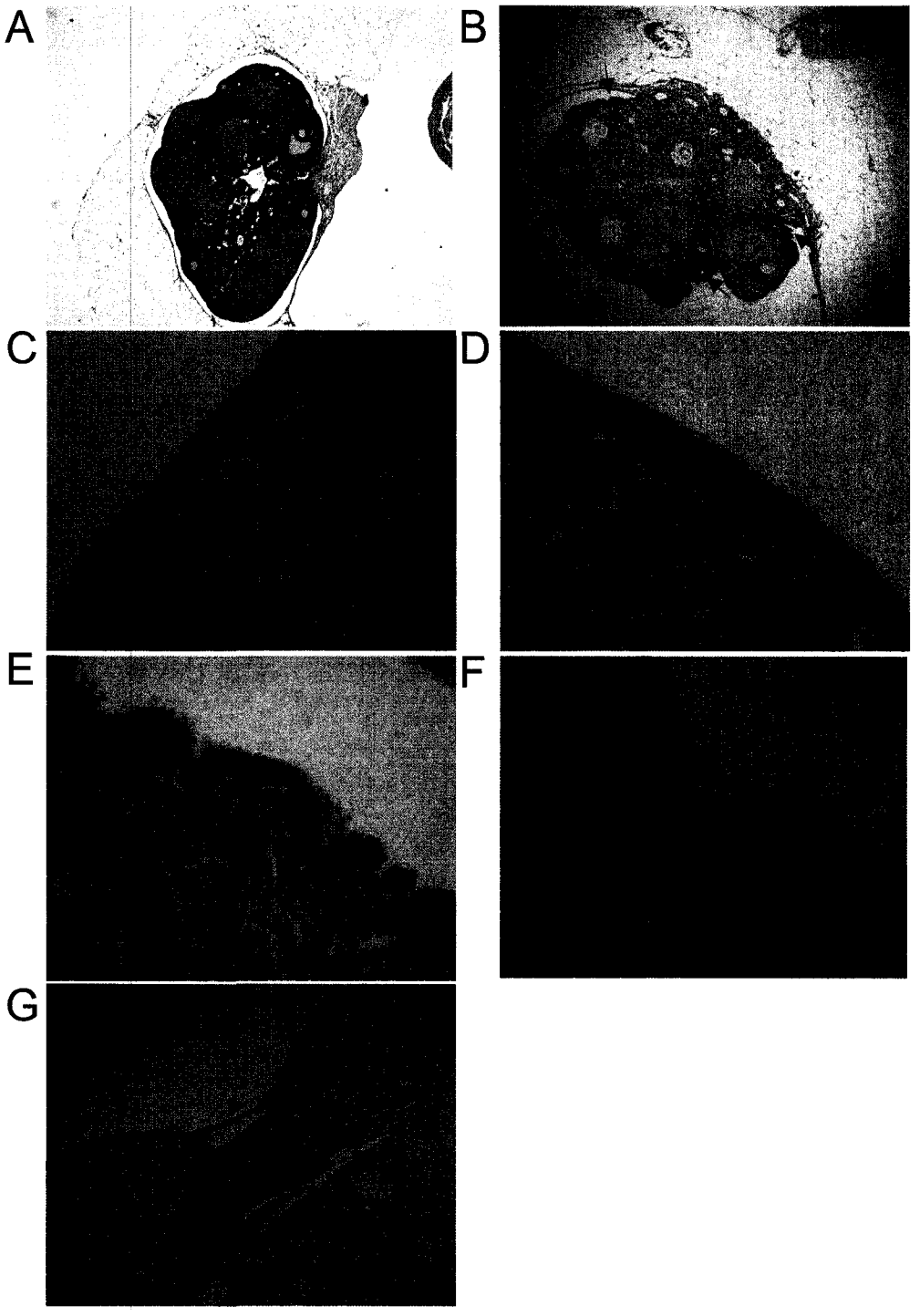
A
B
C
D
E
F
G

Table 1: Distribution of morphological features in the OSE over time following conditional inactivation of *Brca1*.

	Time (Days)			
Epithelial Morphology	**60**	**120**	**180**	**240**
Areas of Columnar Cells				
Brca1$^{\Delta 5\text{-}13}$	0.99±021^{a*} (n=9)	2.50±0.52^{a} (n=7)	4.23±0.62^{b} (n=9)	5.22±0.38^{b} (n=10)
Brca1$^{loxP/loxP}$	2.26±0.28^{a} (n=10)	2.73±0.26^{a} (n=8)	3.50±0.21^{a} (n=8)	3.61±0.71^{b} (n=10)
Areas of Hyperplasia				
Brca1$^{\Delta 5\text{-}13}$	1.16±0.47^{a}	2.96±1.58^{a}	4.54±0.88^{a}	4.94±0.89^{b}
Brca1$^{loxP/loxP}$	1.80±0.44^{a}	1.65±0.50^{a}	2.68±0.42^{a,b}	5.46±0.67^{b}
Epithelial Invaginations				
Brca1$^{\Delta 5\text{-}13}$	0^{a}	0.26±0.26^{a}	0.60±0.33^{a}	1.44±0.70^{b*}
Brca1$^{loxP/loxP}$	0.08±0.06^{a}	0.05±0.05^{a}	0.08±0.05^{a}	0.34±0.14^{a}
Inclusion Cysts				
Brca1$^{\Delta 5\text{-}13}$	0	0	0.19±0.19	0.80±0.00
Brca1$^{loxP/loxP}$	0	0	0	0
Total Changes				
Brca1$^{\Delta 5\text{-}13}$	2.14±0.54^{a}	5.71±1.67^{a,b}	9.56±1.69^{b}	12.96±1.21^{b*}
Brca1$^{loxP/loxP}$	4.14±0.63^{a}	4.43±0.73^{a}	6.25±0.58^{a,b}	9.42±0.76^{b}

Numbers represent the mean ±SEM number of morphological changes per section over five non-consecutive sections in n ovaries. Time is the number of days after intrabursal injection of AdCre (Brca1$^{\Delta 5\text{-}13}$) or AdGFP (Brca1$^{loxP/loxP}$). Superscript letters are used to denote a significant difference between time points for that treatment group. * Indicates a significant difference between the Brca1$^{\Delta 5\text{-}13}$ group and the Brca1$^{loxP/loxP}$ group at that time point ($P<0.05$).

Brca1$^{loxP/loxP}$ group (P<0.01). This pattern was also seen in terms of increases in the number of areas of columnar epithelium over time. There was a significant increase in the number of invaginations of the OSE in the *Brca1*$^{\Delta 5\text{-}13}$ group between the 60 and 240-day time points (P<0.05), whereas there was no significant change in the number of invaginations in the *Brca1*$^{loxP/loxP}$ group during the course of the study.

Not only the time course of morphological changes was affected by *Brca1* inactivation, but there was also a more significant increase in the number of epithelial changes in the OSE of the *Brca1*$^{\Delta 5\text{-}13}$ mice versus *Brca1*$^{loxP/loxP}$ mice over time. The total number of morphologic changes in the surface epithelium increased 6-fold between 60 days and 240 days post-intrabursal injection in the *Brca1*$^{\Delta 5\text{-}13}$ mice, whereas only a 2-fold increase was observed in the *Brca1*$^{loxP/loxP}$ mice over the same time period.

Overall, there were significantly more surface epithelial changes observed in ovaries in which *Brca1* had been inactivated in the OSE than in control ovaries after 240 days (12.96±1.21 versus 9.42±0.76, P<0.05). Significantly more areas of columnar epithelium were observed in the *Brca1*$^{loxP/loxP}$ ovaries at the 60-day time point (0.99±0.21 versus 2.26±0.28, P<0.05); however, this was not sustained at later time points. There were no differences in the number of areas of hyperplasia between the *Brca1*$^{loxP/loxP}$ and *Brca1*$^{\Delta 5\text{-}13}$ ovaries at any time point examined. There were 4-fold more epithelial invaginations in the *Brca1*$^{\Delta 5\text{-}13}$ ovaries as compared to *Brca1*$^{loxP/loxP}$ at 240 days post-intrabursal injection (1.44±0.70 versus 0.34±0.14, P<0.05). Epithelial inclusion cysts were only observed in the *Brca1*$^{\Delta 5\text{-}13}$ ovaries and only at the 180 and 240-day time points.

To ensure that changes in ovarian surface epithelial morphology were not due to non-specific effects of Cre recombinase, non-transgenic FVBn mice were also subjected to intrabursal injection of either AdCre or a mock injection and their ovaries were collected at 60, 120, 180, and 240 days post-injection. Two mice were injected per group per time point. The number of surface epithelial changes increased with time in both groups, however there was no difference between the AdCre-injected ovaries and the mock-injected ovaries at any of the time points examined (**Table 2**).

3.4 An increase in morphological changes in the *Brca1*$^{\Delta 5\text{-}13}$ OSE is not due to an increase in proliferation.

Very few (≤ 5, on average) Ki67-positive cells were found in the OSE in any of the sections examined (**Figure 11A**). There was no significant difference in the number of Ki67-positive cells in the OSE between the *Brca1*$^{loxP/loxP}$ and *Brca1*$^{\Delta 5\text{-}13}$ group at the 240 day time point (**Figure 11B**). No association was seen between morphological features of the OSE such as hyperplasia, invaginations, or inclusion cysts and the presence of Ki67-positive cells. There was also no association between the location of Ki67-positive cells in the OSE and underlying follicular structures.

3.5 Expression of proteins involved in ovarian cancer initiation and progression.

Immunohistochemical analysis was performed to determine the expression of p53, E-cadherin, and Collagen IV, proteins which have all been shown to be involved in ovarian cancer initiation and progression in humans, often with alterations in expression patterns seen in prophylactic oophorectomy specimens (Hutson, et. al., 1995; Maines-

Table 2: Distribution of morphological features in the OSE of non-transgenic FVBn mice over time following intrabursal injection of adenoviral Cre or mock injection.

	Time (Days)			
Treatment	**60**	**120**	**180**	**240**
AdCre	2.05±0.35[a]	5.20±1.51[a]	6.95±0.86[a]	10.40±0.70[b]
mock	1.75±0.54[a]	7.00±1.81[a]	5.60±1.40[a]	10.05±0.50[b]

Numbers represent the mean ±SEM of the mean number of morphological changes per section over five non-consecutive sections in n=4 ovaries. Letters are used to denote a significant difference between time points for that treatment group.

Figure 11: Ki67 expression following inactivation of *Brca1* in the OSE *in vivo*. A) Section of an ovary stained for the presence of Ki67. There are very few positive cells in the OSE (arrow, 100X), whereas the growing follicles contain many granulosa cells positive for Ki67. **B)** There is no difference in the number of Ki67 positive cells in the OSE in which *Brca1* has been inactivated versus wildtype at the 240 day time point. Numbers represent the mean number of Ki67-positive cells in the OSE per section, where five non-consecutive sections/ovary were analyzed for 10 ovaries in each group. Error bars represent SEM.

A

B

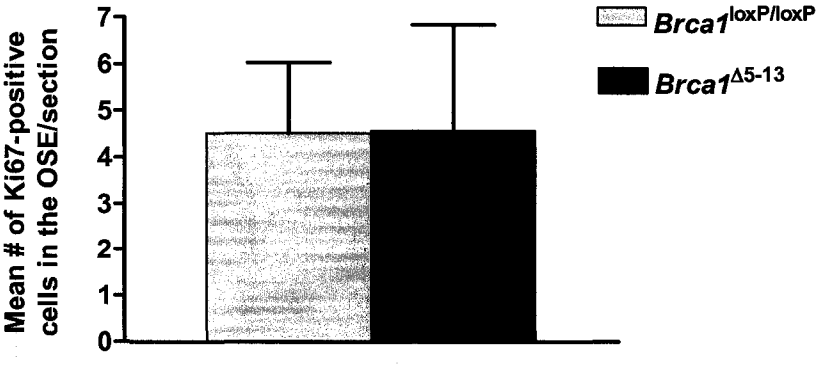
Mean # of Ki67-positive cells in the OSE/section
0
1
2
3
4
5
6
7
Brca1loxP/loxP
Brca1Δ5-13

Bandiera and Auersperg, 1997; Capo-chichi, et. al., 2002). p53 expression was not detected in the OSE of any of the ovaries examined in our study, nor was it found in the epithelial invaginations or inclusion cysts, although it was expressed strongly in mouse SV40 TAg-induced ovarian tumours (**Figure 12G-I**). E-cadherin expression was detected uniformly in the OSE of all the mouse ovaries we examined, with no observable difference in expression levels in normal versus morphologically altered OSE (**Figure 12A-C**). Consistent Collagen IV expression was observed in the basement membrane beneath the OSE in all of the mouse ovaries irrespective of morphological changes in the OSE (**Figure 12D-F**).

3.6 Inactivation of *Brca1* in MOSE cells *in vitro* results in a suppression of proliferation with increased apoptosis

Proliferation assays were performed on the adherent cells of primary cultures of $Brca1^{loxP/loxP}$ MOSE cells infected with either AdCre ($Brca1^{\Delta 5\text{-}13}$) or AdGFP ($Brca1^{loxP/loxP}$). The doubling time of these cells is quite long (approximately 48 hours, before adenoviral infection) and there were no differences in the proliferation rates of the $Brca1^{\Delta 5\text{-}13}$ or $Brca1^{loxP/loxP}$ cells at 24, 48, or 72-hours after plating, however by 96 hours the $Brca1^{loxP/loxP}$ cells outgrew the $Brca1^{\Delta 5\text{-}13}$ cells (**Figure 13A**). A later set of experiments in which the proliferation curve was extended to 120 hours demonstrated that this inhibition of proliferation in the $Brca1^{\Delta 5\text{-}13}$ cells was also significant at this later time point, with a decrease in cell number of 40% as compared to $Brca1^{loxP/loxP}$ cells (**Figure 13B**). Flow cytometric analysis of both adherent and floating cells demonstrated

Figure 12: Immunohistochemical analysis of expression of proteins known to be involved in ovarian tumourigenesis. Expression of E-cadherin (A-C; brown stain), Collagen IV (D-F; reddish-brown stain), and p53 (G-I; nuclear stain) in the OSE of control (AdGFP-injected) $Brca1^{loxP/loxP}$ mice (B, E, H) and OSE of (AdCre-injected) $Brca1^{\Delta 5-13}$ mice (C, F, I). Mouse uterine epithelium (A), mouse liver (D), and a mouse ovarian tumour (G) were used as positive controls. Scale bars are equal to 25μm (A, D, G) or 50μm (B, C, E, F, H, I).

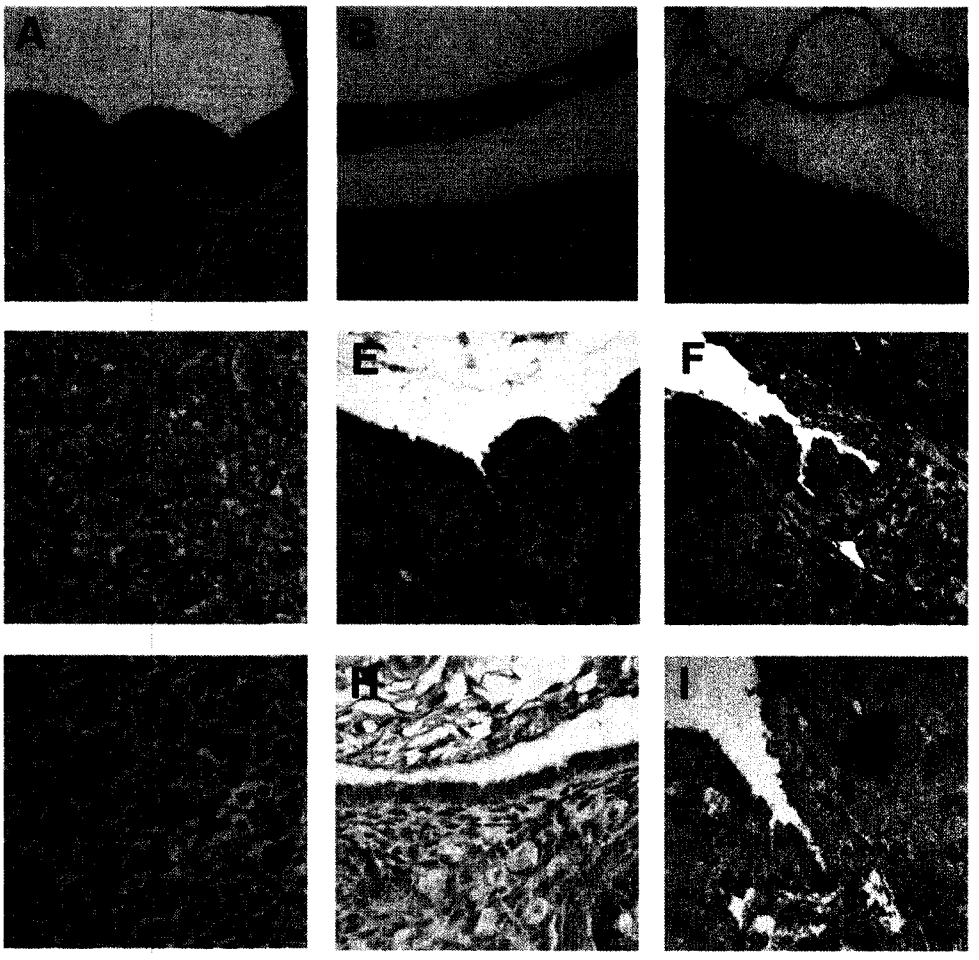
A
E
F
H
I

Figure 13: Proliferation of MOSE cells following inactivation of *Brca1 in vitro* A) Proliferation of *Brca1*$^{loxP/loxP}$ MOSE following infection with AdCre (*Brca1*$^{\Delta 5\text{-}13}$) to inactivate Brca1 or with AdGFP (*Brca1*$^{loxP/loxP}$) followed up to 96 hours after replating **B)** A subsequent experiment examining the proliferation of Brca1$^{loxP/loxP}$ MOSE following infection with AdCre (*Brca1*$^{\Delta 5\text{-}13}$) to inactivate Brca1 or with AdGFP (*Brca1*$^{loxP/loxP}$) followed up to 120 hours after replating. * Indicates a significant difference between groups at that time point where $P<0.05$, and ** indicates a significant difference where $P<0.01$. Error bars indicate the SEM. All proliferation experiments were performed three times in triplicate.

A

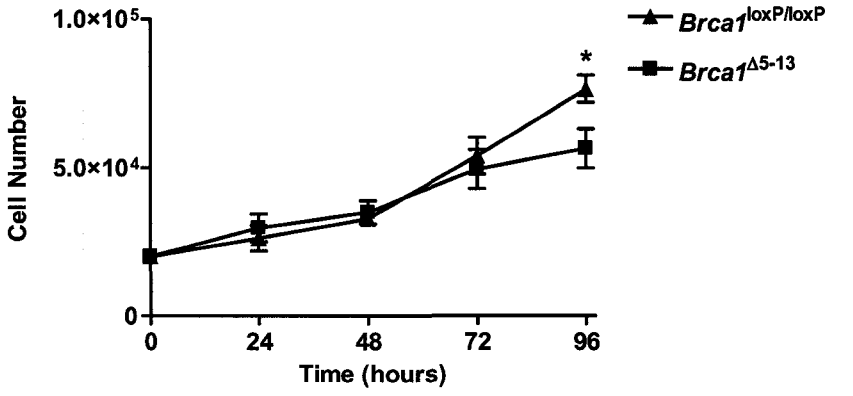
1.0×10^5
5.0×10^4
0
Cell Number
0
24
48
72
96
Time (hours)
*
Brca1loxP/loxP
Brca1Δ5-13

B

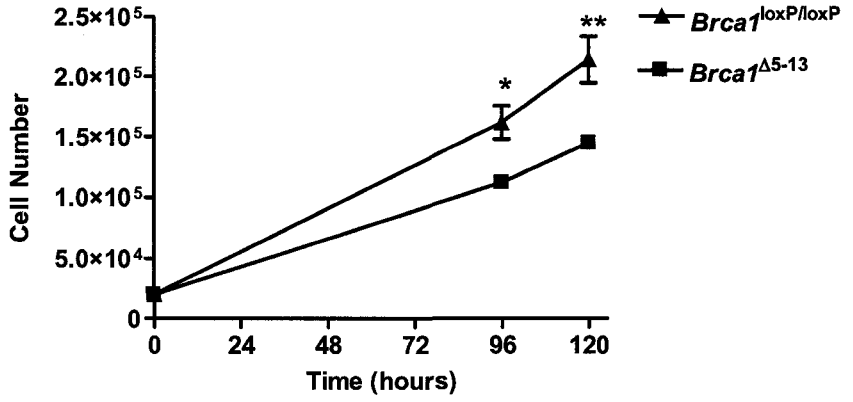
2.5×10^5
2.0×10^5
1.5×10^5
1.0×10^5
5.0×10^4
0
Cell Number
0
24
48
72
96
120
Time (hours)
*
**
Brca1loxP/loxP
Brca1Δ5-13

a sub-G1 fraction in the *Brca1*$^{\Delta 5\text{-}13}$ cells that was nearly double that of the *Brca1*$^{loxP/loxP}$ cells after 96 hours (31.00%±5.63% versus 17.44%± 3.87%, P<0.05, **Figure 14**).

In order to ensure that changes in proliferation were not due to nonspecific effects of Cre recombinase infection, primary cultures of MOSE cells collected from non-transgenic FVBn mice were infected *in vitro* with either AdCre or AdGFP in the same manner as the transgenic MOSE cultures. The cells were replated 72 hours after infection and the cells were counted 96 hours later. There was no significant difference seen in the number of cells in either group at the 96 hour time point (**Figure 15**).

3.7 *Brca1*$^{\Delta 5\text{-}13}$ OSE cells have an increased sensitivity to cisplatin.

Brca1$^{loxP/loxP}$ OSE cells were treated with 0, 1, 5, 10, 20, 50, or 100 μM of cisplatin for 48 hours in order to determine the optimal dosage at which to treat the cells in subsequent experiments (**Figure 16**). Based on these results, *Brca1*$^{loxP/loxP}$ and *Brca1*$^{\Delta 5\text{-}13}$ OSE cells were treated with either 1μM or 5μM cisplatin for 24 or 48 hours. At the 24-hour time point at either concentration, there was no difference between the cell types in cisplatin sensitivity, as measured by the number of adherent cells in treated groups compared to cells not exposed to cisplatin (**Figure 17A**). By 48-hours, however, the number of adherent *Brca1*$^{\Delta 5\text{-}13}$ cells remaining following treatment with 5μM of cisplatin was significantly reduced compared to *Brca1*$^{loxP/loxP}$ cells (47.35±3.04% versus 66.18±6.10%, P<0.05, results expressed as a percentage of untreated cells, **Figure 17B**). Both the *Brca1*$^{loxP/loxP}$ cells and the *Brca1*$^{\Delta 5\text{-}13}$ cells displayed a significant increase in the sub-G1 fraction following treatment with cisplatin, as assessed by flow cytometry, however there was a larger fraction seen in the *Brca1*$^{\Delta 5\text{-}13}$ cells (**Figure 18**).

Figure 14: Apoptosis in MOSE cells following inactivation of *Brca1 in vitro*. Percentage of cells in the sub-G1 fraction as measured by flow cytometry at the 96 hour time point following infection with AdCre ($Brca1^{\Delta 5\text{-}13}$) or AdGFP ($Brca1^{loxP/loxP}$). * Indicates a significant difference between groups where $P<0.05$. Error bars indicated the SEM. Results represent three independent experiments.

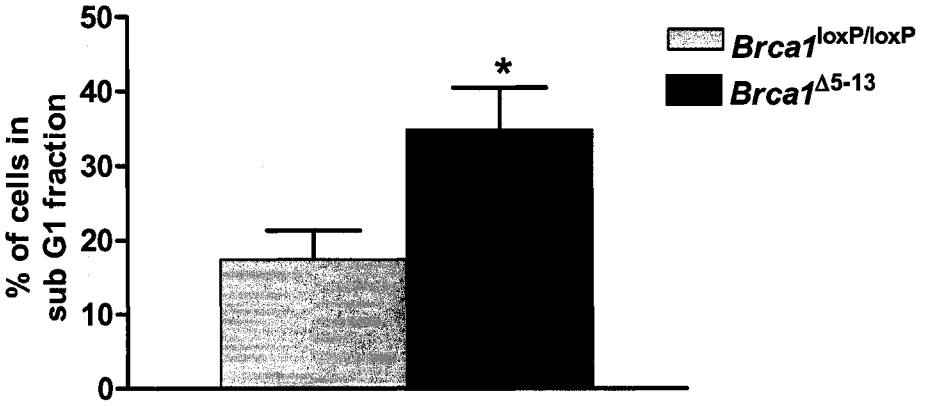
50
40
30
20
10
0
% of cells in sub G1 fraction
*
Brca1loxP/loxP
Brca1Δ5-13

Figure 15: Proliferation of non-transgenic MOSE cells treated with AdCre. Proliferation of FVBn MOSE cells following infection with AdCre or a mock infection, 96 hours after replating. Error bars indicate the SEM. No significant differences were observed. All proliferation experiments were performed three times in triplicate.

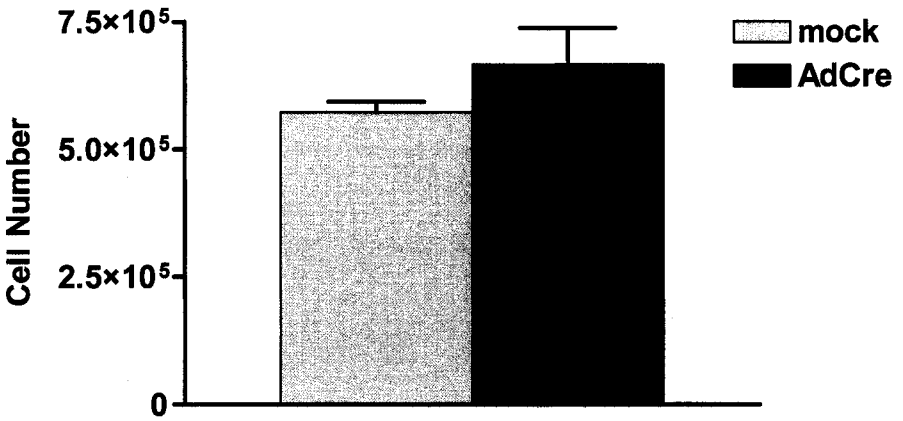
7.5×10^5
5.0×10^5
2.5×10^5
0
Cell Number
mock
AdCre

Figure 16: Dose-response curve of MOSE cells treated with cisplatin. MOSE cells were plated at a density of 1.75 X 10^5 cells per well in 6-well plates and were treated with various doses of cisplatin for 48 hours in order to determine the optimal dose at which to carry out subsequent cisplatin-treatment experiments. Error bars represent the SEM.

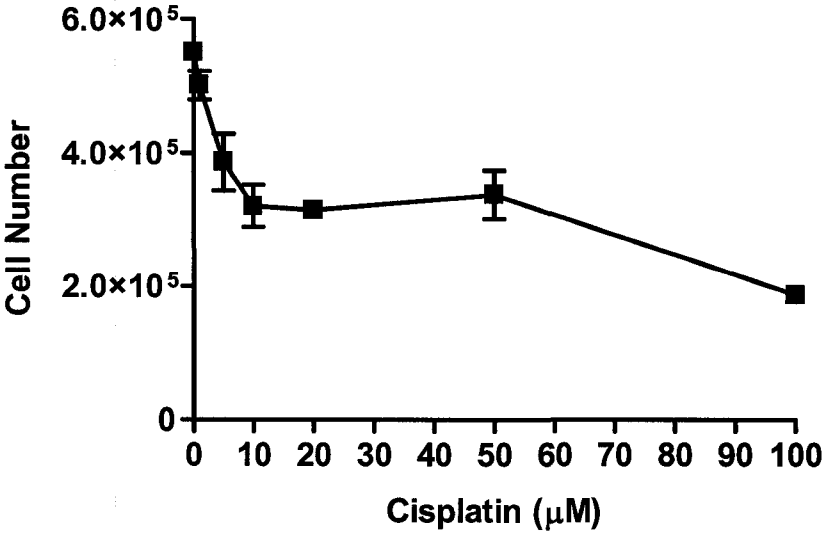
6.0×10⁵
4.0×10⁵
2.0×10⁵
0
Cell Number
0 10 20 30 40 50 60 70 80 90 100
Cisplatin (μM)

Figure 17: ***Brca1*$^{\Delta 5\text{-}13}$ MOSE cells treated with the DNA-damaging agent cisplatin *in vitro*** **A)** *Brca1*$^{loxP/loxP}$ MOSE cells infected with either AdCre (*Brca1*$^{\Delta 5\text{-}13}$) or AdGFP (*Brca1*$^{loxP/loxP}$) and treated with 1 or 5μM of cisplatin for 24 hours **B)** *Brca1*$^{loxP/loxP}$ MOSE cells infected with either AdCre (*Brca1*$^{\Delta 5\text{-}13}$) or AdGFP (*Brca1*$^{loxP/loxP}$) and treated with 5μM cisplatin for 48 hours. Values are the number adherent cells presented as a proportion of similar cells exposed to the vehicle control (untreated cells). * indicates a significant difference where $P<0.05$. Error bars represent the SEM. Experiments were performed three times in triplicate.

A

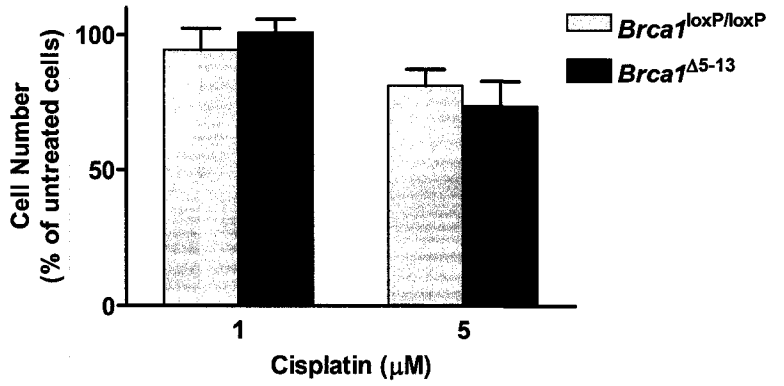
Brca1loxP/loxP
Brca1Δ5-13
Cell Number
(% of untreated cells)
100
50
0
1
5
Cisplatin (μM)

B

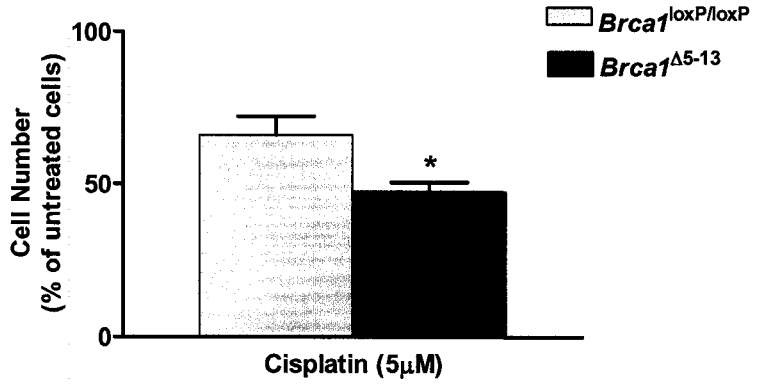
Brca1loxP/loxP
Brca1Δ5-13
Cell Number
(% of untreated cells)
100
50
0
*
Cisplatin (5μM)

Figure 18: Brca1$^{\Delta 5\text{-}13}$ MOSE cells display an increased level of apoptosis in response to treatment with cisplatin as measured by flow cytometry. Percentage of cells in the sub-G1 fraction following 48 hours of treatment with 5μM of cisplatin or vehicle control. * indicates a significant difference where $P<0.05$ and ** indicates a significant difference where $P<0.01$. Error bars represent the SEM. Results are from three independent experiments.

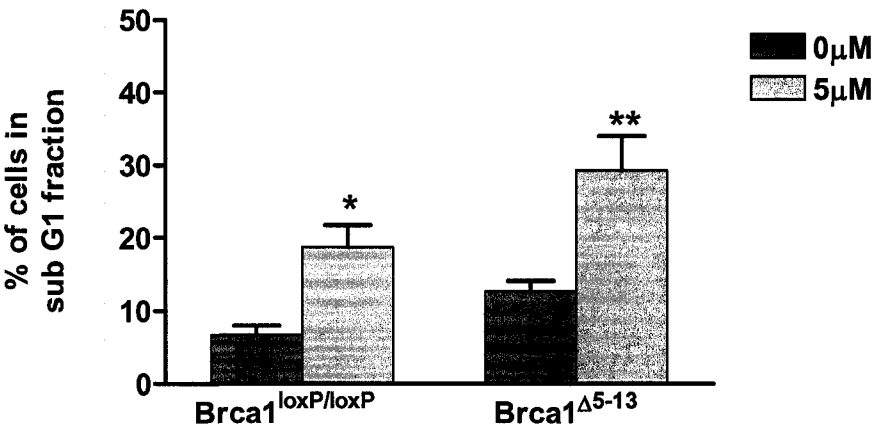
50
40
30
20
10
0
% of cells in sub G1 fraction
0μM
5μM
*
**
Brca1loxP/loxP
Brca1Δ5-13

Further cell cycle analysis revealed a trend towards a greater proportion of *Brca1*$^{\Delta 5\text{-}13}$ cells in the G2/M phase of the cell cycle than Brca1$^{loxP/loxP}$ cells following 48 hours of cisplatin treatment; however these results did not reach significance (26.89%±5.58% vs. 12.19%±2.91%, P=0.08) (**Figure 19**). As assessed by western blotting, *Brca1*$^{\Delta 5\text{-}13}$ cells displayed a greater increase in p53 protein expression after both 24 and 48 hours of treatment with 5μM cisplatin than was observed in the *Brca1*$^{loxP/loxP}$ cells (**Figure 20**).

3.8 *Brca1*$^{\Delta 5\text{-}13}$ OSE cells demonstrate a decreased sensitivity to paclitaxel.

Primary cultures of *Brca1*$^{loxP/loxP}$ MOSE cells were treated with doses of 0, 25, 50, 75, 100, and 250nM of paclitaxel for 96 hours in order to determine the ideal dose at which to treat the cells in subsequent experiments (**Figure 21**). Based on these results, *Brca1*$^{loxP/loxP}$ and *Brca1*$^{\Delta 5\text{-}13}$ MOSE cells were treated with 25nM of paclitaxel or an equal volume of vehicle control (DMSO) for 96 hours. At this time point, the *Brca1*$^{\Delta 5\text{-}13}$ cells were found to be significantly less sensitive to treatment with paclitaxel than the *Brca1*$^{loxP/loxP}$ cells (60.61% ± 1.89% versus 54.90% ± 2.35%, P<0.05, numbers expressed as a percentage of the adherent vehicle control-treated cells, **Figure 22A**). Because this difference, while significant, was relatively modest, we also treated the cells for 72 hours with 25 nM paclitaxel and for 96 hours with 12.5 nM of drug. When treated with 12.5 nM paclitaxel for 96 hours the *Brca1*$^{\Delta 5\text{-}13}$ cells were also slightly less sensitive to the treatment than the *Brca1*$^{loxP/loxP}$ cells, however the results were not significant (52.83% ± 2.41% versus 48.23% ± 2.00%, P=0.13, **Figure 22B**). The same effect was seen when the cells were treated with 25 nM paclitaxel for 72 hours, with the *Brca1*$^{\Delta 5\text{-}13}$ cells being

Figure 19: Cell cycle distribution following cisplatin treatment. A) Percentage of *Brca1*$^{loxP/loxP}$ and *Brca1*$^{\Delta 5\text{-}13}$ cells in the G1, S, and G2/M phases of the cell cycle as determined by flow cytometry. Cells were analysed after 48 hours of treatment with 5μM of cisplatin. Error bars represent the SEM. No significant differences were observed between the two groups. Results are compiled from three independent experiments. No significant differences were observed. **B)** A representative flow cytometry profile of *Brca1*$^{loxP/loxP}$ cells at the 48 hour time point with no cisplatin treatment. **C)** A representative flow cytometry profile of *Brca1*$^{\Delta 5\text{-}13}$ cells at the 48 hour time point with no cisplatin treatment. **D)** A representative flow cytometry profile of *Brca1*$^{loxP/loxP}$ cells following 48 hours of treatment with 5μM of cisplatin. **E)** A representative flow cytometry profile of *Brca1*$^{\Delta 5\text{-}13}$ cells following 48 hours of treatment with 5μM of cisplatin.

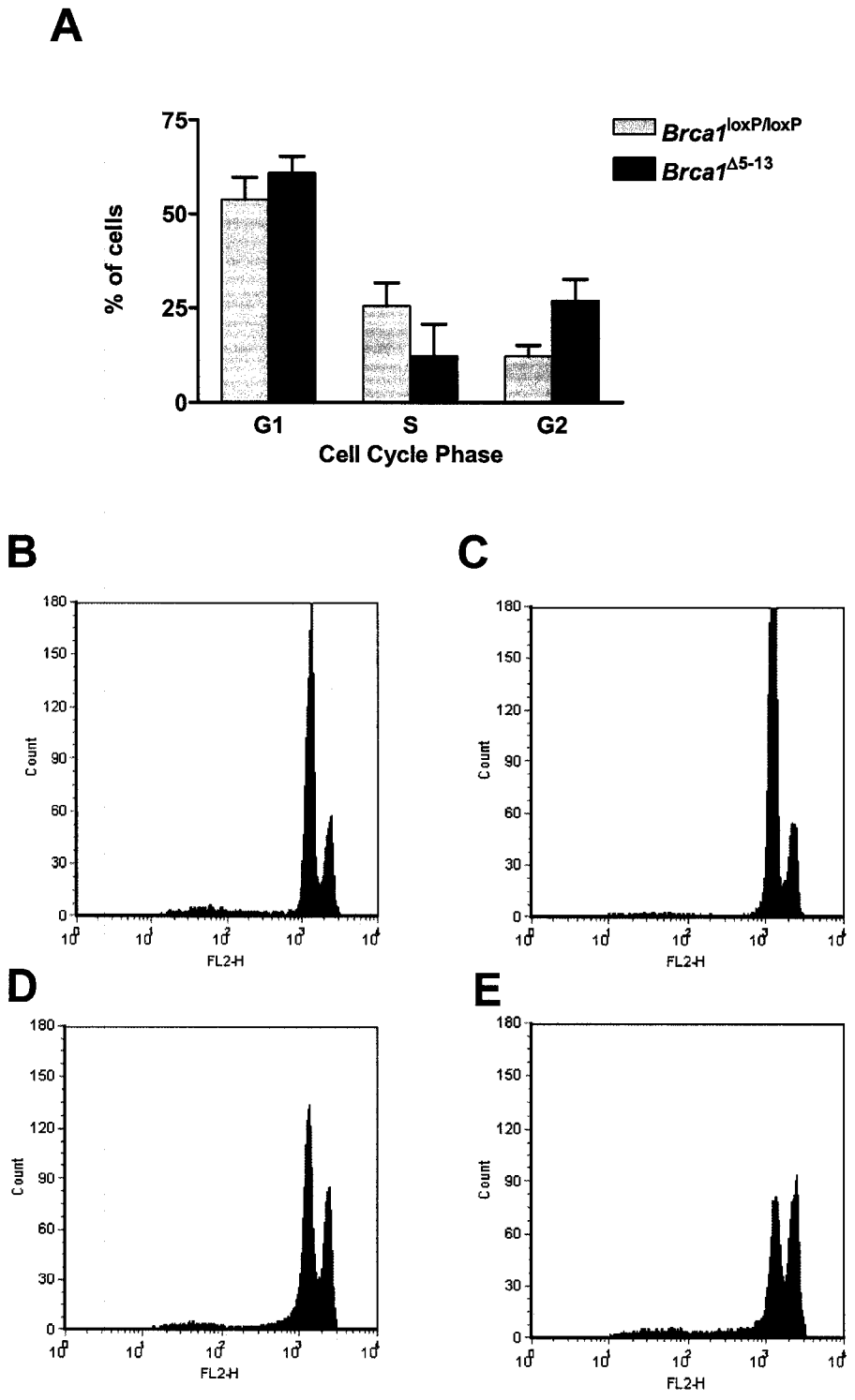
A
75
50
25
0
% of cells
G1
S
G2
Cell Cycle Phase
Brca1loxP/loxP
Brca1Δ5-13
B
C
D
E
Count
FL2-H
180
150
120
90
60
30
0

Figure 20: p53 protein expression in *Brca1*$^{\Delta 5\text{-}13}$ cells following treatment with cisplatin. Protein was collected from Brca1$^{\Delta 5\text{-}13}$ and Brca1$^{loxP/loxP}$ cells after 0, 24, and 48 hours of treatment with 5μM cisplatin and subjected to Western blotting with an anti-p53 antibody. GAPDH expression was used as a loading control.

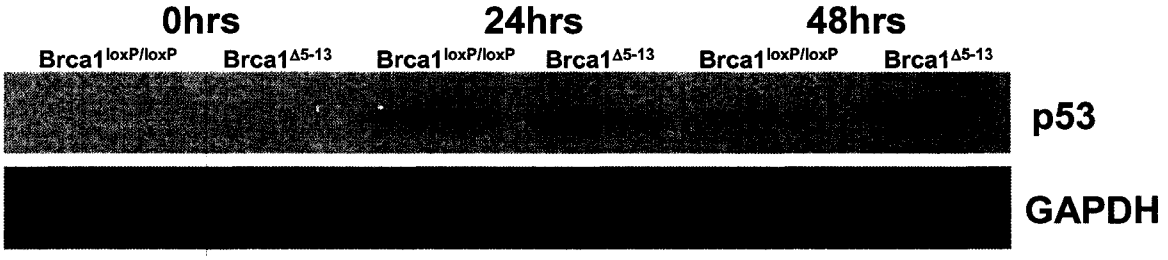
0hrs
24hrs
48hrs
Brca1loxP/loxP
Brca1Δ5-13
Brca1loxP/loxP
Brca1Δ5-13
Brca1loxP/loxP
Brca1Δ5-13
p53
GAPDH

Figure 21: Dose-response curve of MOSE cells treated with paclitaxel. MOSE cells were plated at a density of 2.0 X 10^4 cells per well in 6-well tissue culture plates and were treated with various doses of paclitaxel for 96 hours in order to determine the optimal dose at which to carry out subsequent paclitaxel-treatment experiments. The cell number is the number of adherent cells remaining following treatment. Error bars represent the SEM.

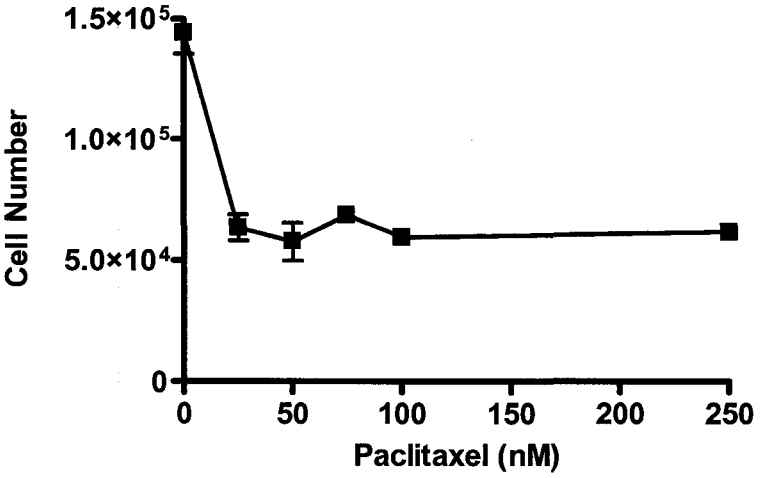
1.5×10^5
1.0×10^5
5.0×10^4
0
Cell Number
0
50
100
150
200
250
Paclitaxel (nM)

Figure 22: ***Brca1*** **MOSE treated with paclitaxel.** *Brca1*$^{loxP/loxP}$ MOSE cells infected with either AdCre (*Brca1*$^{\Delta 5\text{-}13}$) or AdGFP (*Brca1*$^{loxP/loxP}$) and treated with 25nM of paclitaxel for 96 hours. Values are the number adherent cells presented as a proportion of similar cells exposed to the vehicle control (untreated cells). * indicates a significant difference where $P<0.05$. Error bars represent the SEM. Experiments were performed three times in triplicate.

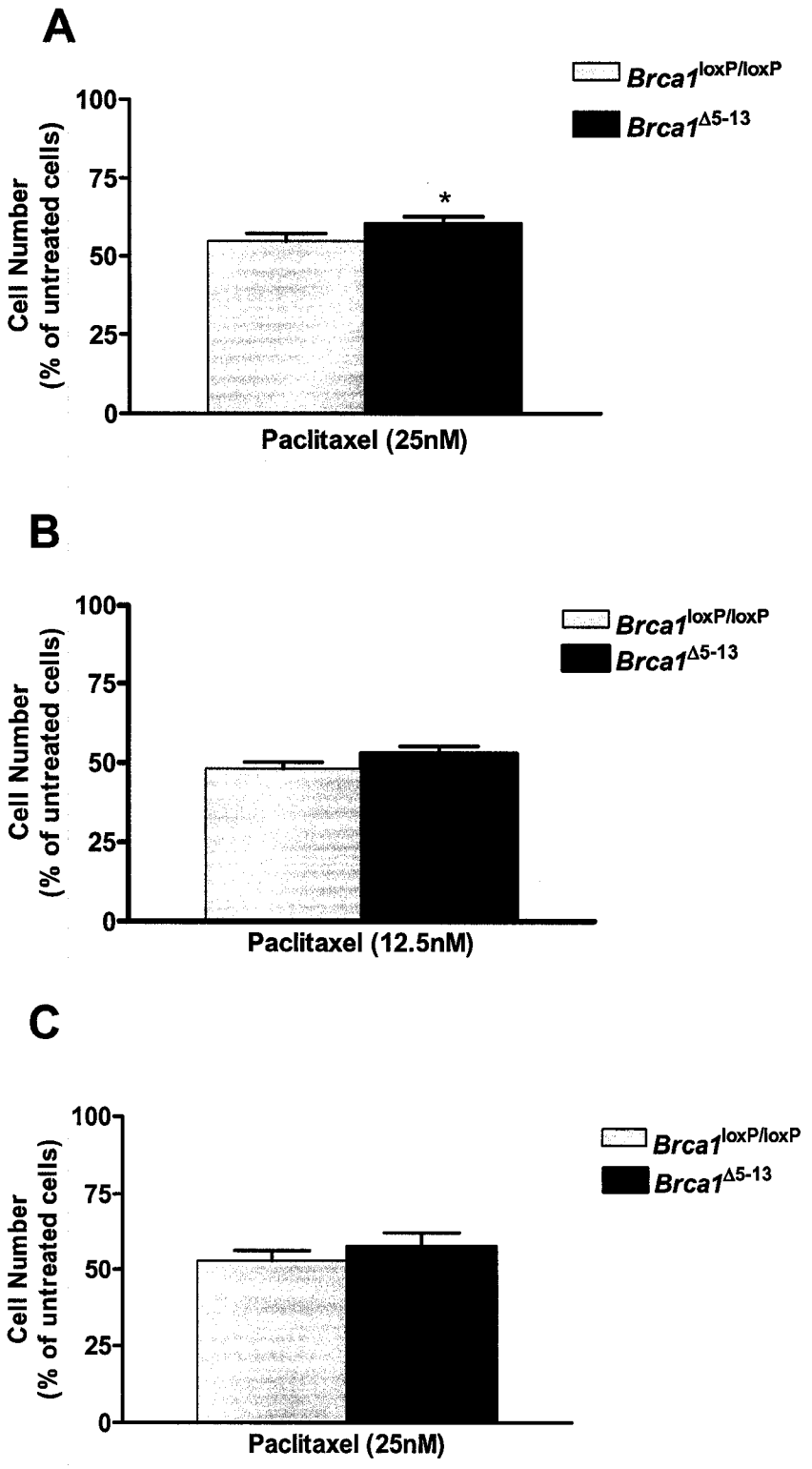
A
Brca1loxP/loxP
Brca1Δ5-13
100
75
50
25
0
Cell Number
(% of untreated cells)
*
Paclitaxel (25nM)
B
Brca1loxP/loxP
Brca1Δ5-13
100
75
50
25
0
Cell Number
(% of untreated cells)
Paclitaxel (12.5nM)
C
Brca1loxP/loxP
Brca1Δ5-13
100
75
50
25
0
Cell Number
(% of untreated cells)
Paclitaxel (25nM)

slightly, but not significantly, less sensitive to treatment than the *Brca1*$^{loxP/loxP}$ cells (57.98% ± 4.51% versus 52.92% ± 5.53%, P=0.13, **Figure 22C**).

3.9 Several passages following AdCre exposure, *Brca1*$^{\Delta 5\text{-}13}$ cells are overtaken in culture by any remaining wildtype *Brca1*$^{loxP/loxP}$ cells.

Following adenoviral infection, *Brca1*$^{\Delta 5\text{-}13}$ cells and their AdGFP-infected counterparts were cultured for several passages and then their proliferation was compared again. It was found that there was no longer any difference in the proliferation rate between the *Brca1*$^{\Delta 5\text{-}13}$ cells and the *Brca1*$^{loxP/loxP}$ cells at any of the time points examined (**Figure 23B**). When the recombination status of the *Brca1*$^{\Delta 5\text{-}13}$ cells was analyzed at this stage, it was found that while recombination at the loxP sites could still be detected; non-recombined DNA was now also predominant in these cells (**Figure 23A**). When these cells were treated with 5μM of cisplatin for 48 hours, the *Brca1*$^{\Delta 5\text{-}13}$ cells no longer displayed the increased sensitivity to this treatment (**Figure 23C**).

Figure 23: Proliferation and cisplatin sensitivity of *Brca1* MOSE cells several passages following inactivation of *Brca1*. **A)** PCR of genomic DNA collected from cultured *Brca1*$^{loxP/loxP}$ OSE cells 1 or 6 passages following *in vitro* infection with AdCre (*Brca1*$^{\Delta 5\text{-}13}$) or AdGFP (*Brca1*$^{loxP/loxP}$) **B)** Proliferation of *Brca1*$^{loxP/loxP}$ MOSE 6 passages following infection with AdCre (*Brca1*$^{\Delta 5\text{-}13}$) to inactivate Brca1 or with AdGFP (*Brca1*$^{loxP/loxP}$). **C)** *Brca1*$^{loxP/loxP}$ MOSE cells 6 passages following infection with either AdCre (*Brca1*$^{\Delta 5\text{-}13}$) or AdGFP (*Brca1*$^{loxP/loxP}$) and treated with 5μM cisplatin for 48 hours. Values are the number adherent cells presented as a proportion of similar cells exposed to the vehicle control (untreated cells). No significant differences were observed. Experiments were performed three times in triplicate. Error bars represent the SEM.

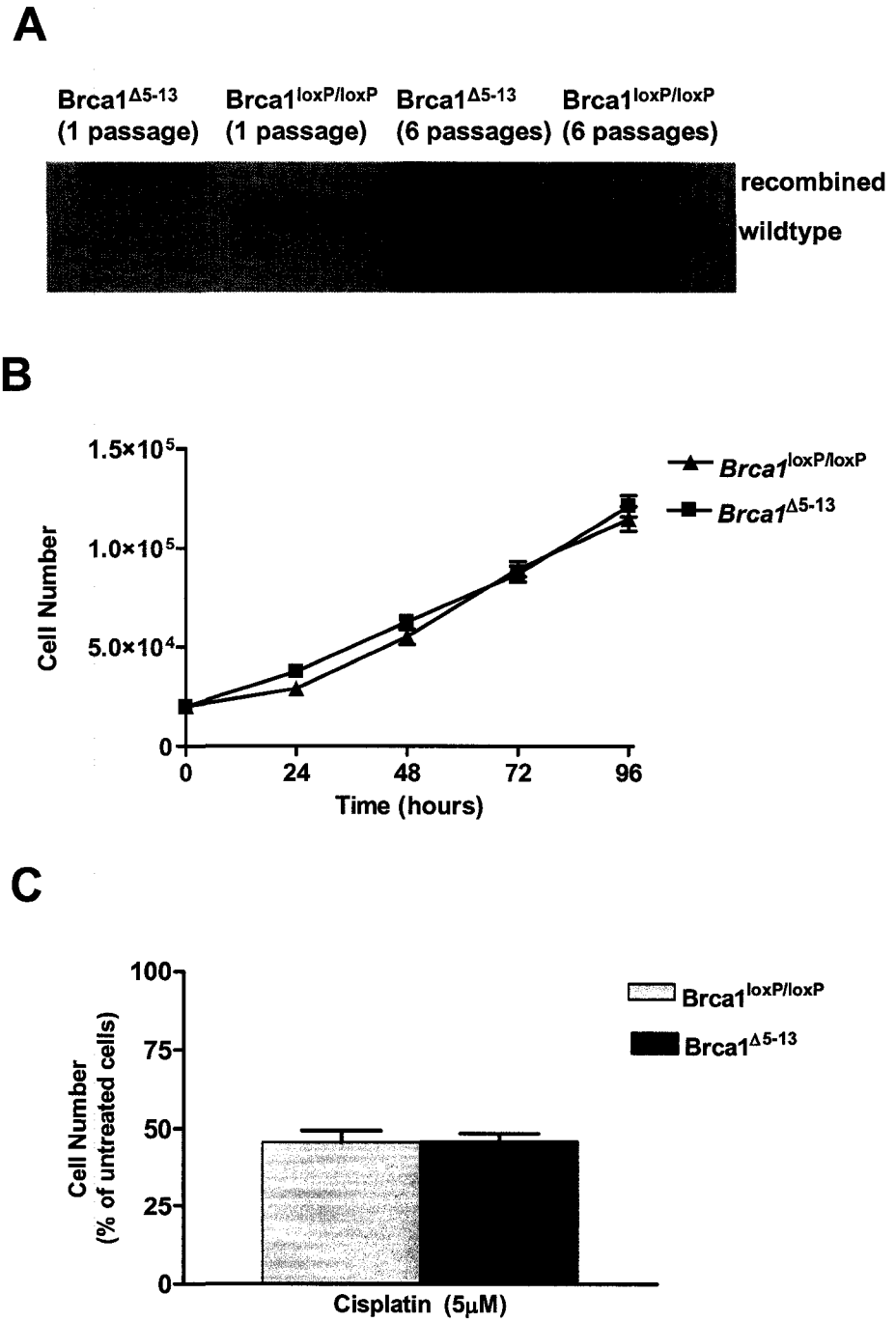
A
Brca1Δ5-13 (1 passage)
Brca1loxP/loxP (1 passage)
Brca1Δ5-13 (6 passages)
Brca1loxP/loxP (6 passages)
recombined
wildtype
B
1.5×10^5
1.0×10^5
5.0×10^4
0
Cell Number
0
24
48
72
96
Time (hours)
Brca1loxP/loxP
Brca1Δ5-13
C
100
75
50
25
0
Cell Number (% of untreated cells)
Cisplatin (5μM)
Brca1loxP/loxP
Brca1Δ5-13

Chapter 4 – Results:

Conditional inactivation of *Brca1* in conjunction with the tumour suppressors *p53* and/or *Rb* in the mouse OSE both *in vitro* and *in vivo*

4.1 Effect of *p53* or *Rb* inactivation on MOSE cell proliferation immediately following inactivation.

Cultures of $Brca1^{loxP/loxP}$, $p53^{loxP/loxP}$, and $Rb^{loxP/loxP}$ MOSE cells were infected with AdCre or AdGFP to inactivate each of these genes individually and the effect on proliferation was assessed 72 hours following infection. As was demonstrated in Chapter 3, section 3.6, inactivation of *Brca1* in MOSE cells negatively impacted their proliferation after 96 hours (**Figure 13A**). Inactivation of *p53* in $p53^{loxP/loxP}$ MOSE cells however, had no effect on proliferation at any of the time points examined (**Figure 24A**). Likewise, conditional inactivation of *Rb* in $Rb^{loxP/loxP}$ MOSE cells had no effect on proliferation at any of the time points examined (**Figure 24B**).

4.2 Effect of concomitant inactivation of multiple tumour suppressor genes on proliferation of MOSE cells *in vitro* immediately following inactivation.

4.2.1 *Brca1/p53*

When both *Brca1* and *p53* were inactivated in $Brca1^{loxP/loxP}/p53^{loxP/loxP}$ MOSE cells the proliferation rate of these cells was dramatically increased, with approximately 1.5-fold more cells counted at both the 72 hour and 96 hour time points ($P<0.01$ and $P<0.001$, respectively; **Figure 25A**). The $Brca1^{\Delta 5\text{-}13}/Trp53^{\Delta 2\text{-}10}$ cells showed a 2-fold

Figure 24: Proliferation of MOSE cells immediately following inactivation of either *p53* or *Rb in vitro*. **A)** Proliferation of $p53^{loxP/loxP}$ MOSE immediately following infection with AdCre ($Trp53^{\Delta 2\text{-}10}$) to inactivate *p53* or with AdGFP ($p53^{loxP/loxP}$). **B)** Proliferation of $Rb^{loxP/loxP}$ MOSE cells immediately following infection with AdCre ($Rb^{\Delta 19)}$ to inactivate *Rb* or with AdGFP ($Rb^{loxP/loxP}$). Error bars represent the SEM. Experiments were performed three times in triplicate.

A

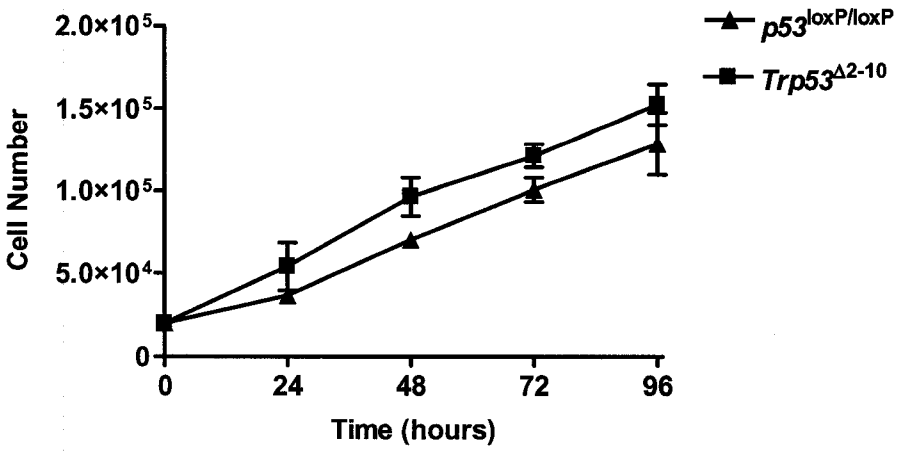
2.0×10^5
1.5×10^5
1.0×10^5
5.0×10^4
0
Cell Number
0
24
48
72
96
Time (hours)
p53^loxP/loxP
Trp53^Δ2-10

B

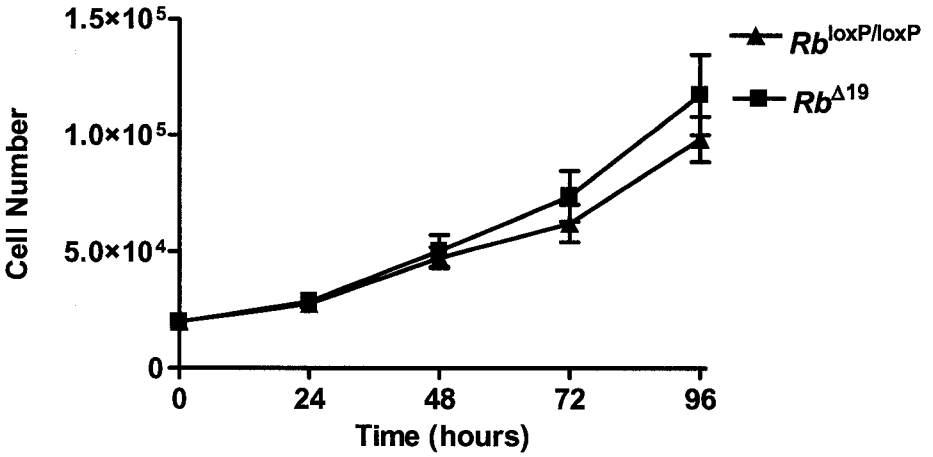
1.5×10^5
1.0×10^5
5.0×10^4
0
Cell Number
0
24
48
72
96
Time (hours)
Rb^loxP/loxP
Rb^Δ19

Figure 25: MOSE cell proliferation following inactivation of multiple tumour suppressors. A) Proliferation of *Brca1*$^{loxP/loxP}$/*p53*$^{loxP/loxP}$ MOSE immediately following infection with AdCre (*Brca1*$^{\Delta 5\text{-}13}$/*Trp53*$^{\Delta 2\text{-}10}$) to inactivate *Brca1* and *p53* or with AdGFP (*Brca1*$^{loxP/loxP}$/*p53*$^{loxP/loxP}$). **B)** Proliferation of *Rb*$^{loxP/loxP}$/*Brca1*$^{loxP/loxP}$ MOSE cells immediately following infection with AdCre (Rb$^{\Delta 19}$/*Brca1*$^{\Delta 5\text{-}13}$) to inactivate *Rb* and *Brca1* or with AdGFP (*Rb*$^{loxP/loxP}$/*Brca1*$^{loxP/loxP}$). **C)** Proliferation of *Rb*$^{loxP/loxP}$/*p53*$^{loxP/loxP}$ MOSE immediately following infection with AdCre (*Rb*$^{\Delta 19}$/*Trp53*$^{\Delta 2\text{-}10}$) to inactivate *Rb* and *p53* or AdGFP (*Rb*$^{loxP/loxP}$/*p53*$^{loxP/loxP}$). **D)** Proliferation of *Rb*$^{loxP/loxP}$/*p53*$^{loxP/loxP}$/*Brca1*$^{loxP/loxP}$ MOSE immediately following infection with AdCre (*Rb*$^{\Delta 19}$/*p53*$^{\Delta 2\text{-}10}$/*Brca1*$^{\Delta 5\text{-}13}$) or AdGFP (*Rb*$^{loxP/loxP}$/*p53*$^{loxP/loxP}$/*Brca1*$^{loxP/loxP}$). ** indicates a significant difference where $P<0.01$ and *** indicates a difference where $P<0.001$. Error bars represent the SEM of data obtained from three experiments performed in triplicate.

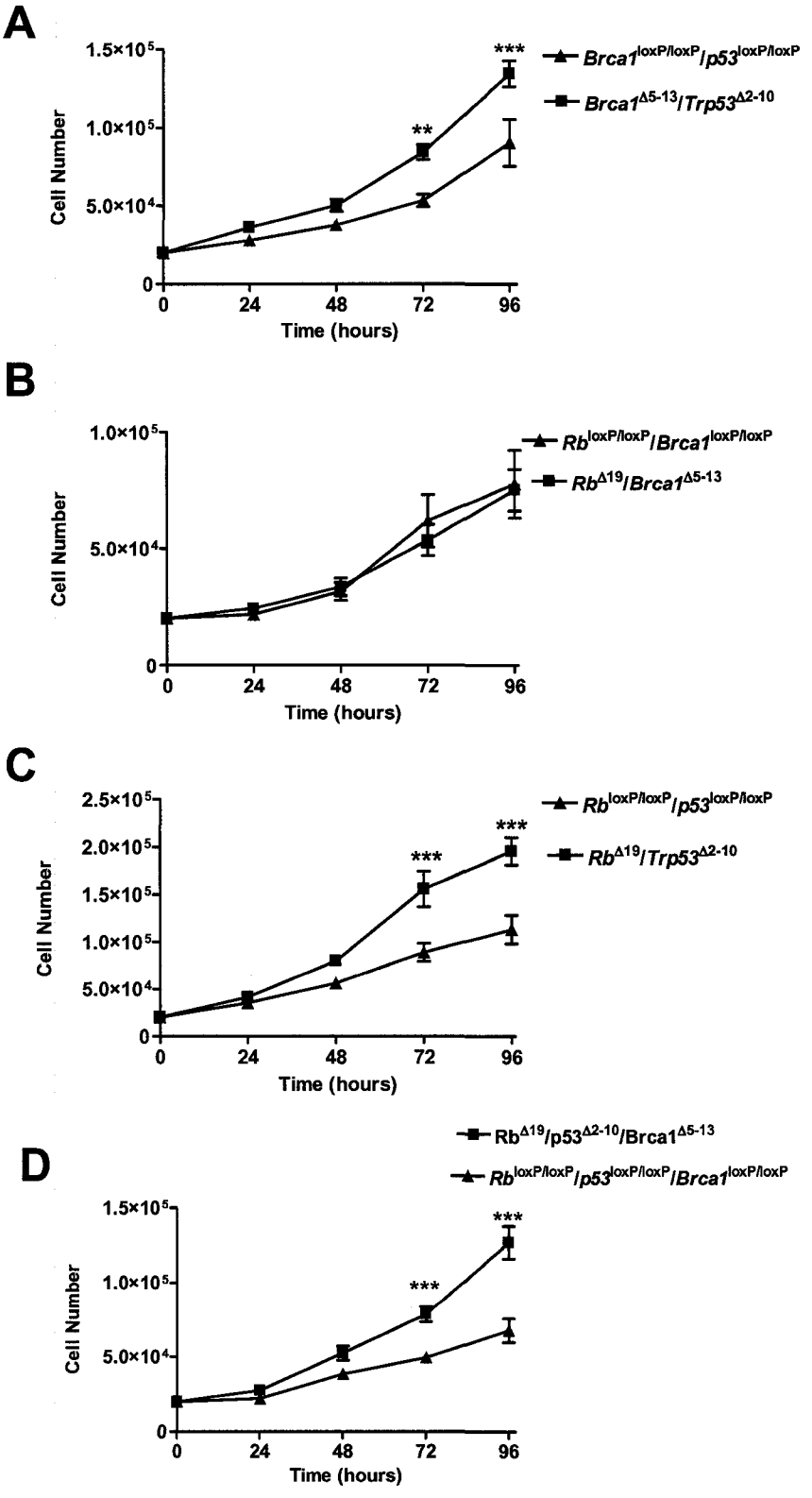
A
1.5×10^5
1.0×10^5
5.0×10^4
0
Cell Number
0
24
48
72
96
Time (hours)
**
***
Brca1loxP/loxP/p53loxP/loxP
Brca1Δ5-13/Trp53Δ2-10
B
1.0×10^5
5.0×10^4
0
Cell Number
0
24
48
72
96
Time (hours)
RbloxP/loxP/Brca1loxP/loxP
RbΔ19/Brca1Δ5-13
C
2.5×10^5
2.0×10^5
1.5×10^5
1.0×10^5
5.0×10^4
0
Cell Number
0
24
48
72
96
Time (hours)
***
***
RbloxP/loxP/p53loxP/loxP
RbΔ19/Trp53Δ2-10
D
1.5×10^5
1.0×10^5
5.0×10^4
0
Cell Number
0
24
48
72
96
Time (hours)
***
***
RbΔ19/p53Δ2-10/Brca1Δ5-13
RbloxP/loxP/p53loxP/loxP/Brca1loxP/loxP

greater increase in cell number between 48 and 72 hours and a 1.3-fold greater increase between 72 and 96 hours than that seen in the *Brca1*$^{loxP/loxP}$/*p53*$^{loxP/loxP}$ cells.

4.2.2 *Rb/Brca1*

When both *Brca1* and *Rb* were inactivated in *Rb*$^{loxP/loxP}$/*Brca1*$^{loxP/loxP}$ MOSE cells the proliferation defect seen when *Brca1* was inactivated alone was eliminated, however there was no significant increase in the proliferation rate of the *Rb/Brca1*-deficient cells at any of the time points examined (**Figure 25B**).

4.2.3 *Rb/p53*

When *p53* was inactivated in conjunction with *Rb* in *Rb*$^{loxP/loxP}$/*p53*$^{loxP/loxP}$ MOSE cells, the resulting *Rb/p53*-deficient cells showed a dramatic increase in proliferation as compared to their control-infected counterparts, with significantly more cells counted at both the 72 and 96 hour time points ($P<0.001$ for both time points; **Figure 25C**). There was a greater than 2-fold increase in the number of *Rb*$^{\Delta 19}$/*Trp53*$^{\Delta 2\text{-}10}$ cells between 48 and 72 hours than that of the *Rb*$^{loxP/loxP}$/*p53*$^{loxP/loxP}$ cells, and this was also observed between 72 and 96 hours, though the difference in increase in cell number was just above 1.5-fold.

4.2.4 *Rb/p53/Brca1*

When all three tumour suppressor genes were conditionally inactivated in the *Rb*$^{loxP/loxP}$/*p53*$^{loxP/loxP}$/*Brca1*$^{loxP/loxP}$ MOSE cells there was a significant increase in their proliferation at both the 72 and 96 hour time points as compared to the control-infected cells ($P<0.001$ for both time points; **Figure 25D**). The increase in cell number was 2.4 times greater between 48 and 72 hours for the *Rb*$^{\Delta 19}$/*Trp53*$^{\Delta 2\text{-}10}$/*Brca1*$^{\Delta 5\text{-}13}$ cells than the *Rb*$^{loxP/loxP}$/*p53*$^{loxP/loxP}$/*Brca1*$^{loxP/loxP}$ cells and 2.7 times greater between 72 and 96 hours.

4.3 Within several passages after inactivation, loss of either *p53* or *Rb* is sufficient to cause an increase in MOSE cell proliferation.

When the proliferation rate of $Trp53^{\Delta 2\text{-}10}$ MOSE cells was examined several passages following AdCre infection, it was found that the p53-deficient MOSE now had a significantly increased rate of proliferation detectable at both the 72 and 96 hour time points as compared to the AdGFP-infected cells, which had also been passaged for the same length of time following the initial infection ($P<0.001$ for both time points, **Figure 26A**). The increase in cell number of the *p53*-deficient cells between 48 and 72 hours was nearly four times that of the *p53* wildtype cells, and was three times as great between 72 and 96 hours.

The $Rb^{\Delta 19}$ MOSE cells also had a significantly increased rate of proliferation as compared to their AdGFP-infected counterparts when examined several passages following initial infection. In the case of the $Rb^{\Delta 19}$ MOSE cells, this difference was evident as early as the 48-hour time point ($P<0.05$), and was more pronounced at the 72 and 96-hour time points ($P<0.001$ for both time points, **Figure 26B**). The *Rb*-deficient cells demonstrated an increase in cell number between 48 and 96 hours that was 1.6 times greater than that observed in the *Rb* wildtype cells.

4.3 Effect of inactivation of single tumour suppressor genes on sensitivity to cisplatin in MOSE cells *in vitro*.

As was demonstrated in Chapter 3, section 3.7, inactivation of *Brca1* in $Brca1^{loxP/loxP}$ MOSE cells *in vitro* rendered them significantly more sensitive to treatment with the chemotherapeutic agent cisplatin (**Figure 17B**). When *p53* was inactivated in

Figure 26: Proliferation of MOSE cells several passages following inactivation of *p53* or *Rb*. **A)** Proliferation of $p53^{loxP/loxP}$ MOSE several passages following infection with AdCre ($Trp53^{\Delta 2\text{-}10}$) to inactivate *p53* or with AdGFP ($p53^{loxP/loxP}$). **B)** Proliferation of $Rb^{loxP/loxP}$ MOSE cells several passages following infection with AdCre ($Rb^{\Delta 19)}$ to inactivate *Rb* or with AdGFP ($Rb^{loxP/loxP}$). Error bars represent the SEM. Experiments were performed three times in triplicate.

A

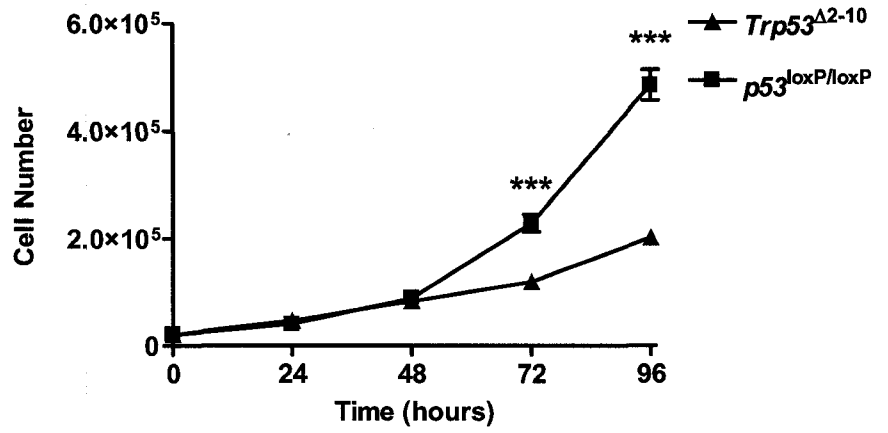
6.0×10^5
4.0×10^5
2.0×10^5
0
Cell Number
0
24
48
72
96
Time (hours)
***
***
Trp53^Δ2-10
p53^loxP/loxP

B

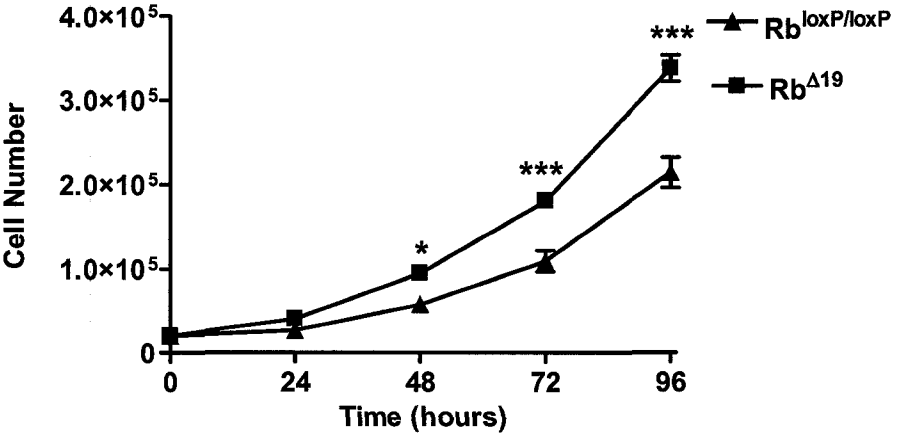
4.0×10^5
3.0×10^5
2.0×10^5
1.0×10^5
0
Cell Number
0
24
48
72
96
Time (hours)
*
***
***
Rb^loxP/loxP
Rb^Δ19

$p53^{loxP/loxP}$ cells and the cells were exposed to cisplatin, it was found that the $Trp53^{\Delta 2\text{-}10}$ cells were also significantly more sensitive to cisplatin treatment after 48 hours of exposure (31.18%±2.13% versus 39.68%±2.81%, $P<0.05$, results expressed as a percentage of untreated cells, **Figure 27A**). The $Rb^{\Delta 19}$ MOSE cells were also significantly more sensitive to cisplatin treatment than the $Rb^{loxP/loxP}$ cells (33.28%±0.95% versus 46.85%±2.42%, $P<0.01$, results expressed as a percentage of untreated cells, **Figure 27B**).

4.4 Effect of inactivation of multiple tumour suppressor genes on sensitivity to cisplatin in MOSE cells *in vitro*.

4.4.1 *Brca1/p53*

When MOSE cells in which both Brca1 and p53 had been conditionally inactivated were treated with cisplatin, it was found that there was no significant difference between the sensitivities of the $Brca1^{\Delta 5\text{-}13}/Trp53^{\Delta 2\text{-}10}$ cells and the $Brca1^{loxP/loxP}/p53^{loxP/loxP}$ cells after 48 hours (59.96±3.52% versus 70.46±5.90%, $P=0.14$, results expressed as a percentage of untreated cells; **Figure 28A**).

4.4.2 *Rb/Brca1*

When both *Rb* and *Brca1* where inactivated via exposure to Cre recombinase in $Rb^{loxP/loxP}/Brca1^{loxP/loxP}$ MOSE cells, it was found that, as was seen with their proliferation, there was no difference in terms of sensitivity to cisplatin treatment as compared to their control-infected counterparts (45.42%±4.51% versus 46.73%±5.76%, $P=0.80$, results expressed as a percentage of untreated cells, **Figure 28B**).

Figure 27: Treatment of MOSE cells with cisplatin following inactivation of *p53* or *Rb*. **A)** $p53^{loxP/loxP}$ MOSE cells infected with either AdCre ($Trp53^{\Delta 2\text{-}10}$) or AdGFP ($p53^{loxP/loxP}$) and treated with 5μM cisplatin for 48 hours. **B)** $Rb^{loxP/loxP}$ MOSE cells infected with either AdCre ($Rb^{\Delta 19}$) or AdGFP ($Rb^{loxP/loxP}$) and treated with 5μM cisplatin for 48 hours. Values are the number of adherent cells presented as a proportion of similar cells exposed to the vehicle control (untreated cells). * indicates a significant difference where $P<0.05$ and ** indicates a difference where $P<0.01$. Error bars represent the SEM. Experiments were performed three times in triplicate.

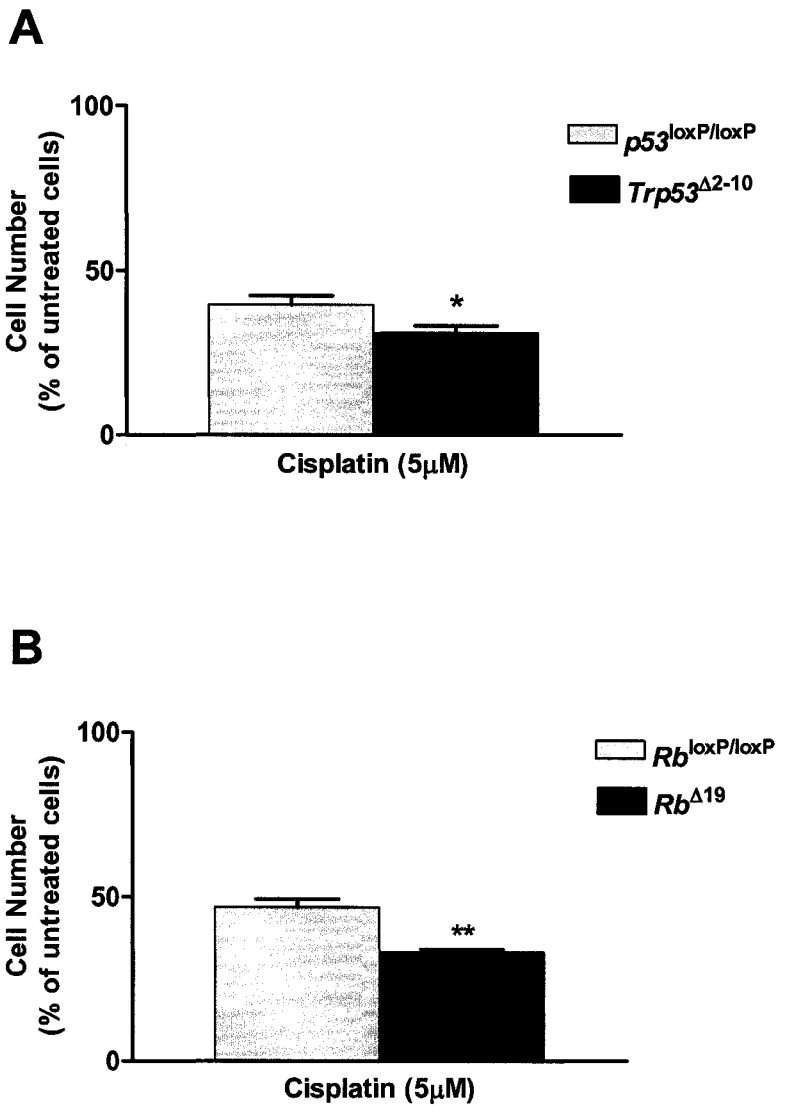
A
100
50
0
Cell Number
(% of untreated cells)
p53loxP/loxP
Trp53Δ2-10
*
Cisplatin (5μM)
B
100
50
0
Cell Number
(% of untreated cells)
RbloxP/loxP
RbΔ19
**
Cisplatin (5μM)

Figure 28: Treatment of MOSE cells with cisplatin following inactivation of multiple tumour suppressors. MOSE cells with specific inactivation of *Brca1*, *p53*, and/or *Rb* in various combinations were tested for their sensitivity to cisplatin by treatment with 5μM cisplatin for 48 hours. **A)** $Brca1^{loxP/loxP}/p53^{loxP/loxP}$ MOSE cells infected with either AdCre ($Brca1^{\Delta 5\text{-}13}/Trp53^{\Delta 2\text{-}10}$) or AdGFP ($Brca1^{loxP/loxP}/p53^{loxP/loxP}$). **B)** $Rb^{loxP/loxP}/Brca1^{loxP/loxP}$ MOSE cells infected with either AdCre ($Rb^{\Delta 19}/Brca1^{\Delta 5\text{-}13}$) or AdGFP ($Rb^{loxP/loxP}/Brca1^{loxP/loxP}$). **C)** $Rb^{loxP/loxP}/p53^{loxP/loxP}$ MOSE cells infected with either AdCre ($Rb^{\Delta 19}/Trp53^{\Delta 2\text{-}10}$) or AdGFP ($Rb^{loxP/loxP}/p53^{loxP/loxP}$). **D)** $Rb^{loxP/loxP}/p53^{loxP/loxP}/Brca1^{loxP/loxP}$ MOSE cells infected with either AdCre ($Rb^{\Delta 19}/Trp53^{\Delta 2\text{-}10}/Brca1^{\Delta 5\text{-}13}$) or AdGFP ($Rb^{loxP/loxP}/p53^{loxP/loxP}/Brca1^{loxP/loxP}$). Values are the number adherent cells presented as a proportion of similar cells exposed to the vehicle control (untreated cells). Error bars represent the SEM. No significant differences were observed. Experiments were performed three times in triplicate.

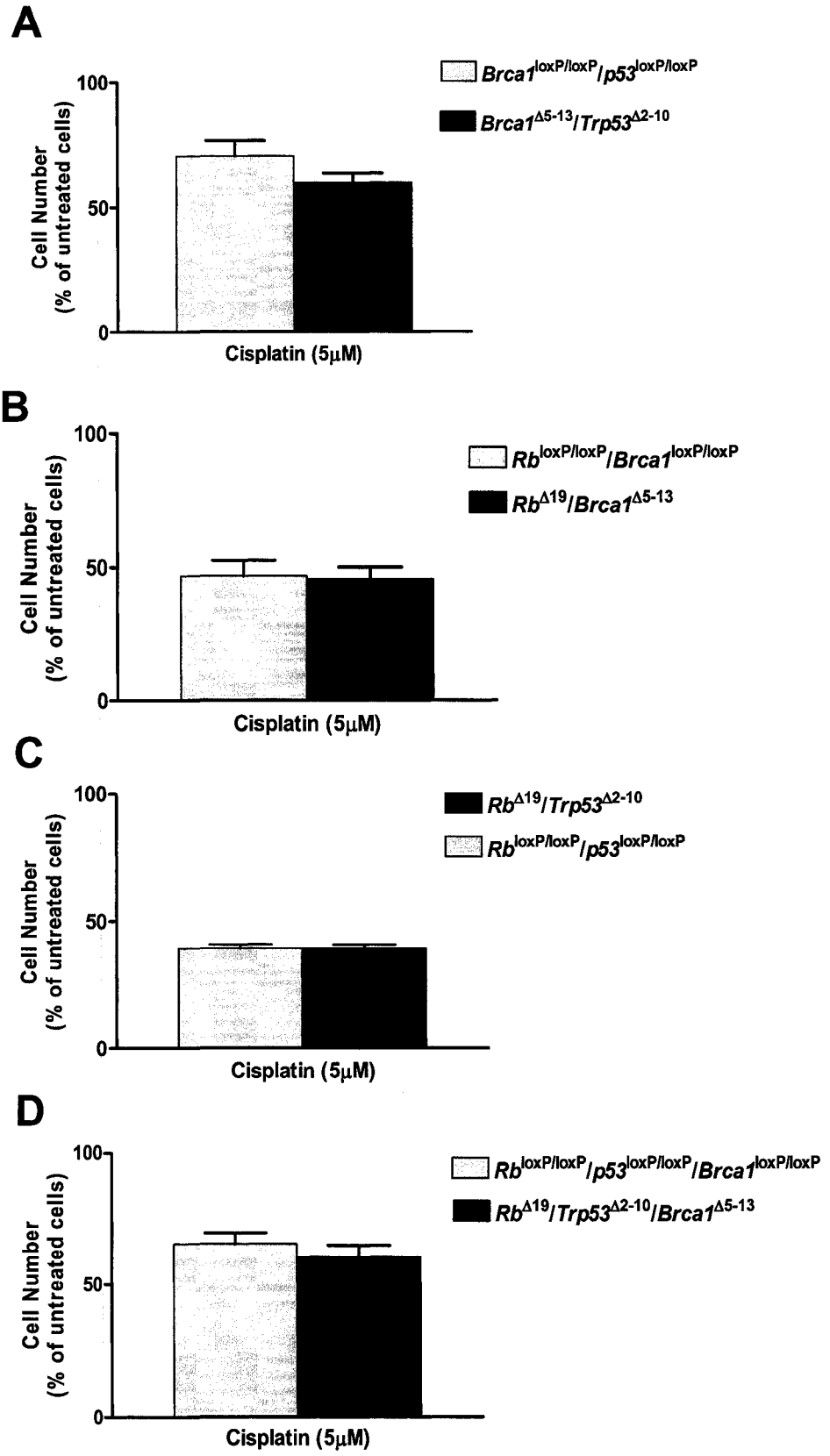
A
Brca1loxP/loxP/p53loxP/loxP
Brca1Δ5-13/Trp53Δ2-10
Cell Number (% of untreated cells)
100
50
0
Cisplatin (5μM)
B
RbloxP/loxP/Brca1loxP/loxP
RbΔ19/Brca1Δ5-13
Cell Number (% of untreated cells)
100
50
0
Cisplatin (5μM)
C
RbΔ19/Trp53Δ2-10
RbloxP/loxP/p53loxP/loxP
Cell Number (% of untreated cells)
100
50
0
Cisplatin (5μM)
D
RbloxP/loxP/p53loxP/loxP/Brca1loxP/loxP
RbΔ19/Trp53Δ2-10/Brca1Δ5-13
Cell Number (% of untreated cells)
100
50
0
Cisplatin (5μM)

4.4.3 *Rb/p53*

The MOSE cells in which both *Rb* and *p53* were inactivated also did not display any significant difference in sensitivity to cisplatin as compared to the control-infected $Rb^{loxP/loxP}/p53^{loxP/loxP}$ cells (39.22%±1.39% versus 39.33%±1.43%, P=0.96, results expressed as a percentage of untreated cells, **Figure 28C**).

4.4.4 *Rb/p53/Brca1*

The concomitant conditional inactivation of all three tumour suppressor genes in the $Rb^{loxP/loxP}/p53^{loxP/loxP}/Brca1^{loxP/loxP}$ cells had no impact on the sensitivity of these cells to treatment with 5μM of cisplatin for 48 hours as compared to the corresponding control-infected cells (60.32%±4.80% versus 65.72%±4.27%, P=0.41, results expressed as a percentage of untreated cells, **Figure 28D**).

4.6 Effect of inactivation of single tumour suppressor genes on sensitivity to paclitaxel in MOSE cells *in vitro*.

As was shown in Chapter 3, section 3.8, $Brca1^{\Delta 5\text{-}13}$ cells, where *Brca1* has been inactivated, display a modest decrease in sensitivity to treatment with paclitaxel (**Figure 22**). When *p53* alone was inactivated, however, it was found that there was no significant difference seen in terms of sensitivity to paclitaxel treatment between the *p53* wildtype $p53^{loxP/loxP}$ cells and their *p53*-deficient counterparts the $Trp53^{\Delta 2\text{-}10}$ MOSE cells (24.57%±2.44% versus 28.73%±4.32%, P=0.41, results expressed as a percentage of untreated cells, **Figure 29A**). A similar result was also observed with the $Rb^{loxP/loxP}$ and the $Rb^{\Delta 19}$ cells when they were subjected to treatment with paclitaxel. While both sets of

Figure 29: Treatment of MOSE cells with paclitaxel following inactivation of *p53* or *Rb*. **A)** $p53^{loxP/loxP}$ MOSE cells infected with either AdCre ($Trp53^{\Delta 2\text{-}10}$) or AdGFP ($p53^{loxP/loxP}$) and treated with 25nM paclitaxel for 96 hours. **B)** $Rb^{loxP/loxP}$ MOSE cells infected with either AdCre ($Rb^{\Delta 19}$) or AdGFP ($Rb^{loxP/loxP}$) and treated with 25nM paclitaxel for 96 hours. Values are the number adherent cells presented as a proportion of similar cells exposed to the vehicle control (untreated cells). Error bars represent the SEM. No significant differences were observed. Experiments were performed three times in triplicate.

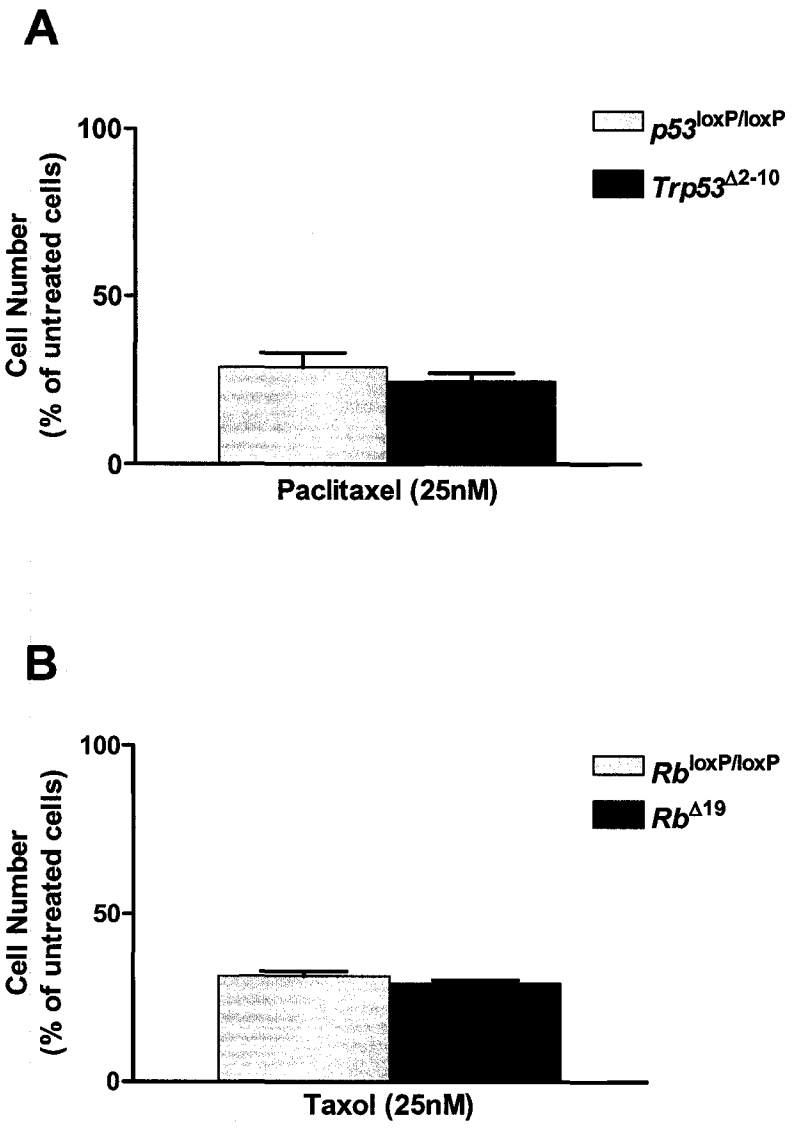
A
100
50
0
Cell Number
(% of untreated cells)
p53loxP/loxP
Trp53Δ2-10
Paclitaxel (25nM)
B
100
50
0
Cell Number
(% of untreated cells)
RbloxP/loxP
RbΔ19
Taxol (25nM)

cells were sensitive to the treatment, there was no significant difference in sensitivity as related to the *Rb* status of the cells (29.13%±0.99% for $Rb^{\Delta 19}$ versus 31.42%±1.49% for $Rb^{loxP/loxP}$, P=0.21, results expressed as a percentage of untreated cells, **Figure 29B**).

4.7 Effect of concomitant inactivation of multiple tumour suppressor genes on sensitivity to paclitaxel *in vitro*.

4.7.1 *Brca1/p53*

When MOSE cells in which both *Brca1* and *p53* were inactivated via Cre-loxP mediated recombination were treated with paclitaxel, it was found that their *Brca1* and *p53* status had no effect on their sensitivity to the drug, when treated with 25 nM for 96 hours (57.11%±6.22% for the $Brca1^{\Delta 5\text{-}13}/Trp53^{\Delta 2\text{-}10}$ cells versus 55.40%±7.21% for the $Brca1^{loxP/loxP}/p53^{loxP/loxP}$ cells, P=0.86, results expressed as a percentage of untreated cells, **Figure 30A**).

4.7.2 *Rb/Brca1*

When both *Rb* and *Brca1* were inactivated in the $Rb^{loxP/loxP}/Brca1^{loxP/loxP}$ MOSE cells and subsequently exposed to 25 nM of paclitaxel for 96 hours, it was found that while paclitaxel elicited a 50% killing of both the *Rb/Brca1*-deficient and the *Rb/Brca1* wildtype cells, there was no significant difference in sensitivity dependent on genotype (49.91%±2.30% versus 46.38%±2.72%, P=0.33, results expressed as a percentage of untreated cells, **Figure 30B**).

Figure 30: Treatment of MOSE cells with paclitaxel following inactivation of multiple tumour suppressors. MOSE cells with specific inactivation of *Brca1*, *p53*, and/or *Rb* in various combinations were tested for their sensitivity to paclitaxel by treatment with 25nM paclitaxel for 96 hours. **A)** $Brca1^{loxP/loxP}/p53^{loxP/loxP}$ MOSE cells infected with either AdCre ($Brca1^{\Delta 5\text{-}13}/Trp53^{\Delta 2\text{-}10}$) or AdGFP ($Brca1^{loxP/loxP}/p53^{loxP/loxP}$). **B)** $Rb^{loxP/loxP}/Brca1^{loxP/loxP}$ MOSE cells infected with either AdCre ($Rb^{\Delta 19}/Brca1^{\Delta 5\text{-}13}$) or AdGFP ($Rb^{loxP/loxP}/Brca1^{loxP/loxP}$). **C)** $Rb^{loxP/loxP}/p53^{loxP/loxP}$ MOSE cells infected with either AdCre ($Rb^{\Delta 19}/Trp53^{\Delta 2\text{-}10}$) or AdGFP ($Rb^{loxP/loxP}/p53^{loxP/loxP}$). **D)** $Rb^{loxP/loxP}/p53^{loxP/loxP}/Brca1^{loxP/loxP}$ MOSE cells infected with either AdCre ($Rb^{\Delta 19}/Trp53^{\Delta 2\text{-}10}/Brca1^{\Delta 5\text{-}13}$) or AdGFP ($Rb^{loxP/loxP}/p53^{loxP/loxP}/Brca1^{loxP/loxP}$). Values are the number adherent cells presented as a proportion of similar cells exposed to the vehicle control (untreated cells). No significant differences were observed. Error bars represent the SEM. Experiments were performed three times in triplicate.

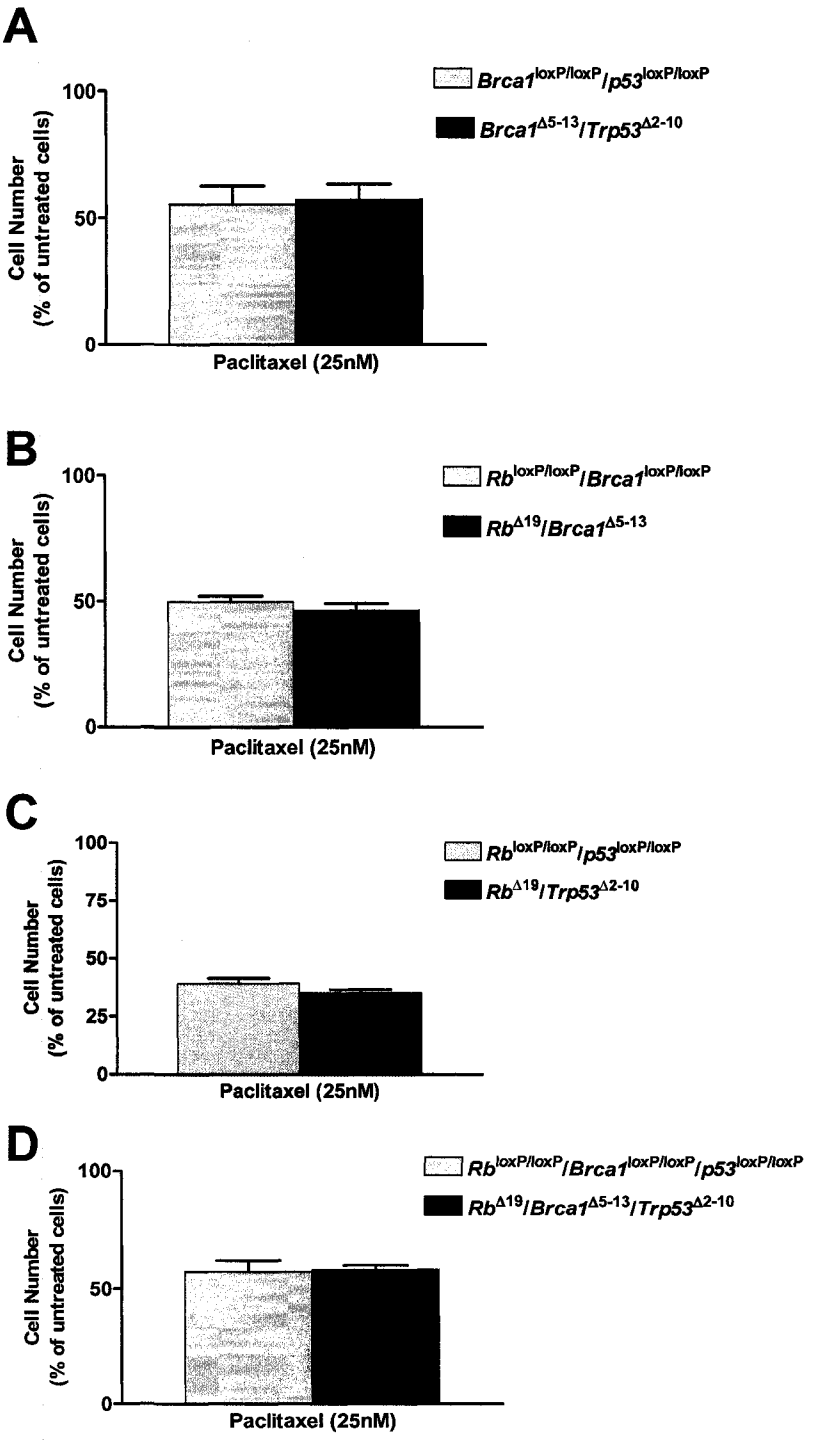
A
Brca1loxP/loxP/p53loxP/loxP
Brca1Δ5-13/Trp53Δ2-10
Cell Number (% of untreated cells)
100
50
0
Paclitaxel (25nM)
B
RbloxP/loxP/Brca1loxP/loxP
RbΔ19/Brca1Δ5-13
Cell Number (% of untreated cells)
100
50
0
Paclitaxel (25nM)
C
RbloxP/loxP/p53loxP/loxP
RbΔ19/Trp53Δ2-10
Cell Number (% of untreated cells)
100
75
50
25
0
Paclitaxel (25nM)
D
RbloxP/loxP/Brca1loxP/loxP/p53loxP/loxP
RbΔ19/Brca1Δ5-13/Trp53Δ2-10
Cell Number (% of untreated cells)
100
50
0
Paclitaxel (25nM)

4.7.3 *Rb/p53*

When both *Rb* and *p53* were conditionally inactivated in the $Rb^{\Delta 19}/Trp53^{\Delta 2\text{-}10}$ MOSE cells and exposed to 25 nM of paclitaxel for 96 hours. Both the *Rb/p53*-deficient cells and their wildtype counterparts were sensitive to the paclitaxel treatment; however there was no significant difference in sensitivity between the two (35.24%±1.47% versus 39.38%±2.14%, P=0.12, results expressed as a percentage of untreated cells, **Figure 30C**).

4.7.4 *Rb/p53/Brca1*

When all three tumour suppressors were concurrently inactivated and then treated with paclitaxel, it was found that the $Rb^{\Delta 19}/Trp53^{\Delta 2\text{-}10}/Brca1^{\Delta 5\text{-}13}$ cells were not significantly more or less sensitive to the treatment than their $Rb^{loxP/loxP}/p53^{loxP/loxP}/Brca1^{loxP/loxP}$ counterparts (57.32%±4.70% versus 58.07%±1.98%, P=0.89, results expressed as a percentage of untreated cells, **Figure 30D**).

4.8 Anchorage-independent growth assay

In order to assess whether or not inactivation of various tumour suppressor genes in MOSE cells *in vitro* resulted in the ability of the cells to proliferate in an anchorage-independent environment, the cells of the various genotypes were plated on either poly-HEMA-coated tissue culture plates as well as in soft agar. Some, but not all of the cells in which one or more tumour suppressors had been inactivated were capable of anchorage-independent growth (**Table 3**). The AdGFP-infected counterparts of each

Table 3: MOSE cell anchorage-independent growth assay results

MOSE Genotype	Poly-HEMA	Soft Agar
$Brca1^{\Delta 5-13}$	No	No
$Rb^{\Delta 19}$	Yes	Yes
$Trp53^{\Delta 2-10}$	Yes	Yes
$Rb^{\Delta 19}$/ $Brca1^{\Delta 5-13}$	No	No
$Brca1^{\Delta 5-13}$/ $Trp53^{\Delta 2-10}$	Yes	No
$Rb^{\Delta 19}$/ $Trp53^{\Delta 2-10}$	Yes	Yes
$Rb^{\Delta 19}$/ $Trp53^{\Delta 2-10}$/ $Brca1^{\Delta 5-13}$	Yes	Yes

genotype were also assessed and none were capable of anchorage-independent growth under either condition.

When *Brca1* was inactivated alone, it was found that the resulting $Brca1^{\Delta 5\text{-}13}$ cells were not capable of proliferation on poly-HEMA-coated plates or colony formation in soft agar. Both the $Trp53^{\Delta 2\text{-}10}$ and the $Rb^{\Delta 19}$ MOSE cells were capable of proliferation both on poly-HEMA-coated plates as well as colony formation in soft agar (**Figure 31**).

When both *Rb* and *Brca1* were inactivated in tandem, the $Rb^{\Delta 19}/Brca1^{\Delta 5\text{-}13}$ cells that resulted did not proliferate in either anchorage-independent setting. The $Rb^{\Delta 19}/Trp53^{\Delta 2\text{-}10}$ cells demonstrated proliferation on poly-HEMA-coated plates as well as colony formation in soft agar (**Figure 31**).

The $Brca1^{\Delta 5\text{-}13}/Trp53^{\Delta 2\text{-}10}$ cells, in which both *Brca1* and *p53* were conditionally inactivated, were capable of proliferation on poly-HEMA-coated plates; however the phenotype they produced in this milieu differed from that of the other genotypes examined. While they did form the small floating spheroids that were observed in other genotypes (see **Figure 31**), they also formed for the most part flat sheets of floating cells in the soft agar (**Figure 32A**). These sheets continued to expand over several days in culture and were capable of re-plating as a monolayer on regular tissue culture plastic (**Figure 32B**). Interestingly, the $Brca1^{\Delta 5\text{-}13}/Trp53^{\Delta 2\text{-}10}$ cells were not capable of colony formation in soft agar with no colonies ever observed in any wells in three separate assays.

Figure 31: Anchorage-independent growth of MOSE cells in which *Brca1*, *p53*, and/or *Rb* have been inactivated. Cells were plated on poly-HEMA coated plates to prevent attachment or in soft agar and anchorage-independent growth was assessed by the formation of floating cell spheres in the coated plates and colony formation in soft agar.

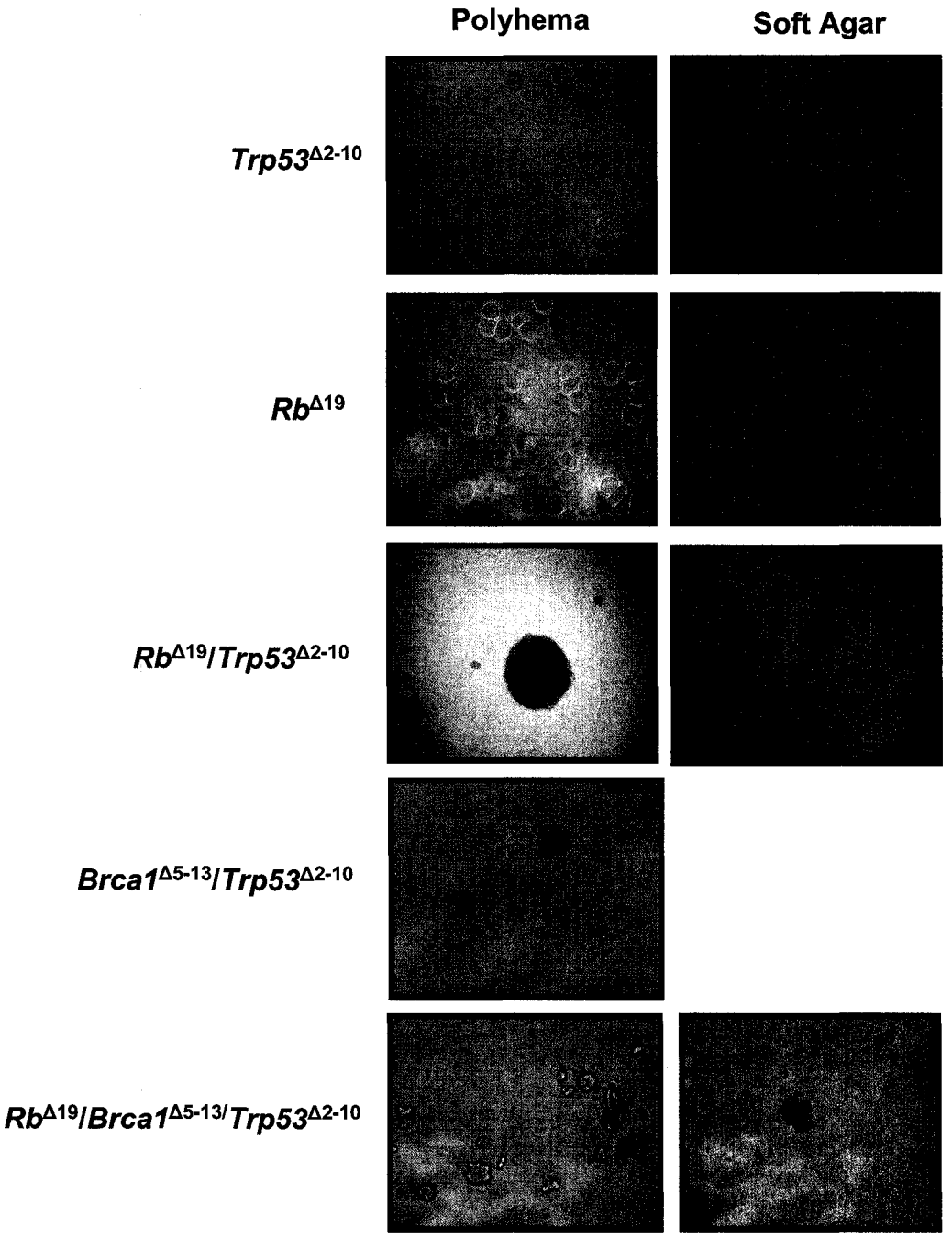
Polyhema
Soft Agar
Trp53Δ2-10
RbΔ19
RbΔ19/Trp53Δ2-10
Brca1Δ5-13/Trp53Δ2-10
RbΔ19/Brca1Δ5-13/Trp53Δ2-10

Figure 32: Anchorage-independent growth on poly-HEMA-coated plates of *Brca1*$^{\Delta 5\text{-}13}$/*Trp53*$^{\Delta 2\text{-}10}$ MOSE cells. A) Representative image of the floating flat sheets of cells observed after four days of anchorage-independent growth (200X, right panel and 400X, left panel). **B)** These floating sheets were replated on standard attachment culture plates to ensure the cells composing the sheets were in fact viable. Image was taken four days following replating.

A

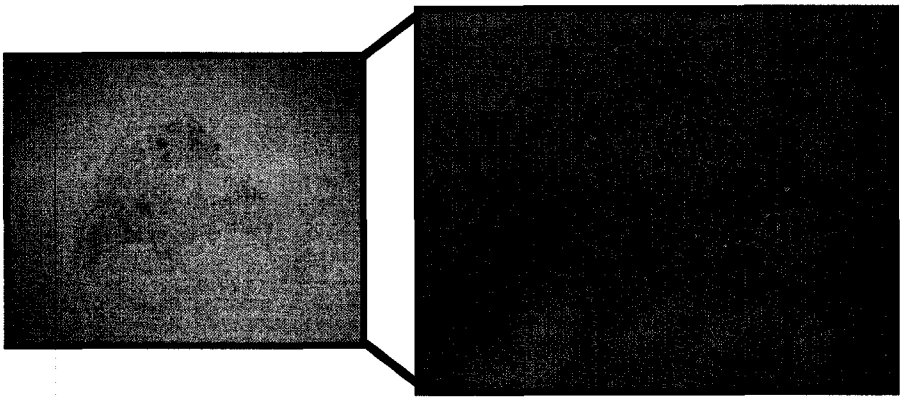

B

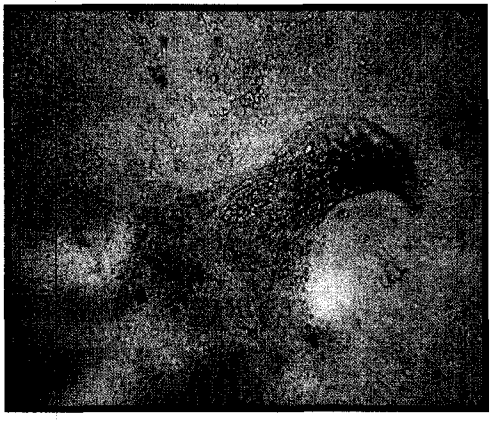

The $Rb^{\Delta 19}/Brca1^{\Delta 5\text{-}13}/Trp53^{\Delta 2\text{-}10}$ cells, on the other hand, were capable of both proliferation as spheroids on poly-HEMA-coated plates as well as colony formation in soft agar (**Figure 31**). None of the AdGFP-infected cells from any of the genotypes were able to proliferate in soft agar or on poly-HEMA-coated plates.

4.9 Conditional inactivation of *Brca1* in conjunction with *p53* and/or *Rb* in the OSE *in vivo*.

The OSE in which *Brca1* was inactivated via intrabursal injection of AdCre displayed more morphologic changes than the AdGFP-injected controls, but no tumour formation was seen. Thus it was of interest to examine the effect of concomitant inactivation of other tumour suppressors, such as *Rb* and *p53*, in conjunction with *Brca1* on OSE morphology and ovarian tumour formation, particularly as dual inactivation of *Rb* and *p53* in the OSE via intrabursal AdCre injection had previously been shown to result in the formation of epithelial ovarian tumours .

No tumour formation was seen in mice in which Rb was conditionally inactivated in the OSE, even when they were followed past one year following intrabursal injection. There were no significant differences in the number of morphological changes in the OSE between the $Rb^{\Delta 19}$ mice and the $Rb^{loxP/loxP}$ mice at any of the time points examined (**Table 4**). Rather surprisingly, there was no age-related increase in the total number of changes, as was seen in the $Brca1^{\Delta 5\text{-}13}$ mice. However, the number of changes in the OSE doubled between 120 and 180 days in the $Rb^{\Delta 19}$ mice (4.32±0.78 versus 8.52±0.80, $P<0.05$, numbers represent the mean ±SEM number of morphological changes per

Table 4: Distribution of morphological features in the OSE over time following inactivation of *Rb*.

	Time (Days)			
Epithelial Morphology	**60**	**120**	**180**	**240**
Areas of Columnar Cells				
$\mathbf{Rb^{\Delta 19}}$	3.34±0.33[a] (n=10)	2.38±0.49[a] (n=10)	4.00±0.53[a] (n=10)	4.33±0.67[a] (n=8)
$\mathbf{Rb^{loxP/loxP}}$	2.48±0.28[a] (n=10)	2.99±0.53[a] (n=8)	4.76±0.53[b] (n=10)	4.02±0.36[a] (n=10)
Areas of Hyperplasia				
$\mathbf{Rb^{\Delta 19}}$	2.60±0.77[a]	1.90±0.54[a]	4.52±0.67[a]	2.08±0.38[a]
$\mathbf{Rb^{loxP/loxP}}$	2.43±0.69[a]	2.96±0.93[a]	3.04±0.70[a]	2.32±0.50[a]
Epithelial Invaginations				
$\mathbf{Rb^{\Delta 19}}$	0.13±0.07[a]	0.04±0.04[a]	0[a]	0.06±0.06[a]
$\mathbf{Rb^{loxP/loxP}}$	0[a]	0.03±0.03[a]	0[a]	0[a]
Inclusion Cysts				
$\mathbf{Rb^{\Delta 19}}$	0	0	0	0
$\mathbf{Rb^{loxP/loxP}}$	0	0	0	0
Total Changes				
$\mathbf{Rb^{\Delta 19}}$	6.05±0.86[a]	4.32±0.78[a]	8.52±0.80[b]	6.40±0.80[a]
$\mathbf{Rb^{loxP/loxP}}$	4.90±0.79[a]	5.98±1.16[a]	7.80±1.10[a]	6.40±0.63[a]

Numbers represent the mean ±SEM number of morphological changes per section over five non-consecutive sections in n ovaries. Letters are used to denote a significant difference between time points for that treatment group.

section over five non-consecutive sections per ovary), whereas this difference was not seen in the $Rb^{loxP/loxP}$ mice.

Tumour formation was also not seen in mice in which both *Rb* and *Brca1* were concomitantly inactivated in the OSE via intrabursal injection of adenoviral Cre recombinase. The number of morphological changes in the OSE increased over time in both groups, however there were no significant differences between the $Rb^{\Delta 19}/Brca1^{\Delta 5\text{-}13}$ ovaries and the $Rb^{loxP/loxP}/Brca1^{loxP/loxP}$ ovaries at any time point examined (**Table 5**). There was a significant increase in the number of areas of columnar cells between 60 and 240 days in the $Rb^{\Delta 19}/Brca1^{\Delta 5\text{-}13}$ mice (1.96±0.45 versus 5.18±0.70, $P<0.01$) that was not seen in the $Rb^{loxP/loxP}/Brca1^{loxP/loxP}$ mice.

Tumour formation was observed in the $Trp53^{\Delta 2\text{-}10}$ mice, the $Rb^{\Delta 19}/Trp53^{\Delta 2\text{-}10}$ mice, the $Brca1^{\Delta 5\text{-}13}/Trp53^{\Delta 2\text{-}10}$ mice, and the $Rb^{\Delta 19}/Trp53^{\Delta 2\text{-}10}/Brca1^{\Delta 5\text{-}13}$ mice (**Table 6**). No tumours were ever observed in any of the mice injected with adenoviral GFP when followed to one year post-intrabursal injection. The presentation of the mice when they reached their loss-of-wellness endpoint was similar in all of the groups examined. Endpoint was reached because the mice had a large, palpable mass(es) on their backs or because they had severe abdominal distention (**Figure 33A-B**), and the time between when these symptoms appeared and when they were deemed to have reached their survival endpoint was quite short, generally one week or less. **Figure 34** illustrates the general appearance of the tumours upon necropsy for each genotype.

Table 5: Distribution of morphological features in the OSE over time following inactivation of *Rb* and *Brca1*.

	Time (Days)			
Epithelial Morphology	**60**	**120**	**180**	**240**
Areas of Columnar Cells				
$Rb^{\Delta 19}/Brca1^{\Delta 5\text{-}13}$	1.96±0.45[a] (n=10)	4.00±0.59[a] (n=10)	4.27±0.49[a] (n=12)	5.18±0.70[b] (n=10)
$Rb^{loxP/loxP}/Brca1^{loxP/loxP}$	3.24±0.43[a] (n=10)	3.38±0.31[a] (n=10)	3.30±0.32[a] (n=12)	5.02±0.85[a] (n=10)
Areas of Hyperplasia				
$Rb^{\Delta 19}/Brca1^{\Delta 5\text{-}13}$	2.64±0.68[a]	2.70±0.84[a]	4.23±0.75[a]	4.14±0.84[a]
$Rb^{loxP/loxP}/Brca1^{loxP/loxP}$	1.76±0.40[a]	2.80±0.62[a]	3.08±0.68[a]	2.42±0.87[a]
Epithelial Invaginations				
$Rb^{\Delta 19}/Brca1^{\Delta 5\text{-}13}$	0	0	0.35±0.25	0.20±0.11
$Rb^{loxP/loxP}/Brca1^{loxP/loxP}$	0	0	0	0
Inclusion Cysts				
$Rb^{\Delta 19}/Brca1^{\Delta 5\text{-}13}$	0	0	0	0
$Rb^{loxP/loxP}/Brca1^{loxP/loxP}$	0	0	0	0
Total Changes				
$Rb^{\Delta 19}/Brca1^{\Delta 5\text{-}13}$	4.62±1.08[a]	8.85±1.06[a]	8.52±0.80[a]	9.52±1.51[a]
$Rb^{loxP/loxP}/Brca1^{loxP/loxP}$	5.00±0.72[a]	6.38±0.90[a]	7.80±1.10[a]	7.44±1.62[a]

Numbers represent the mean ±SEM of the mean number of morphological changes per section over five non-consecutive sections in n ovaries. Letters are used to denote a significant difference between time points for that treatment group.

Table 6: Tumour formation following intrabursal injection of adenoviral Cre recombinase

Genotype	# of mice[a]	# of mice with tumours	Median Survival in Days (range)	% with ascites
$Brca1^{\Delta 5-13}$	5	0		
$Rb^{\Delta 19}$	5	0		
$Rb^{\Delta 19}$/ $Brca1^{\Delta 5-13}$	5	0		
$Trp53^{\Delta 2-10}$	8	8	179.5 (101-200)	50
$Rb^{\Delta 19}$/ $Trp53^{\Delta 2-10}$	10	10	170 (99-207)	30
$Brca1^{\Delta 5-13}$/ $Trp53^{\Delta 2-10}$	12	12	147.5 (105-166)	42
$Rb^{\Delta 19}$/ $Trp53^{\Delta 2-10}$/ $Brca1^{\Delta 5-13}$	14	14	118.5 (89-183)	0

[a]Number of mice indicates the number of animals who received intrabursal adenoviral Cre recombinase and were sacrificed when they had reached a loss-of-wellness endpoint due to tumour burden or had reached the 240 day time point.

Figure 33: General presentation of mice at loss-of-wellness endpoint following intrabursal administration of AdCre. A) Severe abdominal distention caused by peritoneal ascites fluid accumulation. **B)** Large palpable unilateral or bilateral (shown) dorsal mass(es).

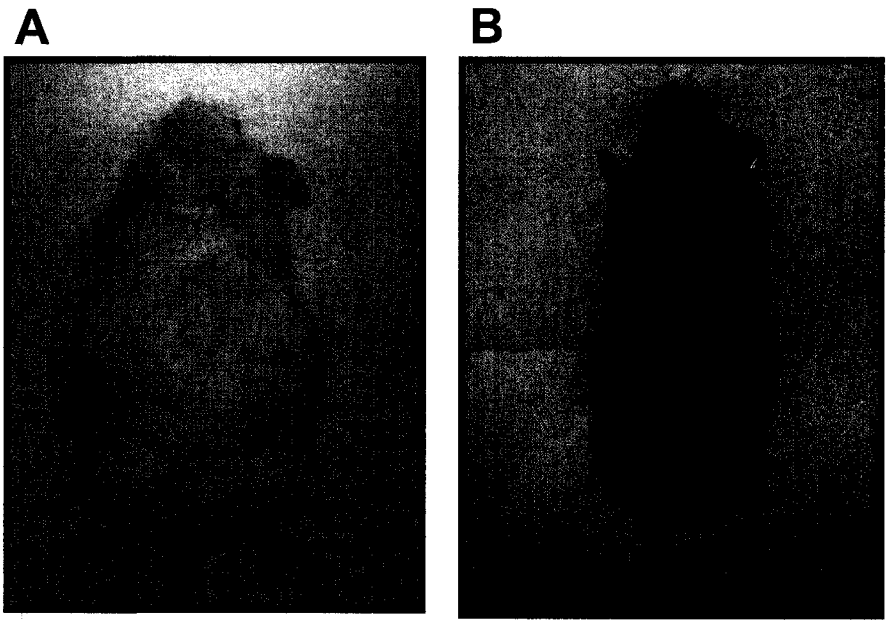
A
B

Figure 34: Gross tumour presentation of mice at survival endpoint following intrabursal administration of AdCre. A) Representative image of a tumour from a *Trp53*$^{\Delta 2\text{-}10}$ mouse. **B)** Representative image of a tumour from a *Brca1*$^{\Delta 5\text{-}13}$/*Trp53*$^{\Delta 2\text{-}10}$ mouse. **C)** Representative image of a tumour from an *Rb*$^{\Delta 19}$/*Trp53*$^{\Delta 2\text{-}10}$ mouse. **D)** Representative image of a tumour from an *Rb*$^{\Delta 19}$/*Trp53*$^{\Delta 2\text{-}10}$/ *Brca1*$^{\Delta 5\text{-}13}$ mouse.

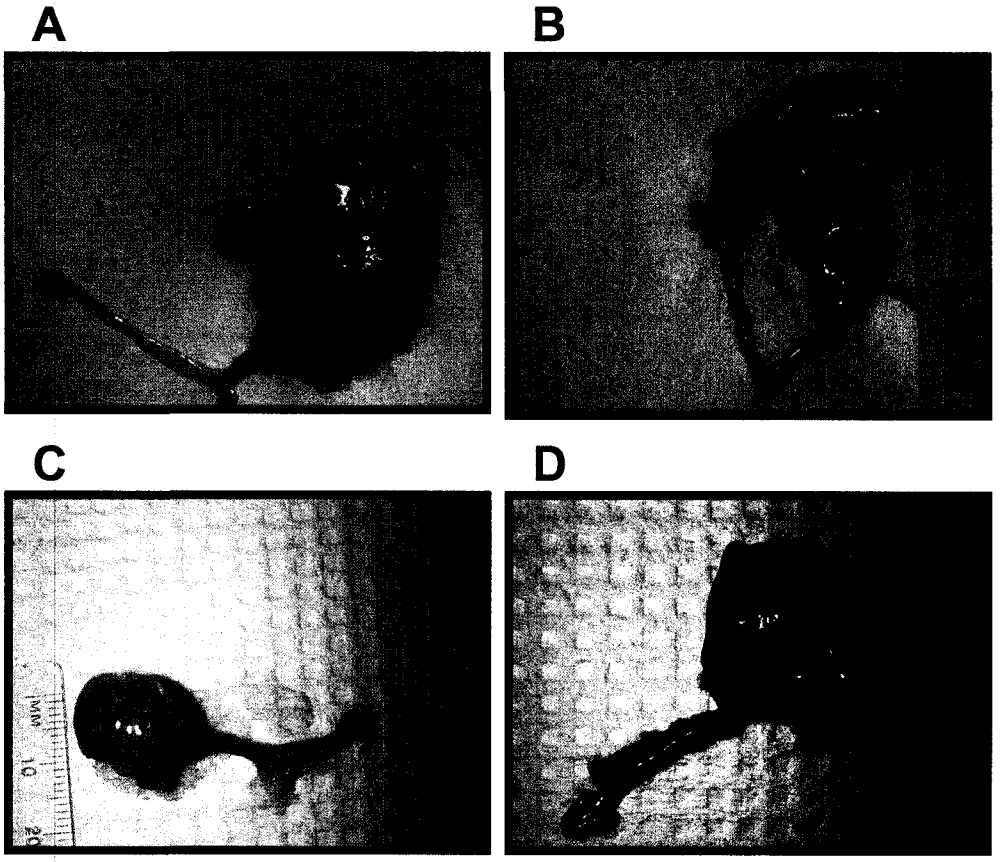
A
B
C
D

The tumours were generally located at the end of the uterine horn involving the ovary and sometimes engulfing surrounding organs such as the pancreas and the spleen. It should be noted that while both ovaries were subjected to intrabursal injection in all animals, bilateral tumours were only ever observed in the $Rb^{\Delta 19}/Trp53^{\Delta 2\text{-}10}/Brca1^{\Delta 5\text{-}13}$ mice, and only in two animals. It was originally anticipated, based on the previous work of Flesken-Nikitin, *et al* that the $Rb^{\Delta 19}/Trp53^{\Delta 2\text{-}10}$ mice would likely succumb to tumours around 200 days post-injection and that there would be minimal tumour formation seen in the $Trp53^{\Delta 2\text{-}10}$ mice (Flesken-Nikitin, et. al., 2003). As such, the experimental design originally involved allowing five mice to go to loss-of-wellness endpoint and to collect ovaries from earlier time points (60, 120, 180, and 240 days, if possible) from another five animals per time point. When it became apparent that different results were being obtained, the experimental plan was altered such that it essentially became a survival experiment with tissues collected when the mice reached a loss-of-wellness endpoint. When possible, ovaries were obtained from the earlier time points of 60 and 120 days post-injection. Thus the $Trp53^{\Delta 2\text{-}10}$, $Rb^{\Delta 19}/\ Trp53^{\Delta 2\text{-}10}$, $Brca1^{\Delta 5\text{-}13}/\ Trp53^{\Delta 2\text{-}10}$, and the $Rb^{\Delta 19}/\ Trp53^{\Delta 2\text{-}10}/\ Brca1^{\Delta 5\text{-}13}$ animals included in Table 6 are those that were euthanized at a loss-of-wellness endpoint, and not a predetermined time point.

The median time to loss-of-wellness endpoint of the $Trp53^{\Delta 2\text{-}10}$ mice was 179.5 days post intrabursal injection with a range of 101 to 200 days. Fifty percent of these mice were found to have bloody peritoneal ascites upon autopsy. All of the primary tumours were associated with one ovary, despite both ovaries having been subjected to intrabursal injection. Fifty percent of these mice were found to have tumours elsewhere

in the peritoneal cavity, generally smaller nodules associated with the body wall, intestines, or spleen, with half of these mice also presenting with ascites.

The $Rb^{\Delta 19}$/ $Trp53^{\Delta 2\text{-}10}$ mice had a mean time to endpoint of 170 days with a similar range of 99 to 207 days. Only 30% of these mice were found to have peritoneal ascites, two with bloody ascites and one with clear fluid. Three of the mice were found to have smaller tumours throughout their peritoneal cavity in addition to the primary tumour, and two of these mice also had ascites. The $Brca1^{\Delta 5\text{-}13}/Trp53^{\Delta 2\text{-}10}$ mice had a median survival time of 147.5 days with a range of 105 to 166 days. Forty-two percent of these mice were found to have peritoneal ascites upon autopsy, and these mice were also more likely to have multiple smaller tumours within the abdominal cavity. Twenty-one percent of the $Rb^{\Delta 19}/Brca1^{\Delta 5\text{-}13}/Trp53^{\Delta 2\text{-}10}$ mice had bilateral tumours associated with the ovaries, which was not seen in any of the other genotypes. The $Rb^{\Delta 19}/Trp53^{\Delta 2\text{-}10}/Brca1^{\Delta 5\text{-}13}$ mice had median survival time of 118.5 days with a range of 89-183 days and none of the mice presented with ascites on autopsy.

Combined inactivation of both *Brca1* and *p53* decreased the median survival of the mice as compared to the inactivation of *p53* alone ($P<0.05$, Table 6 and **Figure 35A**), and was also significantly shorter than that of mice in which both Rb and p53 had been inactivated in tandem ($P<0.01$, **Figure 35C**). The inactivation of all three tumour suppressors significantly decreased the survival as compared to mice in which only both *Rb* and *p53* were inactivated ($P<0.05$, **Figure 35D**). Mice with tumours resulting from concomitant inactivation of both *Rb* and *p53* did not have a significantly different survival time as compared to those in which only *p53* was inactivated ($P=0.78$, **Figure**

Figure 35: Survival of mice following inactivation of multiple tumour suppressors in the OSE *in vivo*. Kaplan-Meier plots showing the time to loss-of-wellness endpoint of the mice in which *Brca1*, *p53*, and/or *Rb* had been inactivated in the OSE. **A)** The median survival time of the $Brca1^{\Delta 5\text{-}13}/Trp53^{\Delta 2\text{-}10}$ mice (147.5 days) is significantly shorter than that of the $Trp53^{\Delta 2\text{-}10}$ mice (179.5 days), $P<0.05$. **B)** There is no significant difference in the median survival time of the $Trp53^{\Delta 2\text{-}10}$ mice (179.5 days) and the $Rb^{\Delta 19}/Trp53^{\Delta 2\text{-}10}$ mice (170 days). **C)** The median survival time of the $Brca1^{\Delta 5\text{-}13}/Trp53^{\Delta 2\text{-}10}$ mice (147.5 days) is significantly less than that of the $Rb^{\Delta 19}/Trp53^{\Delta 2\text{-}10}$ mice (170 days), $P<0.001$. **D)** The median survival time of the $Rb^{\Delta 19}/Trp53^{\Delta 2\text{-}10}/Brca1^{\Delta 5\text{-}13}$ mice (118.5 days) is significantly less than that of the $Rb^{\Delta 19}/Trp53^{\Delta 2\text{-}10}$ mice (170 days), $P<0.05$.

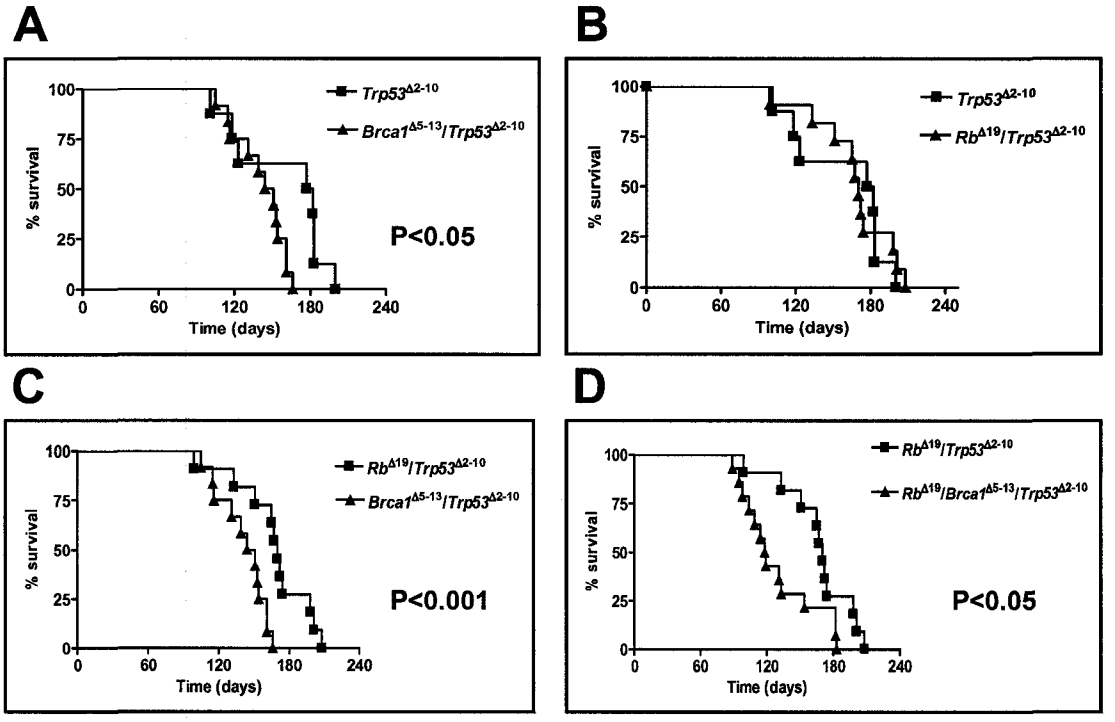
A
B
C
D
% survival
Time (days)
0
25
50
75
100
0
60
120
180
240
Trp53Δ2-10
Brca1Δ5-13/Trp53Δ2-10
Rb Δ19/Trp53Δ2-10
Rb Δ19/Brca1Δ5-13/Trp53Δ2-10
P<0.05
P<0.001
P<0.05

35B). When compiled, these data indicate that loss of *p53* is necessary for tumour formation and that *Brca1* deficiency accelerates tumour initiation and/or progression.

Recombination at the relevant loxP sites was detectable in genomic DNA from all the tumour samples (**Figure 36A**). Wildtype DNA was also detectable in all of the tumour samples, which is not unexpected given that the tumours are likely composed of both tumour cells and the cells of the normal tissue they have invaded. Recombination at the relevant loxP sites was also detectable in samples of genomic DNA from cultured ascites cells from tumour-bearing mice (**Figure 36B**).

There was no obvious difference in the pathology of the tumours as related to their genotype. H&E stained sections revealed densely-packed and highly malignant cells with spindle-shape morphology, as well as the presence of anaplastic giant cells in all of the samples examined (**Figure 37A-D**). Further immunohistochemical analysis revealed that the tumours were predominantly negative for the epithelial marker CK19, with the exception of some glandular structures present in a small number of the tumours (**Figure 38A-D**). These tumours were also stained for the presence of other epithelial markers such as CK8 and pancytokeratin and found to be negative with the exception of the areas noted above. All of the tumours examined were positive for Smooth Muscle Actin (SMA) (**Figure 39A,C,E,G**) as well as Desmin (**Figure 39B,D,F,H**), another muscle marker, and were negative for CD34, a hematological marker (**Figure 40A-D**). Taken together, along with consultation with Dr. Mary Senterman, a pathologist at the Ottawa Hospital, these results strongly indicate that these tumours are malignant leiomyosarcomas, which are of smooth muscle origin.

Figure 36: Recombination at loxP sites in the relevant tumour suppressor genes in tumour and ascites samples. A) PCR of genomic DNA collected from the tumour and the corresponding tail (control for lack of recombination) to detect recombination at loxP sites of the tumour suppressor genes relevant the genotype of the mouse. **B)** PCR of genomic DNA collected from cultured ascites cells from tumour-bearing mice and the corresponding tail sample to detect recombination at loxP sites of the tumour suppressor genes relevant the genotype of the mouse.

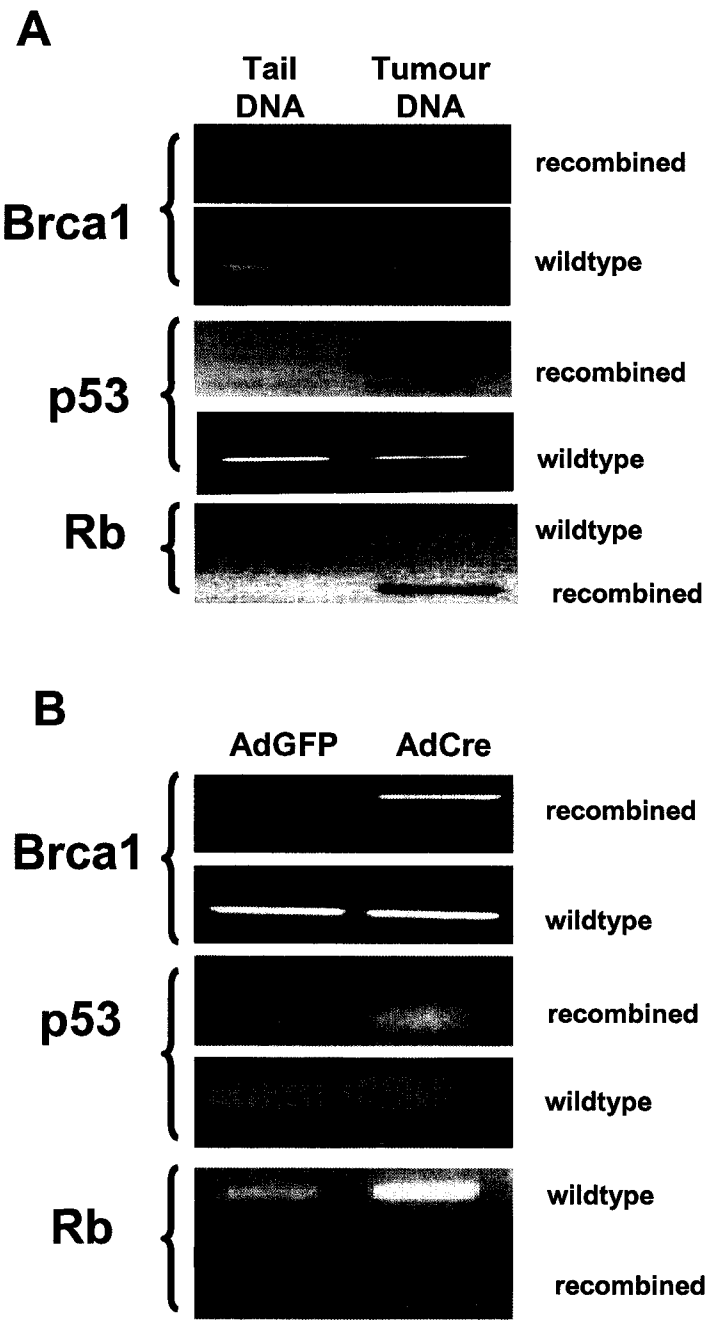
A
Tail DNA
Tumour DNA
Brca1
recombined
wildtype
p53
recombined
wildtype
Rb
wildtype
recombined
B
AdGFP
AdCre
Brca1
recombined
wildtype
p53
recombined
wildtype
Rb
wildtype
recombined

Figure 37: Representative images of tumour histology. Paraffin sections (5μm) of the tumours from each genotype were stained with H&E in order to examine histology **A)** *Trp53*$^{\Delta 2\text{-}10}$ (H&E, 200X) **B)** *Brca1*$^{\Delta 5\text{-}13}$/*Trp53*$^{\Delta 2\text{-}10}$ (H&E, 200X) **C)** *Rb*$^{\Delta 19}$/*Trp53*$^{\Delta 2\text{-}10}$ (H&E, 200X) **D)** *Rb*$^{\Delta 19}$/ *Brca1*$^{\Delta 5\text{-}13}$/*Trp53*$^{\Delta 2\text{-}10}$ (H&E, 200X).

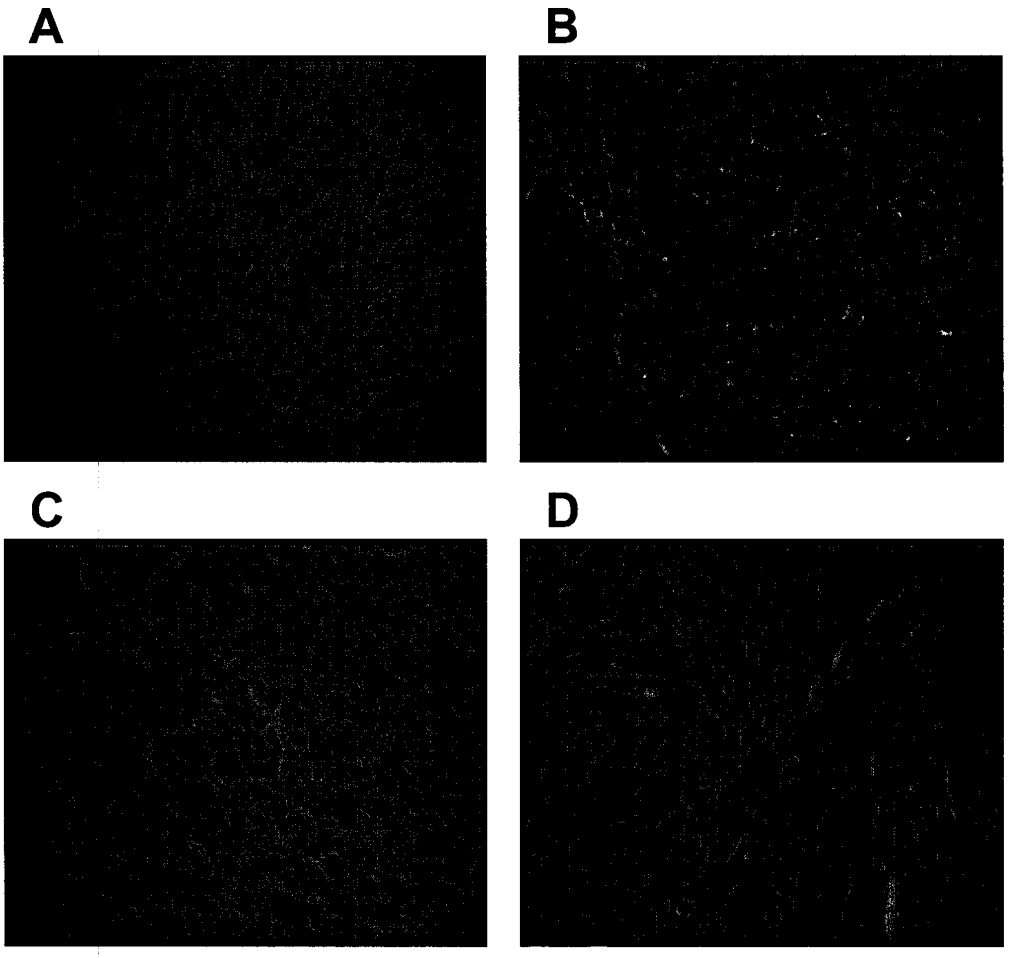
A
B
C
D

Figure 38: Staining of tumours for CK19. Paraffin sections (5μm) of tumours from all of the genotypes were stained for CK19 expression. **A)** *Trp53*$^{\Delta 2\text{-}10}$ (400X) B) *Brca1*$^{\Delta 5\text{-}13}$/*Trp53*$^{\Delta 2\text{-}10}$ (400X) **C)** *Rb*$^{\Delta 19}$/*Trp53*$^{\Delta 2\text{-}10}$ (25X) **D)** *Rb*$^{\Delta 19}$/ *Brca1*$^{\Delta 5\text{-}13}$/*Trp53*$^{\Delta 2\text{-}10}$ (100X). Positive areas (generally glandular structures, arrows) are stained reddish-brown.

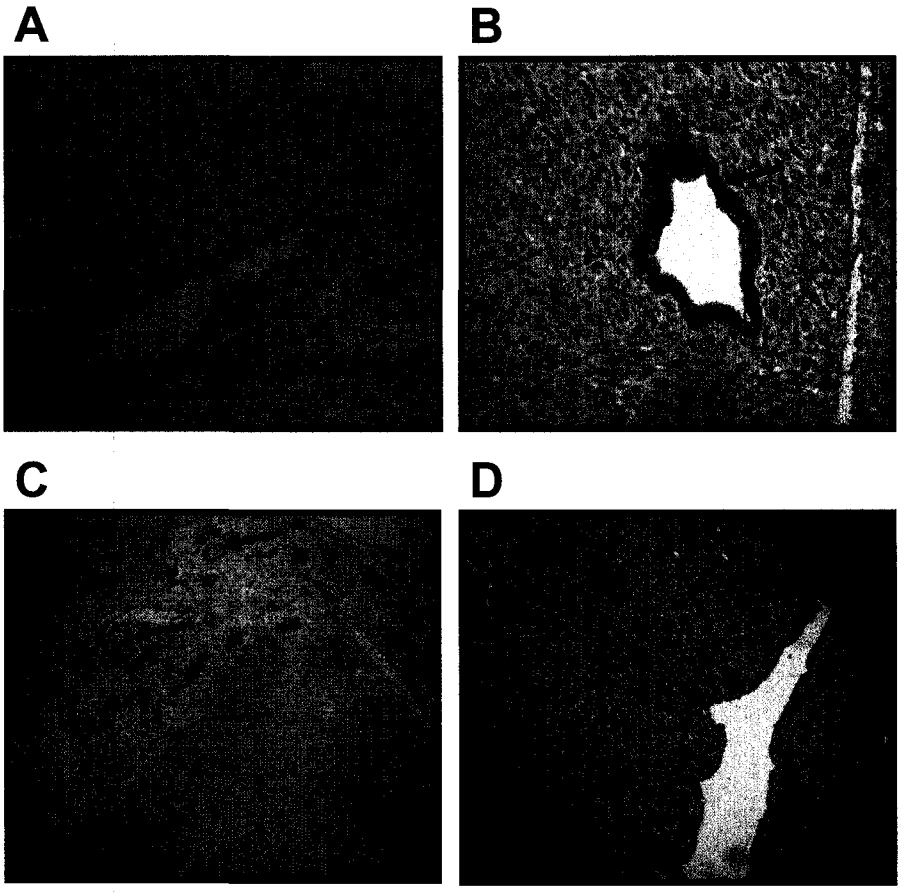
A
B
C
D

Figure 39: Staining of tumours for SMA and Desmin. Sections of tumours from all of the genotypes were stained for the presence of the muscle markers SMA and Desmin. Immunohistochemical staining to detect SMA (A, C, E, and G, brownish-red stain) and Desmin (B, D, F, and H, brownish-red stain) for tumours of the following genotypes: $Trp53^{\Delta 2\text{-}10}$ (A-B), $Brca1^{\Delta 5\text{-}13}/Trp53^{\Delta 2\text{-}10}$ (C-D), $Rb^{\Delta 19}/Trp53^{\Delta 2\text{-}10}$ (E-F), and $Rb^{\Delta 19}/Brca1^{\Delta 5\text{-}13}/Trp53^{\Delta 2\text{-}10}$ (G-H). (Magnification is 200X for A, C, and G, 100X for B , D, and H, 25X for E, and 400X for F).

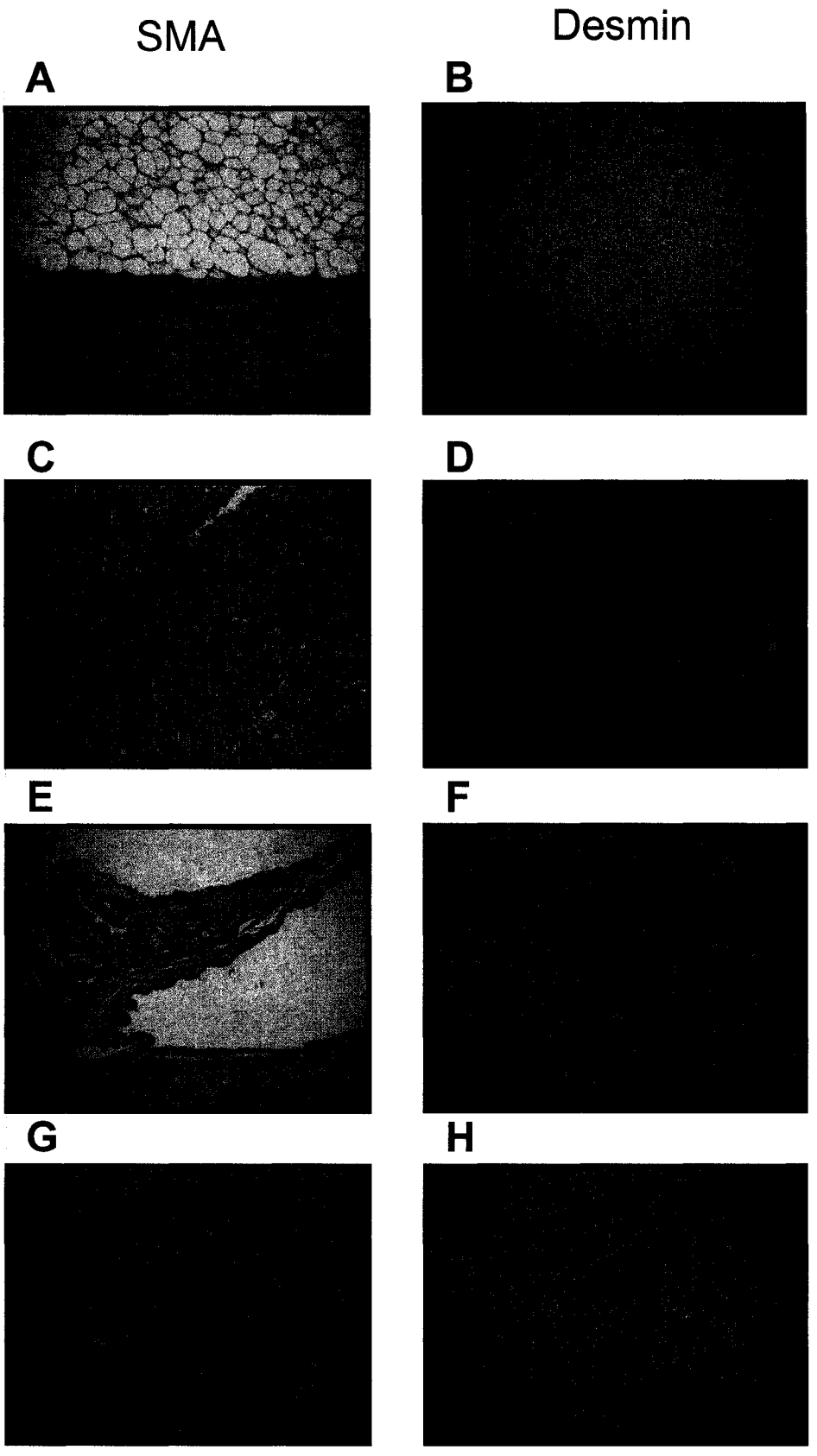
SMA
Desmin
A
B
C
D
E
F
G
H

Figure 40: Staining of tumours for CD34. Sections of tumours from all of the genotypes were stained for expression of CD34. **A)** *Trp53*$^{\Delta 2\text{-}10}$ (200X) B) *Brca1*$^{\Delta 5\text{-}13}$/*Trp53*$^{\Delta 2\text{-}10}$ (200X) **C)** *Rb*$^{\Delta 19}$/*Trp53*$^{\Delta 2\text{-}10}$ (200X) **D)** *Rb*$^{\Delta 19}$/ *Brca1*$^{\Delta 5\text{-}13}$/*Trp53*$^{\Delta 2\text{-}10}$ (400X). Positive areas (blood vessels) are stained reddish-brown.

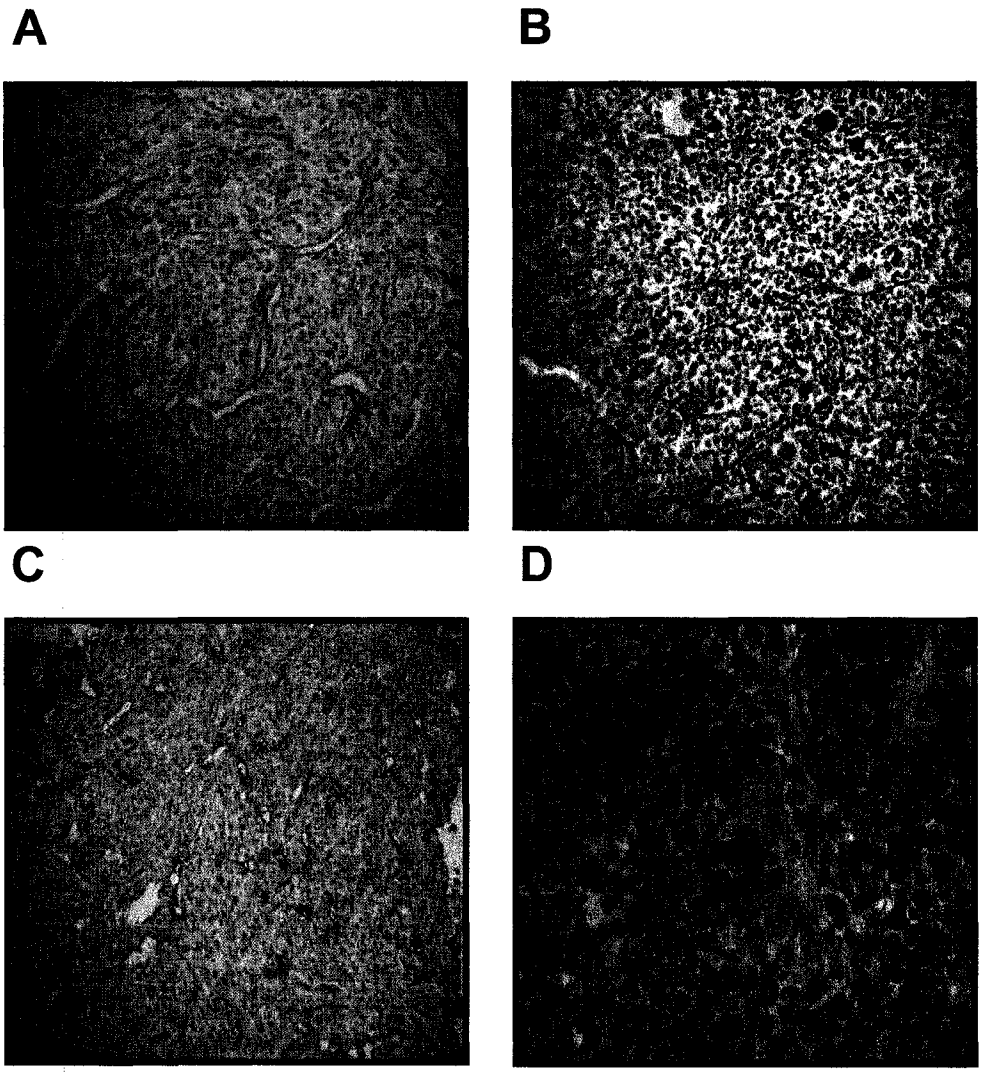
A
B
C
D

The gross pathology along with the H&E sections provided some clues as to the origin of the tumours. In some instances, normal ovary was visible at the edge of a tumour, such that the bursal membrane that surrounds the ovary was flush with the tumour (**Figure 41A**). In some cases, even when normal ovary was not grossly visible on autopsy, the ovary was found within the H&E section of the tumour (**Figure 41B**). In these sections, the tumour also appears to be connected to the bursal membrane (**Figure 41C**). Staining of sections of normal ovaries revealed that the bursa, which is an extension of the oviduct, is highly positive for SMA (**Figure 42A**). Staining also revealed that the inner lining of the bursal membrane is positive for CK19 (**Figure 42B**).

While both ovaries in each mouse were subjected to intrabursal injection, in the vast majority of the AdCre injected mice tumour formation was seen unilaterally. While the contralateral ovary appeared grossly normal on autopsy, H&E sections often revealed a thickened bursal membrane (**Figure 43A-D**).

Ovaries from the 60-day post-intrabursal injection time point were examined from mice from all genotypes. This time point was used as no loss-of-wellness endpoints were reached prior to this point. The *Trp53*$^{\Delta 2\text{-}10}$ mice displayed significantly less overall surface epithelial morphology changes than their AdGFP-injected counterparts at the 60-day time point (1.18±0.33 versus 3.73±0.67, $P<0.01$, numbers represent the mean ±SEM number of morphological changes per section over five non-consecutive sections, **Table 7**). There was no significant difference in the number of areas of columnar cells between these two groups, however there were significantly fewer areas of hyperplasia in the *Trp53*$^{\Delta 2\text{-}10}$ ovaries as compared to their controls (0.40±0.14 versus 2.48±0.54, $P<0.01$, **Table 7**). There were no statistically significant differences in the number of ovarian

Figure 41: Tumours appear to be associated with the ovarian bursal membrane. A) Gross anatomical image of involvement of ovarian bursal membrane with tumour. **B)** and **C)** H&E section illustrating involvement of ovarian bursal membrane with tumour. T= tumour, b= bursal membrane, Ov= oviduct, O= ovary, and u=uterus. (25X)

A

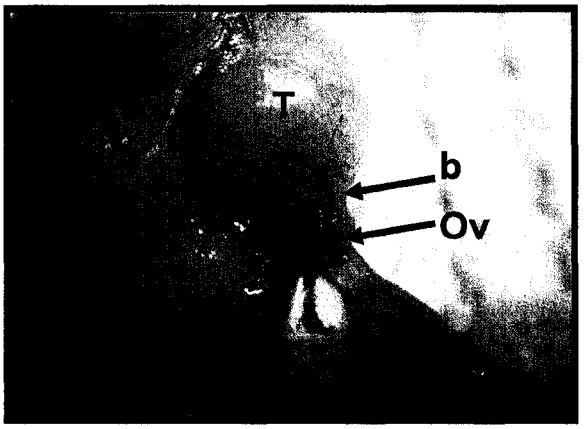

B

C

Figure 42: Staining of the bursal membrane for SMA and CK19. Sections of normal ovary with an intact bursal membrane were stained for expression of SMA and CK19. **A)** SMA staining (reddish-brown stain) of a normal ovary with an intact bursal membrane (25X) **B)** CK19 staining (reddish-brown stain) of a normal ovary with an intact bursal membrane (400X).

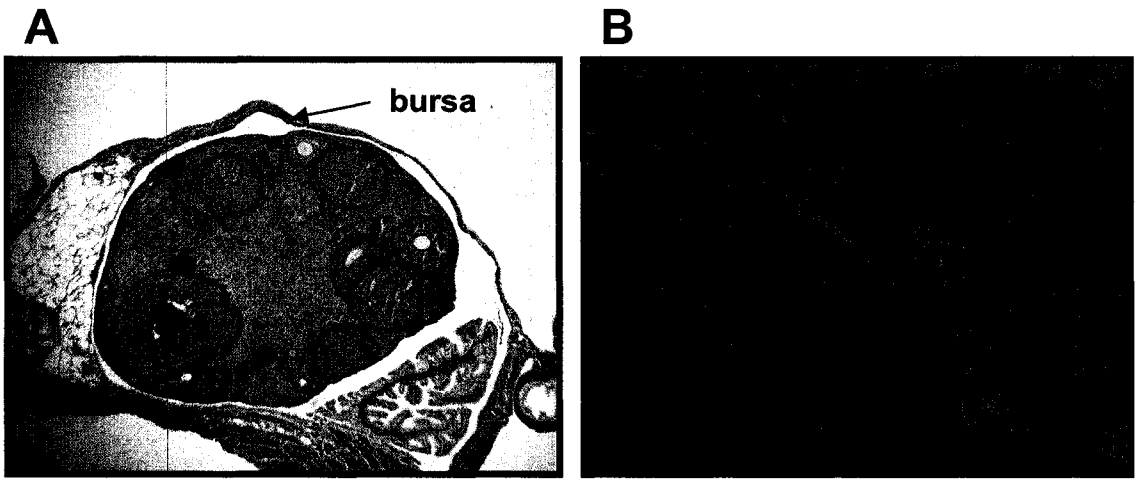
A
bursa
B

Figure 43: Contralateral ovaries display a thickened bursal membrane. A) The normal bursal membrane is quite thin (arrow) **B-D)** representative sections of ovaries from animals in which the other ovary was associated with tumour. Arrows indicated the thickened bursal membrane. (H&E, 25X)

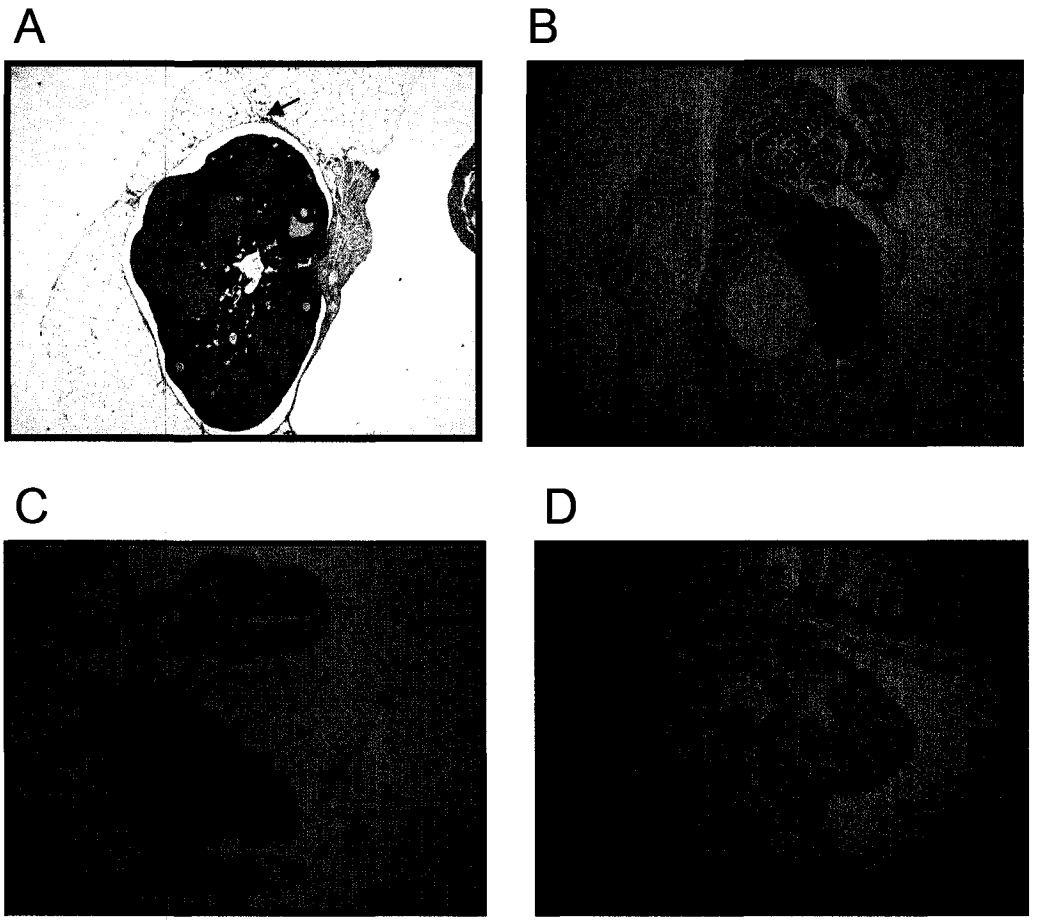
A
B
C
D

Table 7: Distribution of morphological features in the OSE 60 days following conditional inactivation of *p53*.

Epithelial Morphology	Genotype	Number of Events n= number of ovaries
Areas of Columnar Cells	**$Trp53^{\Delta 2\text{-}10}$**	0.78±0.23 (n=9)
	$p53^{loxP/loxP}$	1.25±1.17 (n=8)
Areas of Hyperplasia	**$Trp53^{\Delta 2\text{-}10}$**	0.40±0.14 **
	$p53^{loxP/loxP}$	2.48±0.54
Epithelial Invaginations	**$Trp53^{\Delta 2\text{-}10}$**	0
	$p53^{loxP/loxP}$	0
Inclusion Cysts	**$Trp53^{\Delta 2\text{-}10}$**	0
	$p53^{loxP/loxP}$	0
Total Changes	**$Trp53^{\Delta 2\text{-}10}$**	1.18±0.33 **
	$p53^{loxP/loxP}$	3.73±0.67

Numbers represent the mean ±SEM of the mean number of morphological changes per section over five non-consecutive sections in n ovaries. **indicates a significant difference between the $Trp53^{\Delta 2\text{-}10}$ group and the $p53^{loxP/loxP}$ group at that time point ($P<0.01$).

surface epithelial morphology alterations between the *Brca1*$^{\Delta 5\text{-}13}$/*Trp53*$^{\Delta 2\text{-}10}$ mice and their controls (**Table 8**) or the *Rb*$^{\Delta 19}$/ *Trp53*$^{\Delta 2\text{-}10}$ mice and their controls (**Table 9**) at the 60 day time point. While the ovaries of the *Rb*$^{\Delta 19}$/*Brca1*$^{\Delta 5\text{-}13}$/*Trp53*$^{\Delta 2\text{-}10}$ mice displayed over 1.5 times as many areas of hyperplasia than those of their controls, the difference was not significant (3.06±0.40 versus 1.84±0.43, P=0.05, Table 10) and there was no difference in the total number of surface epithelial changes between these two groups at the 60-day time point (**Table 10**).

Table 8: Distribution of morphological features in the OSE 60 days following conditional inactivation of *Brca1* and *p53*.

Epithelial Morphology	Genotype	Number of Events n= number of ovaries
Areas of Columnar Cells	**$Brca1^{\Delta 5\text{-}13}/Trp53^{\Delta 2\text{-}10}$**	1.62±0.30 (n=10)
	$Brca1^{loxP/loxP}/p53^{loxP/loxP}$	1.22±0.36 (n=9)
Areas of Hyperplasia	**$Brca1^{\Delta 5\text{-}13}/Trp53^{\Delta 2\text{-}10}$**	0.96±0.27
	$Brca1^{loxP/loxP}/p53^{loxP/loxP}$	1.36±0.46
Epithelial Invaginations	**$Brca1^{\Delta 5\text{-}13}/Trp53^{\Delta 2\text{-}10}$**	0
	$Brca1^{loxP/loxP}/p53^{loxP/loxP}$	0
Inclusion Cysts	**$Brca1^{\Delta 5\text{-}13}/Trp53^{\Delta 2\text{-}10}$**	0
	$Brca1^{loxP/loxP}/p53^{loxP/loxP}$	0
Total Changes	**$Brca1^{\Delta 5\text{-}13}/Trp53^{\Delta 2\text{-}10}$**	2.58±0.42
	$Brca1^{loxP/loxP}/p53^{loxP/loxP}$	2.58±0.49

Numbers represent the mean ±SEM of the mean number of morphological changes per section over five non-consecutive sections in n ovaries.

Table 9: Distribution of morphological features in the OSE 60 days following conditional inactivation of *Rb* and *p53*.

Epithelial Morphology	Genotype	Number of Events n= number of ovaries
Areas of Columnar Cells		
	$Rb^{\Delta 19}/Trp53^{\Delta 2\text{-}10}$	1.65±0.34 (n=12)
	$Rb^{loxP/loxP}$ /$p53^{loxP/loxP}$	2.22±0.30 (n=10)
Areas of Hyperplasia		
	$Rb^{\Delta 19}/Trp53^{\Delta 2\text{-}10}$	2.02±0.40
	$Rb^{loxP/loxP}$ /$p53^{loxP/loxP}$	1.22±0.25
Epithelial Invaginations		
	$Rb^{\Delta 19}/Trp53^{\Delta 2\text{-}10}$	0
	$Rb^{loxP/loxP}$ /$p53^{loxP/loxP}$	0
Inclusion Cysts		
	$Rb^{\Delta 19}/Trp53^{\Delta 2\text{-}10}$	0
	$Rb^{loxP/loxP}$ /$p53^{loxP/loxP}$	0
Total Changes		
	$Rb^{\Delta 19}/Trp53^{\Delta 2\text{-}10}$	3.67±0.61
	$Rb^{loxP/loxP}$ /$p53^{loxP/loxP}$	3.44±0.47

Numbers represent the mean ±SEM of the mean number of morphological changes per section over five non-consecutive sections in n ovaries.

Table 10: Distribution of morphological features in the OSE 60 days following conditional inactivation of *Rb, p53* and *Brca1*.

Epithelial Morphology	Genotype	Number of Events n= number of ovaries
Areas of Columnar Cells		
	$Rb^{\Delta 19}/Trp53^{\Delta 2\text{-}10}/Brca1^{\Delta 5\text{-}13}$	2.50±0.34 (n=10)
	$Rb^{loxP/loxP}/p53^{loxP/loxP}/Brca1^{loxP/loxP}$	2.83±0.54 (n=10)
Areas of Hyperplasia		
	$Rb^{\Delta 19}/Trp53^{\Delta 2\text{-}10}/Brca1^{\Delta 5\text{-}13}$	3.06±0.40
	$Rb^{loxP/loxP}/p53^{loxP/loxP}/Brca1^{loxP/loxP}$	1.84±0.43
Epithelial Invaginations		
	$Rb^{\Delta 19}/Trp53^{\Delta 2\text{-}10}/Brca1^{\Delta 5\text{-}13}$	0
	$Rb^{loxP/loxP}/p53^{loxP/loxP}/Brca1^{loxP/loxP}$	0
Inclusion Cysts		
	$Rb^{\Delta 19}/Trp53^{\Delta 2\text{-}10}/Brca1^{\Delta 5\text{-}13}$	0
	$Rb^{loxP/loxP}/p53^{loxP/loxP}/Brca1^{loxP/loxP}$	0
Total Changes		
	$Rb^{\Delta 19}/Trp53^{\Delta 2\text{-}10}/Brca1^{\Delta 5\text{-}13}$	5.56±0.69
	$Rb^{loxP/loxP}/p53^{loxP/loxP}/Brca1^{loxP/loxP}$	4.67±0.80

Numbers represent the mean ±SEM of the mean number of morphological changes per section over five non-consecutive sections in n ovaries.

Chapter 5: Discussion

This study is the first to demonstrate that inactivation of the *Brca1* tumour suppressor gene in the mouse OSE leads to an increase in morphological changes in that tissue that may constitute premalignant lesions similar to those that have been reported in human prophylactic oophorectomy specimens from *BRCA1* germline mutation carriers. The number and scope of morphological changes in the OSE increased in both the ovaries in which *Brca1* had been conditionally inactivated and in control ovaries, which was not unexpected, as an increase in alterations in surface epithelial morphology with age has been previously reported in mice (Tan, et. al., 2005) and humans . Significant increases in these changes arose earlier in the $Brca1^{\Delta 5\text{-}13}$ OSE, however, and there were significantly more epithelial changes overall observed in the ovaries of these animals than in controls at 240 days following intrabursal injection. These data indicate that loss of function of the *Brca1* tumour suppressor gene in this tissue may accelerate the development of morphologic alterations, resulting in the earlier appearance of some of the more complex epithelial changes, such as invaginations and inclusion cysts.

Epithelial invaginations and inclusions cysts have long been proposed to be the precursor lesions of ovarian carcinoma , representing the most advanced morphologic changes in the OSE. Age at diagnosis of ovarian cancer is typically much earlier in *BRCA1* mutation carriers (54 years versus 63 years in non-carriers) (Boyd, et. al., 2000), and as our data and human prophylactic oophorectomy specimens would suggest, preneoplastic changes in the ovarian epithelium also appear earlier. There were significantly more areas of columnar epithelial cells noted in the ovaries of control mice

at the earliest time point; however this difference was not sustained through the later time points. It is possible that this observation was due the expression of, or immune reaction to, eGFP that was not seen in adenoviral Cre recombinase infected cells.

We found no difference in expression levels or patterns of several proteins, specifically p53, E-cadherin, and Collagen IV, known to be markers of human ovarian tumourigenesis between the *Brca1*$^{\Delta 5\text{-}13}$ and control groups, which may point to a species-related difference or may suggest that alteration in the expression of these proteins is not a direct consequence of inactivation of *Brca1* and is related to genetic events that occur later in transformation. We immunostained all of our ovarian sections for p53 expression and found none in any of the samples examined. It could be that such an event occurs later than the time points we examined or was simply not detectable by this method. The same may be said for the lack of differences in expression with the other proteins examined, E-cadherin and collagen IV. E-cadherin expression is absent in the normal human OSE, with overexpression seen in inclusion cysts and tumours . Rodents normally do express E-cadherin in the OSE, thus it was hypothesized that perhaps in mice expression would be reduced or lost with morphologic changes consistent with preneoplasia, however we did not observe any difference in level of expression between the *Brca1*-deficient and the *Brca1* wildtype OSE. Collagen IV expression has been shown to be decreased or lost in the OSE and epithelial inclusion cysts and with tumourigenesis in EOCs (Capo-chichi, et. al., 2002). We did not observe any difference in collagen IV staining between the *Brca1*-deficient and the *Brca1* wildtype ovaries examined. Again, these may be alterations that are simply not detectable until a later time point or may not be related to the *Brca1* status of the cells. As adhesion molecules as well

as components of the ECM may be related to the increased structural changes observed in the *Brca1*-deficient OSE, it would be valuable to expand the immunohistochemical panel to include more ECM components such as laminin and other members of the collagen family, as well as other adhesion molecules such as other cadherin family members and integrins.

We evaluated the proliferative capacity of the OSE in which *Brca1* had been inactivated *in vivo* by staining ovarian sections for the proliferation marker Ki67. Studies of prophylactic oophorectomy specimens have found conflicting results in this area, with some studies demonstrating an increase in proliferation in the OSE of *BRCA1* mutation carriers (Schlosshauer, et. al., 2003), while others found no difference (Barakat, et. al., 2000). Our results indicate that the increase in the number of areas of altered epithelial morphology in the OSE due to inactivation of *Brca1* is not accompanied by a notable change in proliferation, thus the morphological changes observed are not necessarily the result of the loss of the growth suppressor activity of *Brca1*. Our analysis of the effect of inactivation of *Brca1* in MOSE cells *in vitro* also found that the *Brca1*-deficient cells did not proliferate faster than controls and in fact loss of *Brca1* function appeared to suppress their proliferation, which was in fact due to a nearly two-fold increase in basal levels of apoptosis. These results may seem counterintuitive, given the tumour suppressor status of *Brca1*, however *Brca1* null mice die embryonically due to major proliferation defects and increased apoptosis (Hakem, et. al., 1996) and cultures of mouse embryonic fibroblasts with a deletion of exon 11 of *Brca1* display a senescence-like growth defect (Cao, et. al., 2003). With prolonged culture of the $Brca1^{\Delta 5\text{-}13}$ MOSE, there was a decrease in the proportion of the population with recombination at the loxP sites, with a corresponding

resurgence of the wildtype population that remained after the initial infection. This also indicates that these cells are not tolerant of the inactivation of *Brca1*, and hence the culture is overtaken by the remaining *Brca1* wildtype cells. This phenomenon has not been investigated extensively in the ovary; though one study found that human OSE cells from women with a known or suspected germline mutation in *BRCA1* proliferated at a slower rate than the OSE of their normal counterparts (Kruk, et. al., 1999). Our study is the first to demonstrate this effect in a conditional model of *Brca1* inactivation in the mouse OSE, which thereby suggests that this model may be suitable for more thorough investigations of the role of *BRCA1* in the behavior of the ovarian surface epithelium.

It has been postulated that loss of function of *Brca1* results in a destabilized genome that is more sensitive to DNA-damaging assaults. Thus, in the absence of the caretaker function of *Brca1*, other DNA-damage repair and cell cycle regulatory pathways, such as those inducing *p53* and *Rb*, are activated resulting in slowed proliferation as damage is repaired. It may be that complete loss of function of *Brca1* in normal adult tissues simply creates a genetically unstable environment, the impact of which is not wholly evident until further genetic alterations take place. We propose that an unstable genome in OSE cells, resulting from loss of function of *Brca1*, results in altered cell behavior manifested as morphological changes that arise earlier and are more numerous than what can simply be attributed to ageing. Our *in vitro* data would suggest that OSE cells in which *Brca1* has been inactivated are more sensitive to DNA damaging agents, indicating a possible repair defect. Cell death in the OSE due to an inability to recognize and repair DNA damage could possibly result in tissue remodeling that would produce the morphologic alterations reported here, however the exact mechanism by

which these cellular events translate to these more global tissue changes remains unknown.

Alterations in tissue homeostasis due to the imbalance of increased apoptosis with decreased proliferation that accompanies inactivation of *Brca1* in MOSE cells may provide insight into how this genetic change translates into alterations in tissue morphology. Apoptosis has been shown to be a key mediator of tissue remodeling in several developmental scenarios. Coordinated cell death is an integral part of the invagination that occurs during gastrulation (Sanders, et. al., 1997) as well as mammary gland involution following cessation of lactation (Strange, et. al., 1992). It is also a critical component of the lumen formation seen during blastocyst cavitation, terminal end bud development in the mammary gland, as well as development of the neural crest (Zahir and Weaver, 2004). Various *Brca1* mutants display defects in all of these processes (Liu, et. al., 1996; Hakem, et. al., 1998), indicating a role for this gene in the tissue remodeling events necessary for proper development. Increased cell loss via apoptosis without corresponding proliferation to compensate can also be likened to a failure in wound repair. Viable *Brca1*-deficient mice have been shown to have a reduced capacity for wound healing and display features of premature ageing (Cao, et. al., 2003). As well, cultured OSE cells from women with a significant family history of EOC, and hence likely a *BRCA1* mutation, are less likely to undergo epithelial-mesenchymal transition, a process likened to the processes of wound repair (Dyck, et. al., 1996). Thus it may be that the *Brca1*-deficient OSE is displaying the physiologic result of this imbalance in apoptosis and proliferation (**Figure 44**). In order to examine this in greater

Figure 44: Proposed model of inactivation of *Brca1* in the OSE *in vivo*. Inactivation of Brca1 in OSE cells leads to decreased proliferation and increased apoptosis that results in tissue remodeling and aberrant wound healing in this tissue resulting in an increase in preneoplastic changes. This tissue would then be increasingly susceptible to further genetic changes such as the loss of *p53* as well as other tumour suppressor genes or inactivation of oncogenes potentially contributing to transformation and tumourigenesis.

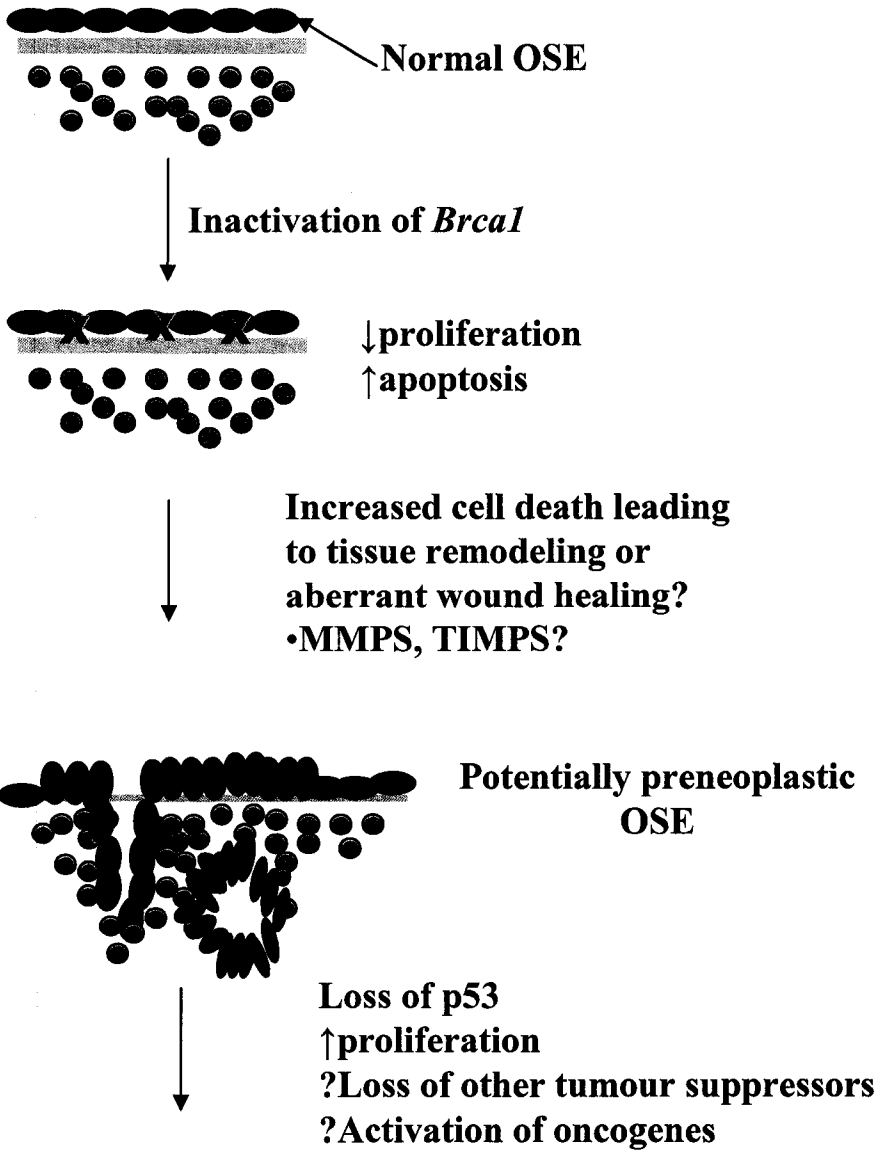

Transformation/Tumourigenesis?

detail, it would be of interest to assess the expression of proteins involved in this type of tissue remodeling, such as matrix metalloproteinases, tissue inhibitors of metalloproteinases, and plasminogen activator in the *Brca1*-deficient and wildtype OSE cells both *in vitro* and *in vivo*. It would also be of interest to examine the wound repair capability of these cells via scratch assays.

There is considerable evidence, from both knockout models and mammary tumour models, that the *p53* tumour suppressor gene plays a significant role in both *Brca1*-associated growth control and tumourigenesis (Cressman, et. al., 1999; Xu, et. al., 2001b). *p53* dysfunction is commonly associated with ovarian carcinoma, particularly in tumours associated with a germline *BRCA1* mutation (Lakhani, et. al., 2004), and prophylactic oophorectomy specimens from *BRCA1* heterozygotes have demonstrated increased p53 immunostaining in the OSE . As mentioned, we immunostained all of our ovarian sections for p53 expression and found none in any of the samples examined. It could be that such an event occurs later than the time points we examined or was simply not detectable by this method.

While upregulation of p53 expression was not observed in MOSE cells in which *Brca1* had simply been inactivated, increased protein levels were seen in these cells when they were challenged with the DNA-damaging agent cisplatin, a chemotherapeutic agent commonly used to treat ovarian cancer. These cells were also more sensitive to treatment with cisplatin, as measured by cell survival, providing further evidence for the hypothesis that loss of *Brca1* in the OSE leads to a DNA-damage repair defect and hence destabilized genome that, in the presence of intact *p53* function, results in a commitment to cell death. Cisplatin treatment did result in an increase in apoptosis, as determined by

the sub G1 fraction, which was more pronounced in the *Brca1*$^{\Delta 5\text{-}13}$ cells. This observation is in keeping with the finding that ovarian cancer patients bearing germline *BRCA1* mutations display an improved initial response to cisplatin treatment and slightly improved survival as a result (Cass, et. al., 2003). The *p53* status of these cells also modulated their sensitivity to cisplatin treatment. While *Trp53*$^{\Delta 2\text{-}10}$ cells were also more sensitive to cisplatin than *p53*$^{loxP/loxP}$ MOSE cells, there was no difference in cisplatin sensitivity seen between the *Brca1*$^{\Delta 5\text{-}13}$/ *Trp53*$^{\Delta 2\text{-}10}$ MOSE and *Brca1*$^{loxP/loxP}$/ p53$^{loxP/loxP}$ MOSE. Loss or aberrant expression of *p53* has been previously associated with an increase in sensitivity to cisplatin in normal human foreskin fibroblasts (Hawkins, et. al., 1996) as well as in ovarian cancer cells lines (Gibb, et. al., 1997). Our result disagrees with a study of *Brca1* inactivation in *p53*-null mouse cells that found that cells deficient in both *Brca1* and *p53* were increasingly sensitive to carboplatin, a platinum-based chemotherapeutic agent highly similar to cisplatin (Fedier, et. al., 2003). A very recent study by Xing and Orsulic concluded that loss of *Brca1* increased the sensitivity of the mouse OSE to cisplatin treatment; however these cells were also *p53*-deficient as well as overexpressing c-myc (Xing and Orsulic, 2006). As it appears that *p53*-deficiency at least partially rescues embryonic lethality phenotype of *Brca1* null mice (Hakem, et. al., 1997), it may be that the phenotype of increased cisplatin sensitivity that was observed in the *Brca1*-deficient MOSE cells is also being "rescued" by concomitant *p53* deficiency. This is not a phenomenon that has been extensively studied in normal cells, and thus these results warrant further investigation.

Whether inactivation of the tumour suppressor *Rb* in conjunction with *Brca1* was able to modify sensitivity to cisplatin was examined and found that it was. The *Rb*$^{\Delta 19}$

MOSE cells were significantly more sensitive to the cisplatin treatment than the *Rb* wildtype MOSE, as was seen with the *Brca1*$^{\Delta 5\text{-}13}$ MOSE cells; however the combined inactivation of both *Rb* and *Brca1* in these cells had no effect on cisplatin sensitivity. The same result was seen when we concomitantly inactivated all three tumour suppressors, *Brca1*, *p53*, and *Rb*, in the MOSE cells, i.e. there was no significant difference in sensitivity to the cisplatin treatment. Loss of *Rb* in Schwann cells was recently shown to result in an increased sensitivity to cisplatin (Seeley, et. al., 2007) and the same phenomenon has been seen in cultured breast cancer cells (Bosco, et. al., 2007), indicating a possible role for this gene as a modifier of chemotherapeutic response, and our results indicate it could potentially have a similar role in ovarian cells. As with loss of *Brca1*, loss of *Rb* has been shown to cause an increase in p53 expression (Mayhew, et. al., 2004) in response to DNA-damaging agents, indicating that its loss may be compensated for by the activation of cell cycle checkpoints that would induce programmed cell death. It would be of interest to examine whether this is the case in *Rb*-deficient MOSE cells. As to why the increased sensitivity to cisplatin treatment observed when only one tumour suppressor gene is inactivated in the MOSE cells is lost when two or more are inactivated simultaneously, it may be that these cells are now beginning to more closely resemble the molecular environment of tumour cells, with multiple abnormalities in several pathways. Ovarian carcinomas notoriously become chemoresistant with disease progression, when the tumour has likely acquired multiple genetic lesions. Cisplatin-resistant ovarian tumour cells, as well as cervical carcinoma cells have been shown to harbour multiple genetic changes, particularly affecting pathways leading to apoptosis that render the cells aberrantly tolerant of accumulated

DNA damage (Perego, et. al., 1998; Lanzi, et. al., 1998). If loss of *Brca1* results in compensation in the cell by the *p53* or *Rb* pathways resulting in increased apoptotic response, which ultimately produces the observed phenotype of increased cisplatin sensitivity, then it stands to reason that loss of either *p53* or *Rb* expression would prevent or at least lessen this phenotype.

Paclitaxel is another chemotherapeutic agent that is commonly used in the treatment of EOC. Unlike platinum-based treatments, which inflict DNA damage, taxanes are microtubule poisons that cause microtubule stabilization to the point where mitosis is impossible. We treated cultured MOSE cells of the various genotypes with and without AdCre exposure to treatment with paclitaxel in order to examine the effect of inactivation of the various tumour suppressors on the sensitivity of these cells to this agent. The $Brca1^{\Delta 5\text{-}13}$ MOSE cells were modestly but statistically significantly less sensitive to treatment with 25 nM of paclitaxel than the *Brca1* wildtype MOSE. *Brca1*-deficient cells have been shown in the past to display decreased sensitivity to treatment with paclitaxel. MCF-7 breast cancer cells treated with a small interfering RNA (siRNA) for *BRCA1* were more less sensitive to paclitaxel treatment (Chabalier, et. al., 2006), and this was also demonstrated in a an ovarian cancer cell line harbouring a *BRCA1* nonsense mutation (Zhou, et. al., 2003). Conversely, overexpression of BRCA1 in a breast carcinoma cell line increased paclitaxel sensitivity (Quinn, et. al., 2003). Chabalier, et al, demonstrated that downregulation of BRCA1 resulted in premature inactivation of the mitotic spindle checkpoint, resulting in the paclitaxel resistance (Chabalier, et. al., 2006) , thus it would be interesting to examine the status of the spindle checkpoint of the $Brca1^{\Delta 5\text{-}13}$ MOSE cells in greater detail, with and without taxane treatment. Of particular

interest would be the examination of cyclin B1 and cdk1 protein levels in these cells, whose degradation is inhibited when the spindle checkpoint is correctly activated (Yu, 2002).

Inactivation of either *p53* or *Rb* alone in the MOSE had no impact on paclitaxel sensitivity. It has in fact been shown in ovarian cancer cell lines that *p53* status may not be related to paclitaxel sensitivity (Takahashi, et. al., 2000). Conditional inactivation of *p53* and/or *Rb* in conjunction with *Brca1* in the MOSE cells also had no impact on sensitivity to paclitaxel. Thus it could be argued that *p53* or *Rb* status does have an effect on paclitaxel sensitivity in *Brca1*-deficient MOSE cells. As with the cisplatin treatment, it could be that the MOSE cells with more than one tumour suppressor pathway compromised are beginning to more closely resemble the molecular state of tumour cells, which often develop resistance to paclitaxel. While these cells are not resistant to paclitaxel treatment, they do not demonstrate increased sensitivity.

This study also found, when OSE cell proliferation was examined *in vitro*, that concomitant inactivation of *p53* in MOSE cells rescued the growth suppression that was seen with inactivation of *Brca1* alone and leads to a substantially increased growth rate as compared to control cells. Inactivation of p53 alone in MOSE cells had no immediate effect on proliferation. Loss of p53 function has been demonstrated to partially rescue the embryonic lethality of complete deletion of *Brca1* and appears to play a critical role in mammary tumourigenesis in mice (Hakem, et. al., 1997). Inactivation of the *Rb* tumour suppressor in conjunction with *Brca1* in MOSE cells also rescued the proliferation defect observed with inactivation of *Brca1* alone, however unlike with the $Brca1^{\Delta 5\text{-}13}/Trp53^{\Delta 2\text{-}10}$ MOSE cells, there was not a significant increase in the proliferation of the $Brca1^{\Delta 5\text{-}}$

$^{13}/Rb^{\Delta 19}$ cells. Examination of expression levels of the *Rb* family members p107 and p130 in these cells may be warranted to determine if there is compensation for the loss of *Rb*, this compensation being the primary reason *Rb*-null mice do not develop retinoblastoma (Robanus-Maandag, et. al., 1998). This could also explain why inactivation of *Rb* alone in the MOSE cells had no immediate effect on their proliferation. Concomitant inactivation of both *p53* and *Rb* did, however, result in a significant increase in proliferation in these MOSE cells. This was also observed by Flesken-Nikitin, *et al* in their MOSE cultures. Conditional inactivation of all three tumour suppressor genes, *Brca1*, *p53*, and *Rb* simultaneously in MOSE cells also resulted in a dramatic increase in proliferation with greater fold-increases in cell number between 48 and 72 hours and 72 and 96 hours than was seen in any of the other genotype combinations.

The study by Flesken-Nikitin, *et al* (2003) had found that inactivation of either *p53* or *Rb* in MOSE cells *in vitro* resulted in increased proliferation when measured three to six passages following adenoviral infection. Our study found similar results, indicating that with prolonged culture, these cells may be acquiring further genetic abnormalities that result in uncontrolled proliferation. Evaluation of other tumour suppressor pathways as well as oncogenic pathways in these cells via microarray would be warranted in order to begin to determine the exact nature of the other genetic changes required for transformation in these particular cells.

As these dramatic increases in proliferation *in vitro* pointed to possible transformation events, the cells of the various genotypes were assayed for their ability to proliferate in an anchorage-independent setting. The ability to proliferate independently of attachment to a substrate is a defining characteristic of cellular transformation. None of

the AdGFP-infected cells were capable of forming colonies in soft agar or proliferating on polyhema-coated plates, indicating that none of the parental MOSE lines had undergone spontaneous transformation. The *Brca1*$^{\Delta 5\text{-}13}$ cells were not capable of anchorage independent growth, and neither were the *Rb*$^{\Delta 19}$/ *Brca1*$^{\Delta 5\text{-}13}$ cells, indicating that inactivation of *Brca1* in MOSE cells *in vitro* is not sufficient to cause transformation, as assessed in this manner. The *Rb*$^{\Delta 19}$ MOSE cells were capable of anchorage-independent growth under both conditions. As inactivation of *Rb* in the *Brca1*-deficient MOSE did not result in the capability for this type of growth, it could mean that these cells have not incurred the additional genetic alterations that may have occurred in the *Rb*$^{\Delta 19}$ MOSE cells with time in culture. Alternatively, it could be that Brca1 mediates some aspect of the Rb-deficient phenotype and that without Brca1 this effect is lost, resulting in a different phenotype. Wildtype *BRCA1* has been shown to require *RB* in order to exert its growth suppressor capabilities (Aprelikova, et. al., 1999) and may also modulate the apoptotic response in *RB*-deficient cells (Wang, et. al., 2000), indicating that both of these genes depend, to a certain extent, on the status of the other. It is likely that had this assay been performed on the *Rb*$^{\Delta 19}$ MOSE cells within one passage of inactivation, no anchorage-independent growth would have been observed, as it is generally accepted that perturbations in more than one genetic pathway are needed to cause transformation in mouse cells (Rangarajan, et. al., 2004; Dimri, et. al., 2005).

The *Trp53*$^{\Delta 2\text{-}10}$ MOSE cells as well as the *Rb*$^{\Delta 19}$/*Trp53*$^{\Delta 2\text{-}10}$ cells were also capable of anchorage-independent growth under both sets of conditions. As with the *Rb*$^{\Delta 19}$, it is likely that the *Trp53*$^{\Delta 2\text{-}10}$ cells would not have exhibited this trait had they been assayed immediately following inactivation, as there was no difference in proliferation noted at

that point. It is not surprising that the MOSE cells in which both *Rb* and *p53* were inactivated display signs of transformation, as it is inactivation of these two pathways via SV40 TAg or human papilloma virus E6/E7 infection that is commonly used to transform cells.

When inactivated in conjunction with *p53*, the *Brca1*-deficient MOSE were capable of growth on polyhema-coated plates, however did not form colonies in soft agar. This discrepancy is intriguing, especially given the interesting morphology of these cells on the polyhema-coated plates. Exploring this phenotype further would warrant examining cell-cell adhesion molecules, as well as alternate matrices such as methylcellulose. Cells in which all three tumour suppressors were inactivated were capable of proliferation under both circumstances. Closer analysis of colony formation, in terms of the number of colonies and time to the appearance of the colonies is merited to accurately assess whether *Brca1*-deficiency precipitated colony formation, or whether alterations to the p53 and *Rb* pathways are more dominant in terms of transformation in these cells. Ultimately, all of the cells capable of any type of anchorage-independent growth should be injected subcutaneously into immunodeficient mice in order to assess their tumourigenicity, a true hallmark of transformation. It would be of great value to learn whether inactivation of *Brca1* decreased the latency of tumour development or influenced tumour pathology, as *BRCA1*-related EOCs are almost always adenocarcinomas of the serous subtype and present with early onset .

When *Brca1* was inactivated *in vivo* via intrabursal injection there was no tumourigenesis observed even when the animals were followed past one year post-injection, despite the development of significantly more premalignant changes in the OSE

of these ovaries. Given that not all women with *BRCA1* germline mutations go on to develop ovarian cancer, this result is not overly surprising. However, it was hypothesized that in the mouse OSE, *Brca1*-related tumourigenesis would require further genetic changes, such as inactivation of other tumour suppressor pathways, changes which perhaps never occur in the cohort of *BRCA1* mutation carriers that do not develop ovarian cancer. Thus identical experiments were undertaken in which *Brca1* was conditionally inactivated in the OSE *in vivo* in conjunction with inactivation of the tumour suppressors *p53* and/or *Rb*.

We repeated work done by Flesken-Nikitin, *et al* (2003) by conditionally inactivating *p53* and *Rb* alone or in tandem in the OSE *in vivo* via intrabursal AdCre administration, and then added the *Brca1*-deficient combinations. Based on their previous work, it was anticipated that the $Rb^{\Delta 19}/Trp53^{\Delta 2\text{-}10}$ mice would develop tumours with a median survival of just over 200 days, and that little to no tumour formation would be seen when either *p53* or *Rb* was inactivated alone. Thus it was surprising when in our study the $Rb^{\Delta 19}/Trp53^{\Delta 2\text{-}10}$ mice died of disease by a median time of 170 days and that the $Trp53^{\Delta 2\text{-}10}$ mice also developed tumours. It was also unforeseen that these tumours were not the adenocarcinomas observed in the Flesken-Nikitin study, but were classified as malignant leiomyosarcomas, tumours of smooth muscle origin. This discrepancy in the results cannot be accounted for in terms of intrabursal injection technique as our laboratory has also used this technique to drive conditional TAg expression (which targets the p53 and Rb pathways) to the OSE *in vivo* that resulted in the development of malignant epithelial ovarian tumours (L. Laviolette, unpublished data). The only notable difference between ours and the Flesken-Nikitin study is that they backcrossed their

animals so that they would be on a pure FVB/n strain background, whereas ours were FVB/n;129sv mixed background, the background on which the mice are maintained in the Mouse Models of Human Cancers Consortium Repository. As we were breeding the single conditional knockout transgenics together in order to achieve the various genotype combinations, it would have taken an unsuitably long period of time to also backcross them to the FVB/n background. We did not anticipate that this minor strain variation, especially as they are not two completely different strains, could have such a significant impact on the phenotype in these mice, however studies have recently begun to show that genetic modifiers based on strain can influence phenotype in mouse models of disease (LeCouter, et. al., 1998; Simpson, et. al., 2004; Woodworth, et. al., 2004).

Despite the unanticipated phenotype, it was found that *Brca1*-deficiency in these tumours influenced the survival time of the mice. Concomitant inactivation of *Brca1* in conjunction with *p53* in these tumours resulted in significantly decreased survival times as compared to the singular inactivation of *p53*, whereas inactivation of *Rb* in conjunction with *p53* did not. As the $Trp53^{\Delta 2\text{-}10}$ mice developed tumours it is not possible to determine if *p53*-deficiency is necessary for *Brca1*-related tumourigenesis of the OSE, however it does appear that *Brca1*-deficiency influences progression in the *p53*-deficient tumours. This is also the first time that *Brca1*-deficiency has been linked in any way to the tumourigenesis of leiomyosarcomas. Aberrations in both the p53 and Rb pathways have been implicated in the development and progression of leiomyosarcomas (de, et. al., 1994; Dei Tos, et. al., 1996; Leiser, et. al., 2006). It may be that the tumour pathology observed is due to strain-dependent tissue susceptibility to transformation, in that the smooth muscle cells of the bursal membrane, which would also be in contact with the

adenoviral Cre recombinase, are more sensitive to these consequences of these recombination events than the OSE.

As we have shown, the bursal membrane is largely composed of smooth muscle cells, much like the uterine and oviductal myometrium with which it is contiguous. The tumours that developed in these mice were generally found to be continuous with the bursal membrane, indicating that this was perhaps the tissue of origin. Despite the fact that both ovaries were subjected to intrabursal injection, the majority of animals developed unilateral tumours. The contralateral ovaries, however, frequently displayed thickened bursal membranes, possibly indicating a premalignant stage in this tissue. In order to accurately test this theory of the bursal membrane as the tissue of origin, one could perform the intrabursal adenoviral injections as was done, and then at a suitable time point following the initial surgery, perform a second surgery in a subset of mice in which the bursal membrane was removed as completely as possible in order to observe whether or not tumours still developed.

Ovaries from early time points of the genotypes which developed tumours were not especially informative in terms of premalignant activity in the OSE, as few differences were observed between the tumour suppressor-deficient groups and their appropriate controls, though the 60-day time point may have been too early to detect any major differences. As the time between the detection of tumours by palpation and loss-of-wellness endpoint was quite short in all of the animals, it would perhaps be beneficial to examine time points in closer proximity to tumour development and at shorter intervals. Inactivation of *Rb* alone in the OSE *in vivo* did not result in tumour formation, nor did it result in the presence of more epithelial morphologic changes than the wildtype ovaries.

This likely indicates that alterations *Rb* alone do not play a significant role in initiating events in ovarian tumourigenesis. Combined inactivation of *Brca1* and *Rb* in the OSE did result in more epithelial changes at the later time points, however the results were not significant. Epithelial invaginations were, however, found only in the *Rb/Brca1*-deficient ovaries and not in their wildtype counterparts. As was seen *in vitro*, it could be that the loss of *Rb* in conjunction with *Brca1* at least partially rescues the proliferation defect caused by *Brca1*-deficiency, which could account for the lack of overt differences in the number of epithelial changes *in vivo*, as this would work to maintain proliferation/apoptosis levels in these cells. The impact of these alterations, whether singular or in combination, on OSE cell proliferation *in vivo* requires further in depth analysis, which could be examined initially via injection and labeling with bromodeoxyuridine (BrdU).

With the results of this work, we propose that *Brca1*-deficiency in the OSE results in decreased proliferation and increased apoptosis, which could potentially result in aberrant tissue remodeling manifesting as premalignant morphologic changes such as epithelial invaginations and inclusion cysts. The sensitivity of these cells to the DNA-damaging agent cisplatin indicates a repair defect that could lead to the accumulation of genetic defects, resulting in the genomic instability so frequently observed in *Brca1*-deficient cells (Deng, 2006). An increase in genomic instability would render these cells and hence this tissue more susceptible to further genetic alterations, particularly loss of *p53*, which would ultimately lead to transformation and tumourigenesis (**Figure 45**).

Figure 45: A simplified hypothetical model of the impact of loss of *Brca1* in OSE cells on the molecular level. Following DNA damage in *Brca1*-deficient cells, loss of Brca1 will either be compensated for by increased expression of gatekeeper tumour suppressors such as p53 and/or Rb, resulting in cell cycle arrest while DNA is repaired followed by a return to the cell cycle or a commitment to apoptosis if the repair fails (left). The genomic instability resulting from *Brca1* deficiency also renders the cells more susceptible to mutations in these gatekeeper genes resulting in a failure to arrest the cell cycle and repair damage, leading to uncontrolled proliferation and eventually transformation (right). Adapted from (Welsch, et. al., 2000)

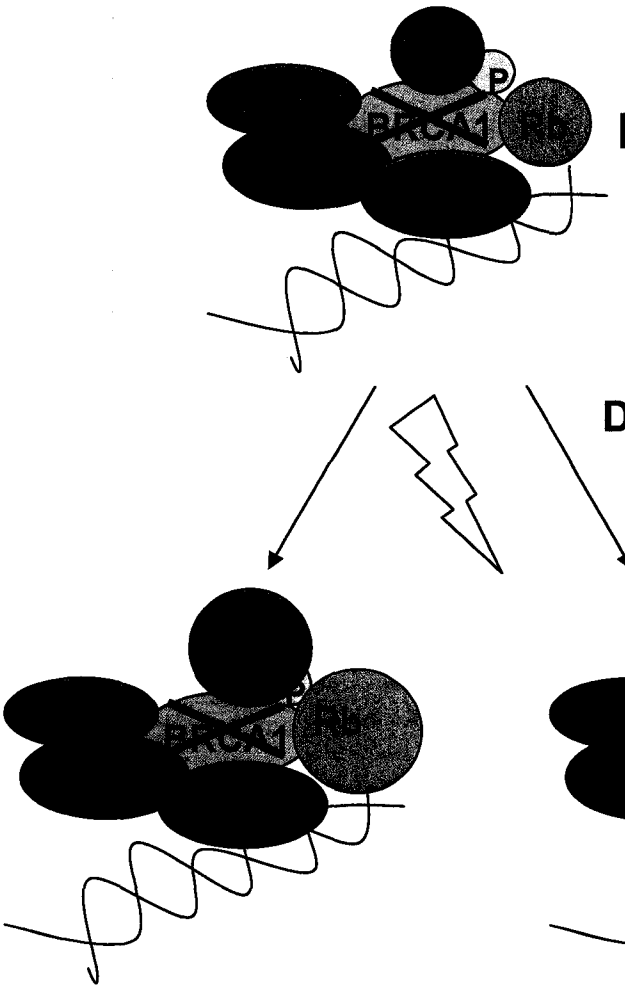

- ↑p53 and Rb
- Cell cycle arrest
- Repair or Apoptosis

- Susceptibility to mutations in p53 and Rb
- No cell cycle arrest
- Repair failure
- ↑proliferation
- transformation

Chodankar, et al, (2005) found that *Brca1* inactivation in the granulosa cells of mouse ovarian follicles led to the development of benign cystadenomas, however no carcinomas were seen. They proposed that, since these tumours possessed normal *Brca1* alleles, *Brca1* might influence tumour development indirectly via an effector secreted by granulosa cells. Our study found that inactivation of *Brca1* in the OSE led to the development of preneoplastic epithelial changes similar to those observed in the ovaries of human *BRCA1* mutation carriers, however was not sufficient for the formation of carcinomas. It may be that inactivation of *Brca1* in both epithelial and non-epithelial tissues of the ovary are necessary for a cooperative effect that would lead to carcinogenesis. Placing conditional inactivation of *Brca1* under the control of a ubiquitous ovarian promoter, such as that of MISIIR, would enable the investigation of this possibility. Utilizing this type of promoter to drive Cre expression specifically to the ovary in conjunction with the double and triple conditional knockout mice we have generated would also allow a more in-depth and specific analysis of the impact of loss of function of these genes, particularly the combined loss of *Brca1* and *p53*, in the ovary than what was able to be accomplished via the intrabursal injection method, given the unanticipated sensitivity of the bursal membrane to transformation.

As germline mutations in *BRCA1* result in an increased risk for cancers of the breast and ovaries, two tissues under the profound influence of hormonal regulation, it would also be of great interest to examine the impact of inactivation of *Brca1* in the OSE in a defined hormonal milieu. Using the model described here, it would be possible to subject the mice to intrabursal AdCre administration and then breed them continually over the course of the experiment order to examine the effect of the hormonal

environment of pregnancy on *Brca1*-deficient OSE cells. It would also be possible to pair the conditional inactivation of *Brca1* in the OSE with a newly developed mouse model of menopause (Hoyer and Sipes, 1996) in order to examine the impact of chronically elevated gonadotropins on *Brca1*-deficient cells. Of particular interest would be the effect of estrogen exposure, as *Brca1*-deficiency in granulosa cells has been shown to lead to increased aromatase activity which would result in increased circulating estrogen (Hu, et. al., 2005) and tamoxifen, a selective estrogen receptor modulator, has been shown to promote mammary tumourigenesis in the *Brca1*-deficient mammary gland (Jones, et. al., 2005).

Given the recent finding that as many as 15% of ovarian carcinomas are related to germline mutations in *BRCA1* (Pal, et. al., 2005a), coupled with the high rates of *BRCA1* dysfunction seen in sporadic ovarian tumours, it is imperative that we further our understanding of the role of this gene in transformation in the ovary. This mouse model of conditional inactivation of *Brca1* in the OSE will provide a useful tool for studying not only the impact of loss of function of *Brca1* in these cells, but also for examining the formation of early preneoplastic lesions in the ovary.

References

Aarnio, M., J. P. Mecklin, L. A. Aaltonen, M. Nystrom-Lahti, and H. J. Jarvinen. 1995. Life-time risk of different cancers in hereditary non-polyposis colorectal cancer (HNPCC) syndrome. Int J Cancer. 64, 430-433.

Abkevich, V., A. Zharkikh, A. M. Deffenbaugh, D. Frank, Y. Chen, D. Shattuck, M. H. Skolnick, A. Gutin, and S. V. Tavtigian. 2004. Analysis of missense variation in human BRCA1 in the context of interspecific sequence variation. J Med. Genet. 41, 492-507.

Adams, J. M. and S. Cory. 1991. Transgenic models of tumor development. Science. 254, 1161-1167.

An, H. J., D. S. Kim, Y. K. Park, S. K. Kim, Y. P. Choi, S. Kang, B. Ding, and N. H. Cho. 2006. Comparative proteomics of ovarian epithelial tumors. J Proteome. Res. 5, 1082-1090.

Andrews, H. N., P. B. Mullan, S. McWilliams, S. Sebelova, J. E. Quinn, P. M. Gilmore, N. McCabe, A. Pace, B. Koller, P. G. Johnston, D. A. Haber, and D. P. Harkin. 2002. BRCA1 regulates the interferon gamma-mediated apoptotic response. Journal of Biological Chemistry. 277, 26225-26232.

Antoniou, A., P. D. Pharoah, S. Narod, H. A. Risch, J. E. Eyfjord, J. L. Hopper, N. Loman, H. Olsson, O. Johannsson, A. Borg, B. Pasini, P. Radice, S. Manoukian, D. M. Eccles, N. Tang, E. Olah, H. nton-Culver, E. Warner, J. Lubinski, J. Gronwald, B. Gorski, H. Tulinius, S. Thorlacius, H. Eerola, H. Nevanlinna, K. Syrjakoski, O. P. Kallioniemi, D. Thompson, C. Evans, J. Peto, F. Lalloo, D. G. Evans, and D. F. Easton. 2003. Average risks of breast and ovarian cancer associated with BRCA1 or BRCA2 mutations detected in case Series unselected for family history: a combined analysis of 22 studies. Am. J. Hum. Genet. 72, 1117-1130.

Aprelikova, O., A. J. Pace, B. Fang, B. H. Koller, and E. T. Liu. 2001. BRCA1 is a selective co-activator of 14-3-3 sigma gene transcription in mouse embryonic stem cells. Journal of Biological Chemistry. 276, 25647-25650.

Aprelikova, O. N., B. S. Fang, E. G. Meissner, S. Cotter, M. Campbell, A. Kuthiala, M. Bessho, R. A. Jensen, and E. T. Liu. 1999. BRCA1-associated growth arrest is RB-dependent. Proc. Natl. Acad. Sci. U. S. A. 96, 11866-11871.

Arizti, P., L. Fang, I. Park, Y. Yin, E. Solomon, T. Ouchi, S. A. Aaronson, and S. W. Lee. 2000. Tumor suppressor p53 is required to modulate BRCA1 expression. Mol. Cell Biol. 20, 7450-7459.

Armstrong, D. K., B. Bundy, L. Wenzel, H. Q. Huang, R. Baergen, S. Lele, L. J. Copeland, J. L. Walker, and R. A. Burger. 2006. Intraperitoneal cisplatin and paclitaxel in ovarian cancer. N. Engl. J Med. 354, 34-43.

Auersperg, N., I. A. Maclaren, and P. A. Kruk. 1991. Ovarian surface epithelium: autonomous production of connective tissue-type extracellular matrix. Biol. Reprod. 44, 717-724.

Auersperg, N., S. Maines-Bandiera, J. H. Booth, H. T. Lynch, A. K. Godwin, and T. C. Hamilton. 1995. Expression of two mucin antigens in cultured human ovarian surface epithelium: Influence of a family history of ovarian cancer. Am. J. Obstet. Gynecol. 173, 558-565.

Auersperg, N., S. L. Maines-Bandiera, and H. G. Dyck. 1997. Ovarian carcinogenesis and the biology of ovarian surface epithelium. J. Cell Physiol. 173, 261-265.

Auersperg, N., S. L. Maines-Bandiera, and H. G. Dyck. 1998. Phenotypic plasticity of ovarian surface epithelium: Possible implications for ovarian carcinogenesis. 3-17.

Auersperg, N., J. Pan, B. D. Grove, T. Peterson, J. Fisher, S. Maines-Bandiera, A. Somasiri, and C. D. Roskelley. 1999. E-cadherin induces mesenchymal-to-epithelial transition in human ovarian surface epithelium. Proceedings of the National Academy of Science USA. 96, 6249-6254.

Auersperg, N., A. S. Wong, K. C. Choi, S. K. Kang, and P. C. Leung. 2001. Ovarian surface epithelium: biology, endocrinology, and pathology. Endocr. Rev. 22, 255-288.

Aunoble, B., R. Sanches, E. Didier, and Y. J. Bignon. 2000. Major oncogenes and tumor suppressor genes involved in epithelial ovarian cancer (review). Int. J. Oncol. 16, 567-576.

Baker, V. V., M. P. Borst, D. Dixon, K. D. Hatch, H. M. Shingleton, and D. Miller. 1990. c-myc amplification in ovarian cancer. Gynecol. Oncol. 38, 340-342.

Barakat, R. R., M. G. Federici, P. E. Saigo, M. E. Robson, K. Offit, and J. Boyd. 2000. Absence of premalignant histologic, molecular, or cell biologic alterations in prophylactic oophorectomy specimens from BRCA1 heterozygotes. Cancer. 89, 383-390.

Baron, U. and H. Bujard. 2000. Tet repressor-based system for regulated gene expression in eukaryotic cells: principles and advances. Methods Enzymol. 327, 401-421.

Bast, R. and R. Woolas. 1993. Screening for ovarian cancer. Multiple markers may outperform CA 125 alone. BMJ. 306, 1684-1685.

Bast, R. C., Jr., D. Badgwell, Z. Lu, R. Marquez, D. Rosen, J. Liu, K. A. Baggerly, E. N. Atkinson, S. Skates, Z. Zhang, A. Lokshin, U. Menon, I. Jacobs, and K. Lu. 2005. New tumor markers: CA125 and beyond. Int. J. Gynecol. Cancer. 15 Suppl 3, 274-281.

Benedet, J. L., H. Bender, H. Jones, III, H. Y. Ngan, and S. Pecorelli. 2000. FIGO staging classifications and clinical practice guidelines in the management of gynecologic cancers. FIGO Committee on Gynecologic Oncology. Int. J. Gynaecol. Obstet. 70, 209-262.

Berkenblit, A. and S. A. Cannistra. 2005. Advances in the management of epithelial ovarian cancer. J. Reprod. Med. 50, 426-438.

Berton, T. R., T. Matsumoto, A. Page, C. J. Conti, C. X. Deng, J. L. Jorcano, and D. G. Johnson. 2003. Tumor formation in mice with conditional inactivation of Brca1 in epithelial tissues. Oncogene. 22, 5415-5426.

Birch, J. M., R. D. Alston, R. J. McNally, D. G. Evans, A. M. Kelsey, M. Harris, O. B. Eden, and J. M. Varley. 2001. Relative frequency and morphology of cancers in carriers of germline TP53 mutations. Oncogene. 20, 4621-4628.

Bohm-Velez, M., E. Mendelson, R. Bree, H. Finberg, E. K. Fishman, H. Hricak, F. Laing, D. Sartoris, A. Thurmond, and S. Goldstein. 2000. Ovarian cancer screening. American College of Radiology. ACR Appropriateness Criteria. Radiology. 215 Suppl, 861-871.

Bosco, E. E., Y. Wang, H. Xu, J. T. Zilfou, K. E. Knudsen, B. J. Aronow, S. W. Lowe, and E. S. Knudsen. 2007. The retinoblastoma tumor suppressor modifies the therapeutic response of breast cancer. J. Clin. Invest. 117, 218-228.

Boyd, J., Y. Sonoda, M. G. Federici, F. Bogomolniy, E. Rhei, D. L. Maresco, P. E. Saigo, L. A. Almadrones, R. R. Barakat, C. L. Brown, D. S. Chi, J. P. Curtin, E. A. Poynor, and W. J. Hoskins. 2000. Clinicopathologic features of BRCA-linked and sporadic ovarian cancer. JAMA. 283, 2260-2265.

Brodie, S. G., X. Xu, W. Qiao, W. M. Li, L. Cao, and C. X. Deng. 2001. Multiple genetic changes are associated with mammary tumorigenesis in Brca1 conditional knockout mice. Oncogene. 20, 7514-7523.

Brugghe, J., J. P. Baak, E. Wiltshaw, and C. Fisher. 1995. Further evaluation of reproducibility and prognostic value of histologic typing and grading in FIGO stage I ovarian cancer patients without systemic locoregional adjuvant treatment. Int J Gynecol. Cancer. 5, 262-268.

Burdette, J. E., S. J. Kurley, S. M. Kilen, K. E. Mayo, and T. K. Woodruff. 2006. Gonadotropin-induced superovulation drives ovarian surface epithelia proliferation in CD1 mice. Endocrinology. 147, 2338-2345.

Buttitta, F., A. Marchetti, A. Gadducci, S. Pellegrini, M. Morganti, V. Carnicelli, S. Cosio, O. Gagetti, A. R. Genazzani, and G. Bevilacqua. 1997. p53 alterations are predictive of chemoresistance and aggressiveness in ovarian carcinomas: a molecular and immunohistochemical study. Br. J. Cancer. 75, 230-235.

Caduff, R. F., S. M. Svoboda-Newman, A. W. Ferguson, C. M. Johnston, and T. S. Frank. 1999. Comparison of mutations of Ki-RAS and p53 immunoreactivity in borderline and malignant epithelial ovarian tumors. Am. J. Surg. Pathol. 23, 323-328.

Callahan, R. and G. H. Smith. 2000. MMTV-induced mammary tumorigenesis: gene discovery, progression to malignancy and cellular pathways. Oncogene. 19, 992-1001.

Canadian Cancer Society. 2006. Canadian Cancer Society: Canadian Cancer Statistics 2006.

Cao, L., W. Li, S. Kim, S. G. Brodie, and C. X. Deng. 2003. Senescence, aging, and malignant transformation mediated by p53 in mice lacking the Brca1 full-length isoform. Genes Dev. 17, 201-213.

Capo-chichi, C. D., E. R. Smith, D. H. Yang, I. H. Roland, L. Vanderveer, C. Cohen, T. C. Hamilton, A. K. Godwin, and X. X. Xu. 2002. Dynamic alterations of the extracellular environment of ovarian surface epithelial cells in premalignant transformation, tumorigenicity, and metastasis. Cancer. 95, 1802-1815.

Cass, I., R. L. Baldwin, T. Varkey, R. Moslehi, S. A. Narod, and B. Y. Karlan. 2003. Improved survival in women with BRCA-associated ovarian carcinoma. Cancer. 97, 2187-2195.

Celik, C., K. Gezginc, M. Aktan, A. Acar, S. T. Yaman, S. Gungor, and C. Akyurek. 2004. Effects of ovulation induction on ovarian morphology: an animal study. Int. J. Gynecol. Cancer. 14, 600-606.

Chabalier, C., C. Lamare, C. Racca, M. Privat, A. Valette, and F. Larminat. 2006. BRCA1 downregulation leads to premature inactivation of spindle checkpoint and confers paclitaxel resistance. Cell Cycle. 5, 1001-1007.

Chamberlain, J. S., M. Boehnke, T. S. Frank, S. Kiousis, J. Xu, S. W. Guo, E. R. Hauser, R. A. Norum, E. A. Helmbold, D. S. Markel, and . 1993. BRCA1 maps proximal to D17S579 on chromosome 17q21 by genetic analysis. Am. J. Hum. Genet. 52, 792-798.

Chen, V. W., B. Ruiz, J. L. Killeen, T. R. Cote, X. C. Wu, and C. N. Correa. 2003. Pathology and classification of ovarian tumors. Cancer. 97, 2631-2642.

Chodankar, R., S. Kwang, F. Sangiorgi, H. Hong, H. Y. Yen, C. Deng, M. C. Pike, C. F. Shuler, R. Maxson, and L. Dubeau. 2005. Cell-nonautonomous induction of ovarian and uterine serous cystadenomas in mice lacking a functional Brca1 in ovarian granulosa cells. Curr. Biol. 15, 561-565.

Cohen, C. J. and T. S. Jennings. 1994. Screening for ovarian cancer: the role of noninvasive imaging techniques. Am. J. Obstet. Gynecol. 170, 1088-1094.

Colgan, T. J., J. Murphy, D. E. Cole, S. Narod, and B. Rosen. 2001. Occult carcinoma in prophylactic oophorectomy specimens: prevalence and association with BRCA germline mutation status. Am. J. Surg. Pathol. 25, 1283-1289.

Colgin, D. C. and W. J. Murdoch. 1997. Evidence for a role of the ovarian surface epithelium in the ovulatory mechanism of the sheep: secretion of urokinase-type plasminogen activator. Anim Reprod. Sci. 47, 197-204.

Connolly, D. C., R. Bao, A. Y. Nikitin, K. C. Stephens, T. W. Poole, X. Hua, S. S. Harris, B. C. Vanderhyden, and T. C. Hamilton. 2003. Female mice chimeric for expression of the simian virus 40 TAg under control of the MISIIR promoter develop epithelial ovarian cancer. Cancer Res. 63, 1389-1397.

Cortez, D., Y. Wang, J. Qin, and S. J. Elledge. 1999. Requirement of ATM-dependent phosphorylation of brca1 in the DNA damage response to double-strand breaks. Science. 286, 1162-1166.

Cramer, D. W., G. B. Hutchison, W. R. Welch, R. E. Scully, and K. J. Ryan. 1983. Determinants of ovarian cancer risk. I. Reproductive experiences and family history. J. Natl. Cancer Inst. 71, 711-716.

Cramer, D. W., R. F. Liberman, L. Titus-Ernstoff, W. R. Welch, E. R. Greenberg, J. A. Baron, and B. L. Harlow. 1999. Genital talc exposure and risk of ovarian cancer. Int. J. Cancer. 81, 351-356.

Cressman, V. L., D. C. Backlund, E. M. Hicks, L. C. Gowen, V. Godfrey, and B. H. Koller. 1999. Mammary tumor formation in p53- and BRCA1-deficient mice. Cell Growth Differ. 10, 1-10.

Daoud, E. and G. Bodor. 1991. CA-125 concentrations in malignant and nonmalignant disease. Clin. Chem. 37, 1968-1974.

de Vries, V. S., S. P. Wilczynski, M. Fleischhacker, and P. Koeffler. 1994. p53 alterations in uterine leiomyosarcomas versus leiomyomas. Gynecol. Oncol. 54, 205-208.

Dei Tos, A. P., R. Maestro, C. Doglioni, S. Piccinin, D. D. Libera, M. Boiocchi, and C. D. Fletcher. 1996. Tumor suppressor genes and related molecules in leiomyosarcoma. Am. J. Pathol. 148, 1037-1045.

Deng, C. X. 2006. BRCA1: cell cycle checkpoint, genetic instability, DNA damage response and cancer evolution. Nucleic Acids Res. 34, 1416-1426.

Deng, C. X. 2001. Tumorigenesis as a consequence of genetic instability in Brca1 mutant mice. Mutat. Res. 477, 183-189.

Deng, C. X. and S. G. Brodie. 2000. Roles of BRCA1 and its interacting proteins. BioEssays. 22, 728-737.

Dimri, G., H. Band, and V. Band. 2005. Mammary epithelial cell transformation: insights from cell culture and mouse models. Breast Cancer Res. 7, 171-179.

Dinulescu, D. M., T. A. Ince, B. J. Quade, S. A. Shafer, D. Crowley, and T. Jacks. 2005. Role of K-ras and Pten in the development of mouse models of endometriosis and endometrioid ovarian cancer. Nat. Med. 11, 63-70.

Dyck, H. G., T. C. Hamilton, A. K. Godwin, H. T. Lynch, S. Maines-Bandiera, and N. Auersperg. 1996. Autonomy of the epithelial phenotype in human ovarian surface epithelium: Changes with neoplastic progression and with a family history of ovarian cancer. Int. J. Cancer. 69, 429-436.

Easton, D. F., D. Ford, and D. T. Bishop. 1995. Breast and ovarian cancer incidence in BRCA1-mutation carriers. Breast Cancer Linkage Consortium. Am. J. Hum. Genet. 56, 265-271.

Ellis, C. A. and G. Clark. 2000. The importance of being K-Ras. Cell Signal. 12, 425-434.

Enomoto, T., C. M. Weghorst, M. Inoue, O. Tanizawa, and J. M. Rice. 1991. K-ras activation occurs frequently in mucinous adenocarcinomas and rarely in other common epithelial tumors of the human ovary. Am. J Pathol. 139, 777-785.

Esteller, M., M. F. Fraga, M. Guo, J. Garcia-Foncillas, I. Hedenfalk, A. K. Godwin, J. Trojan, C. Vaurs-Barriere, Y. J. Bignon, S. Ramus, J. Benitez, T. Caldes, Y. Akiyama, Y. Yuasa, V. Launonen, M. J. Canal, R. Rodriguez, G. Capella, M. A. Peinado, A. Borg, L. A. Aaltonen, B. A. Ponder, S. B. Baylin, and J. G. Herman. 2001. DNA methylation patterns in hereditary human cancers mimic sporadic tumorigenesis. Hum. Mol. Genet. 10, 3001-3007.

Fan, S., R. Yuan, Y. X. Ma, J. Xiong, Q. Meng, M. Erdos, J. N. Zhao, I. D. Goldberg, R. G. Pestell, and E. M. Rosen. 2001. Disruption of BRCA1 LXCXE motif alters BRCA1 functional activity and regulation of RB family but not RB protein binding. Oncogene. 20, 4827-4841.

Fathalla, M. F. 1971. Incessant ovulation--a factor in ovarian neoplasia? Lancet. 2, 163-

Fedier, A., R. A. Steiner, V. A. Schwarz, L. Lenherr, U. Haller, and D. Fink. 2003. The effect of loss of Brca1 on the sensitivity to anticancer agents in p53-deficient cells. Int. J. Oncol. 22, 1169-1173.

Feki, A. and I. Irminger-Finger. 2004. Mutational spectrum of p53 mutations in primary breast and ovarian tumors. Crit Rev. Oncol. Hematol. 52, 103-116.

Finch, A., P. Shaw, B. Rosen, J. Murphy, S. A. Narod, and T. J. Colgan. 2005. Clinical and pathologic findings of prophylactic salpingo-oophorectomies in 159 BRCA1 and BRCA2 carriers. Gynecol. Oncol.

Flesken-Nikitin, A., K. C. Choi, J. P. Eng, E. N. Shmidt, and A. Y. Nikitin. 2003. Induction of carcinogenesis by concurrent inactivation of p53 and Rb1 in the mouse ovarian surface epithelium. Cancer Res. 63, 3459-3463.

Ford, D., D. F. Easton, D. T. Bishop, S. A. Narod, and D. E. Goldgar. 1994. Risks of cancer in BRCA1-mutation carriers. Breast Cancer Linkage Consortium. Lancet. 343, 692-695.

Fredrickson, T. N. 1987. Ovarian tumors of the hen. Environ. Health Perspect. 73:35-51, 35-51.

Fujiwara, K., M. Markman, M. Morgan, and R. L. Coleman. 2005. Intraperitoneal carboplatin-based chemotherapy for epithelial ovarian cancer. Gynecol. Oncol. 97, 10-15.

Gallion, H. H. and S. A. Smith. 1994. Hereditary ovarian carcinoma. Semin. Surg. Oncol. 10, 249-254.

Garte, S. J. 1993. The c-myc oncogene in tumor progression. Crit Rev. Oncog. 4, 435-449.

Gaytan, M., M. A. Sanchez, C. Morales, C. Bellido, Y. Millan, M. J. Martin de Las, J. E. Sanchez-Criado, and F. Gaytan. 2005. Cyclic changes of the ovarian surface epithelium in the rat. Reproduction. 129, 311-321.

Gayther, S. A., W. Warren, S. Mazoyer, P. A. Russell, P. A. Harrington, M. Chiano, S. Seal, R. Hamoudi, E. J. van Rensburg, A. M. Dunning, R. Love, G. Evans, D. Easton, D. Clayton, M. R. Stratton, and B. A. Ponder. 1995. Germline mutations

of the BRCA1 gene in breast and ovarian cancer families provide evidence for a genotype-phenotype correlation. Nat. Genet. 11, 428-433.

Geisler, J. P., M. A. Hatterman-Zogg, J. A. Rathe, T. A. Lallas, P. Kirby, and R. E. Buller. 2001. Ovarian cancer BRCA1 mutation detection: Protein truncation test (PTT) outperforms single strand conformation polymorphism analysis (SSCP). Hum. Mutat. 18, 337-344.

Gertig, D. M., D. J. Hunter, D. W. Cramer, G. A. Colditz, F. E. Speizer, W. C. Willett, and S. E. Hankinson. 2000. Prospective study of talc use and ovarian cancer. J. Natl. Cancer Inst. 92, 249-252.

Ghahremani, M., A. Foghi, and J. H. Dorrington. 1999. Etiology of ovarian cancer: a proposed mechanism. Med Hypotheses. 52, 23-26.

Gibb, R. K., D. D. Taylor, T. Wan, D. M. O'Connor, D. L. Doering, and C. Gercel-Taylor. 1997. Apoptosis as a measure of chemosensitivity to cisplatin and taxol therapy in ovarian cancer cell lines. Gynecol. Oncol. 65, 13-22.

Gilmore, P. M., N. McCabe, J. E. Quinn, R. D. Kennedy, J. J. Gorski, H. N. Andrews, S. McWilliams, M. Carty, P. B. Mullan, W. P. Duprex, E. T. Liu, P. G. Johnston, and D. P. Harkin. 2004. BRCA1 interacts with and is required for paclitaxel-induced activation of mitogen-activated protein kinase kinase kinase 3. Cancer Res. 64, 4148-4154.

Gowen, L. C., B. L. Johnson, A. M. Latour, K. K. Sulik, and B. H. Koller. 1996. Brca1 deficiency results in early embryonic lethality characterized by neuroepithelial abnormalities. Nat. Genet. 12, 191-194.

Gras, E., C. Pons, P. Machin, X. Matias-Guiu, and J. Prat. 2001. Loss of heterozygosity at the RB-1 locus and pRB immunostaining in epithelial ovarian tumors: a molecular, immunohistochemical, and clinicopathologic study. Int. J. Gynecol. Pathol. 20, 335-340.

Gwinn, M. L., N. C. Lee, P. H. Rhodes, P. M. Layde, and G. L. Rubin. 1990. Pregnancy, breast feeding, and oral contraceptives and the risk of epithelial ovarian cancer. J Clin. Epidemiol. 43, 559-568.

Hakem, R., J. L. de la Pompa, A. Elia, J. Potter, and T. W. Mak. 1997. Partial rescue of Brca1 (5-6) early embryonic lethality by p53 or p21 null mutation. Nat. Genet. 16, 298-302.

Hakem, R., J. L. de la Pompa, and T. W. Mak. 1998. Developmental studies of Brca1 and Brca2 knock-out mice. J. Mammary. Gland. Biol. Neoplasia. 3, 431-445.

Hakem, R., J. L. de la Pompa, C. Sirard, R. Mo, M. Woo, A. Hakem, A. Wakeham, J. Potter, A. Reitmair, F. Billia, E. Firpo, C. C. Hui, J. Roberts, J. Rossant, and T. W. Mak. 1996. The tumor suppressor gene Brca1 is required for embryonic cellular proliferation in the mouse. Cell. 85, 1009-1023.

Hall, J. A., E. M. Meisterling, A. M. Benoit, D. A. Cooper, D. A. Coleman, S. P. Lerner, P. E. Lewis, and R. A. Dailey. 1993. Factors contributing to the formation of experimentally-induced ovarian cysts in prepubertal gilts. Domest. Anim Endocrinol. 10, 141-155.

Hamilton, T. C., H. Fox, C. H. Buckley, W. J. Henderson, and K. Griffiths. 1984. Effects of talc on the rat ovary. Br. J. Exp. Pathol. 65, 101-106.

Harkin, D. P., J. M. Bean, D. Miklos, Y. H. Song, V. B. Truong, C. Englert, F. C. Christians, L. W. Ellisen, S. Maheswaran, J. D. Oliner, and D. A. Haber. 1999. Induction of GADD45 and JNK/SAPK-dependent apoptosis following inducible expression of BRCA1. Cell. 97, 575-586.

Harlow, B. L., D. W. Cramer, D. A. Bell, and W. R. Welch. 1992. Perineal exposure to talc and ovarian cancer risk. Obstetrics and Gynecology. 80, 19-26.

Hartman, A. R. and J. M. Ford. 2002. BRCA1 induces DNA damage recognition factors and enhances nucleotide excision repair. Nat. Genet. 32, 180-184.

Hartmann, L. C., K. C. Podratz, G. L. Keeney, N. A. Kamel, J. H. Edmonson, J. P. Grill, J. Q. Su, J. A. Katzmann, and P. C. Roche. 1994. Prognostic significance of p53 immunostaining in epithelial ovarian cancer. Journal of Clinical Oncology. 12, 64-69.

Hashiguchi, Y., H. Tsuda, T. Inoue, S. Nishimura, T. Suzuki, and N. Kawamura. 2004. Alteration of cell cycle regulators correlates with survival in epithelial ovarian cancer patients. Hum. Pathol. 35, 165-175.

Hawkins, D. S., G. W. Demers, and D. A. Galloway. 1996. Inactivation of p53 enhances sensitivity to multiple chemotherapeutic agents. Cancer Res. 56, 892-898.

He, Q. Y., Y. Zhou, E. Wong, T. G. Ehlen, N. Auersperg, J. F. Chiu, and A. S. Wong. 2005. Proteomic analysis of a preneoplastic phenotype in ovarian surface epithelial cells derived from prophylactic oophorectomies. Gynecol. Oncol. 98, 68-76.

Heller, D. S., M. Hameed, and R. Baergen. 2003. Lack of proliferative activity of surface epithelial inclusion cysts of the ovary. Int. J Gynecol. Cancer. 13, 303-307.

Henderson, W. J., T. C. Hamilton, M. S. Baylis, C. G. Pierrepoint, and K. Griffiths. 1986. The demonstration of the migration of talc from the vagina and posterior uterus to the ovary in the rat. Environ. Res. 40, 247-250.

Henderson, W. J., T. C. Hamilton, and K. Griffiths. 1979. Talc in normal and malignant ovarian tissue. Lancet. 1, 499-

Hengstler, J. G., J. Lange, A. Kett, N. Dornhofer, R. Meinert, M. Arand, P. G. Knapstein, R. Becker, F. Oesch, and B. Tanner. 1999. Contribution of c-erbB-2 and topoisomerase IIalpha to chemoresistance in ovarian cancer. Cancer Res. 59, 3206-3214.

Hogervorst, F. B., R. S. Cornelis, M. Bout, V. M. van, J. C. Oosterwijk, R. Olmer, B. Bakker, J. G. Klijn, H. F. Vasen, H. Meijers-Heijboer, and . 1995. Rapid detection of BRCA1 mutations by the protein truncation test. Nat Genet. 10, 208-212.

Holschneider, C. H. and J. S. Berek. 2000. Ovarian cancer: epidemiology, biology, and prognostic factors. Semin Surg Oncol. 19, 3-10.

Holt, J. T., M. E. Thompson, C. Szabo, C. Robinson-Benion, C. L. Arteaga, M. C. King, and R. A. Jensen. 1996. Growth retardation and tumour inhibition by BRCA1 [see comments] [published erratum appears in Nat Genet 1998 May;19(1):102]. Nat. Genet. 12, 298-302.

Hoyer, P. B. and I. G. Sipes. 1996. Assessment of follicle destruction in chemical-induced ovarian toxicity. Annu Rev Pharmacol. Toxicol. 36, 307-331.

Hu, Y., S. Ghosh, A. Amleh, W. Yue, Y. Lu, A. Katz, and R. Li. 2005. Modulation of aromatase expression by BRCA1: a possible link to tissue-specific tumor suppression. Oncogene. 24, 8343-8348.

Husain, A., G. He, E. S. Venkatraman, and D. R. Spriggs. 1998. BRCA1 up-regulation is associated with repair-mediated resistance to cis-diamminedichloroplatinum(II). Cancer Res. 58, 1120-1123.

Hutson, R., J. Ramsdale, and M. Wells. 1995. p53 protein expression in putative precursor lesions of epithelial ovarian cancer. Histopathology. 27, 367-371.

Jacobs, I. J., T. N. Fay, J. Yovich, I. Stabile, C. Frost, J. Turner, D. H. Oram, and J. G. Grudzinskas. 1990. Serum levels of CA 125 during the first trimester of normal outcome, ectopic and anembryonic pregnancies. Hum. Reprod. 5, 116-122.

Jones, L. P., M. Li, E. D. Halama, Y. Ma, R. Lubet, C. J. Grubbs, C. X. Deng, E. M. Rosen, and P. A. Furth. 2005. Promotion of mammary cancer development by tamoxifen in a mouse model of Brca1-mutation-related breast cancer. Oncogene. 24, 3554-3562.

Jonkers, J., R. Meuwissen, G. H. van der, H. Peterse, d. van, V, and A. Berns. 2001. Synergistic tumor suppressor activity of BRCA2 and p53 in a conditional mouse model for breast cancer. Nat Genet. 29, 418-425.

Katsaros, D., C. Theillet, P. Zola, G. Louason, B. Sanfilippo, E. Isaia, R. Arisio, G. Giardina, and P. Sismondi. 1995. Concurrent abnormal expression of *erb*B-2, *myc* and *ras* genes is associated with poor outcome of ovarian cancer patients. Anticancer Res. 15, 1501-1510.

Keri, R. A., K. L. Lozada, F. W. Abdul-Karim, J. H. Nadeau, and J. H. Nilson. 2000. Luteinizing hormone induction of ovarian tumors: oligogenic differences between mouse strains dictates tumor disposition. Proceedings of the National Academy of Science USA. 97, 383-387.

Kido, M. and M. Shibuya. 1998. Isolation and characterization of mouse ovarian surface epithelial cell lines. Pathol. Res. Pract. 194, 725-730.

Kigawa, J., S. Sato, M. Shimada, M. Takahashi, H. Itamochi, Y. Kanamori, and N. Terakawa. 2001. p53 gene status and chemosensitivity in ovarian cancer. Hum. Cell. 14, 165-171.

Kinzler, K. W. and B. Vogelstein. 1997. Cancer-susceptibility genes. Gatekeepers and caretakers. Nature. 386, 761, 763-

Kirchhoff, T., J. M. Satagopan, N. D. Kauff, H. Huang, P. Kolachana, C. Palmer, H. Rapaport, K. Nafa, N. A. Ellis, and K. Offit. 2004. Frequency of BRCA1 and BRCA2 mutations in unselected Ashkenazi Jewish patients with colorectal cancer. J Natl Cancer Inst. 96, 68-70.

Klemi, P. J., L. Pylkkänen, P. Kiilholma, K. Kurvinen, and H. Joensuu. 1995. P53 protein detected by immunohistochemistry as a prognostic factor in patients with epithelial ovarian carcinoma. Cancer. 76, 1201-1208.

Knudson, A. G., Jr. 1984. Genetic predisposition to cancer. Cancer Detect. Prev. 7, 1-8.

Kolasa, I. K., A. Rembiszewska, A. Janiec-Jankowska, A. nsonka-Mieszkowska, A. M. Lewandowska, B. Konopka, and J. Kupryjanczyk. 2006. PTEN mutation, expression and LOH at its locus in ovarian carcinomas. Relation to TP53, K-RAS and BRCA1 mutations. Gynecol. Oncol. 103, 692-697.

Kruk, P. A. and N. Auersperg. 1992. Human ovarian surface epithelial cells are capable of physically restructuring extracellular matrix. Am. J. Obstet. Gynecol. 167, 1437-1443.

Kruk, P. A. and N. Auersperg. 1994. A line of rat ovarian surface epithelium provides a continuous source of complex extracellular matrix. In Vitro Cell. Dev. Biol. 30A, 217-225.

Kruk, P. A., A. K. Godwin, T. C. Hamilton, and N. Auersperg. 1999. Telomeric instability and reduced proliferative potential in ovarian surface epithelial cells from women with a family history of ovarian cancer. Gynecol. Oncol. 73, 229-236.

Kubista, M., M. Rosner, E. Kubista, G. Bernaschek, and M. Hengstschlager. 2002. Brca1 regulates in vitro differentiation of mammary epithelial cells. Oncogene. 21, 4747-4756.

Kumar, T. R., L. A. Donehower, A. Bradley, and M. M. Matzuk. 1995. Transgenic mouse models for tumour-suppressor genes. J. Intern. Med. 238, 233-238.

Kurose, K., X. P. Zhou, T. Araki, S. A. Cannistra, E. R. Maher, and C. Eng. 2001. Frequent loss of PTEN expression is linked to elevated phosphorylated Akt levels, but not associated with p27 and cyclin D1 expression, in primary epithelial ovarian carcinomas. Am. J Pathol. 158, 2097-2106.

Laframboise, S., R. Nedelcu, J. Murphy, D. E. Cole, and B. Rosen. 2002. Use of CA-125 and ultrasound in high-risk women. Int. J. Gynecol. Cancer. 12, 86-91.

Lakhani, S. R., S. Manek, F. Penault-Llorca, A. Flanagan, L. Arnout, S. Merrett, L. McGuffog, D. Steele, P. Devilee, J. G. Klijn, H. Meijers-Heijboer, P. Radice, S. Pilotti, H. Nevanlinna, R. Butzow, H. Sobol, J. Jacquemier, D. S. Lyonet, S. L. Neuhausen, B. Weber, T. Wagner, R. Winqvist, Y. J. Bignon, F. Monti, F. Schmitt, G. Lenoir, S. Seitz, U. Hamman, P. Pharoah, G. Lane, B. Ponder, D. T. Bishop, and D. F. Easton. 2004. Pathology of ovarian cancers in BRCA1 and

Lane, T. F., C. Deng, A. Elson, M. S. Lyu, C. A. Kozak, and P. Leder. 1995. Expression of Brca1 is associated with terminal differentiation of ectodermally and mesodermally derived tissues in mice. Genes Dev. 9, 2712-2722.

Lanzi, C., P. Perego, R. Supino, S. Romanelli, T. Pensa, N. Carenini, I. Viano, D. Colangelo, R. Leone, P. Apostoli, G. Cassinelli, R. A. Gambetta, and F. Zunino. 1998. Decreased drug accumulation and increased tolerance to DNA damage in tumor cells with a low level of cisplatin resistance. Biochem. Pharmacol. 55, 1247-1254.

LeCouter, J. E., B. Kablar, W. R. Hardy, C. Ying, L. A. Megeney, L. L. May, and M. A. Rudnicki. 1998. Strain-dependent myeloid hyperplasia, growth deficiency, and accelerated cell cycle in mice lacking the Rb-related p107 gene. Mol. Cell Biol. 18, 7455-7465.

Lee, J. S. and J. H. Chung. 2001. Diverse functions of BRCA1 in the DNA damage response. Expert. Rev. Mol. Med. 2001, 1-11.

Lee, J. S., K. M. Collins, A. L. Brown, C. H. Lee, and J. H. Chung. 2000. hCds1-mediated phosphorylation of BRCA1 regulates the DNA damage response. Nature. 404, 201-204.

Leiser, A. L., S. E. Anderson, D. Nonaka, S. Chuai, A. B. Olshen, D. S. Chi, and R. A. Soslow. 2006. Apoptotic and cell cycle regulatory markers in uterine leiomyosarcoma. Gynecol. Oncol. 101, 86-91.

Lessa, E. P. and G. Applebaum. 1993. Screening techniques for detecting allelic variation in DNA sequences. Mol Ecol. 2, 119-129.

Li, A. J. and B. Y. Karlan. 2001. Genetic factors in ovarian carcinoma. Curr. Oncol. Rep. 3, 27-32.

Liu, C. Y., A. Flesken-Nikitin, S. Li, Y. Zeng, and W. H. Lee. 1996. Inactivation of the mouse Brca1 gene leads to failure in the morphogenesis of the egg cylinder in early postimplantation development. Genes Dev. 10, 1835-1843.

Liu, H. X., L. Cartegni, M. Q. Zhang, and A. R. Krainer. 2001. A mechanism for exon skipping caused by nonsense or missense mutations in BRCA1 and other genes. Nat Genet. 27, 55-58.

Liu, Y., M. Heyman, Y. Wang, U. Falkmer, C. Hising, L. Székely, and S. Einhorn. 1994. Molecular analysis of the retinoblastoma gene in primary ovarian cancer cells. Int. J. Cancer. 58, 663-667.

Lou, Z., C. C. Chini, K. Minter-Dykhouse, and J. Chen. 2003. Mediator of DNA damage checkpoint protein 1 regulates BRCA1 localization and phosphorylation in DNA damage checkpoint control. Journal of Biological Chemistry. 278, 13599-13602.

Ludwig, T., P. Fisher, S. Ganesan, and A. Efstratiadis. 2001. Tumorigenesis in mice carrying a truncating Brca1 mutation. Genes Dev. 15, 1188-1193.

Lynch, H. T., C. A. Deters, C. L. Snyder, J. F. Lynch, P. Villeneuve, J. Silberstein, H. Martin, S. A. Narod, and R. E. Brand. 2005. BRCA1 and pancreatic cancer: pedigree findings and their causal relationships. Cancer Genet Cytogenet. 158, 119-125.

MacLachlan, N. J. 1987. Ovarian disorders in domestic animals. Environ. Health Perspect. 73, 27-33.

MacLachlan, T. K., K. Somasundaram, M. Sgagias, Y. Shifman, R. J. Muschel, K. H. Cowan, and W. S. El-Deiry. 2000. BRCA1 effects on the cell cycle and the DNA damage response are linked to altered gene expression. Journal of Biological Chemistry. 275, 2777-2785.

Macleod, K. F., Y. Hu, and T. Jacks. 1996. Loss of Rb activates both p53-dependent and independent cell death pathways in the developing mouse nervous system. EMBO J. 15, 6178-6188.

Maines-Bandiera, S. L. and N. Auersperg. 1997. Increased E-cadherin expression in ovarian surface epithelium: an early step in metaplasia and dysplasia? Int. J. Gynecol. Pathol. 16, 250-255.

Maines-Bandiera, S. L., P. A. Kruk, and N. Auersperg. 1992. Simian virus 40-transformed human ovarian surface epithelial cells escape normal growth controls but retain morphogenetic responses to extracellular matrix. Am. J. Obstet. Gynecol. 167, 729-735.

Malpica, A., M. T. Deavers, K. Lu, D. C. Bodurka, E. N. Atkinson, D. M. Gershenson, and E. G. Silva. 2004. Grading ovarian serous carcinoma using a two-tier system. Am. J Surg. Pathol. 28, 496-504.

Markman, M., B. N. Bundy, D. S. Alberts, J. M. Fowler, D. L. Clark-Pearson, L. F. Carson, S. Wadler, and J. Sickel. 2001. Phase III trial of standard-dose intravenous cisplatin plus paclitaxel versus moderately high-dose carboplatin followed by intravenous paclitaxel and intraperitoneal cisplatin in small-volume stage III ovarian carcinoma: an intergroup study of the Gynecologic Oncology Group, Southwestern Oncology Group, and Eastern Cooperative Oncology Group. J Clin. Oncol. 19, 1001-1007.

Marquis, S. T., J. V. Rajan, A. Wynshaw-Boris, J. Xu, G. Y. Yin, K. J. Abel, B. L. Weber, and L. A. Chodosh. 1995. The developmental pattern of Brca1 expression implies a role in differentiation of the breast and other tissues. Nat. Genet. 11, 17-26.

Mayhew, C. N., L. M. Perkin, X. Zhang, J. Sage, T. Jacks, and E. S. Knudsen. 2004. Discrete signaling pathways participate in RB-dependent responses to chemotherapeutic agents. Oncogene. 23, 4107-4120.

Miki, Y., J. Swensen, D. Shattuck-Eidens, P. A. Futreal, K. Harshman, S. Tavtigian, Q. Liu, C. Cochran, L. M. Bennett, W. Ding, R. Bell, J. Rosenthal, C. Hussey, T. Tran, M. McClure, C. Frye, T. Hattier, R. Phelps, A. Haugen-Strano, H. Katcher, K. Yakumo, Z. Gholami, D. Shaffer, and S. Stone. 1994. A strong candidate for the breast and ovarian cancer susceptibility gene *BRCA1*. Science. 266, 66-71.

Mirkovic, N., M. A. Marti-Renom, B. L. Weber, A. Sali, and A. N. Monteiro. 2004. Structure-based assessment of missense mutations in human BRCA1: implications for breast and ovarian cancer predisposition. Cancer Res. 64, 3790-3797.

Mittal, K. R., A. Zeleniuch-Jacquotte, J. L. Cooper, and R. I. Demopoulos. 1993. Contralateral ovary in unilateral ovarian carcinoma: a search for preneoplastic lesions. Int. J. Gynecol. Pathol. 12, 59-63.

Moloughney, B., J. Snider, and L. Villeneuve. 2000. Ovarian cancer in Canada. CMAJ. 162, 690-

Moslehi, R., W. Chu, B. Karlan, D. Fishman, H. Risch, A. Fields, D. Smotkin, Y. Ben-David, J. Rosenblatt, D. Russo, P. Schwartz, N. Tung, E. Warner, B. Rosen, J. Friedman, J. S. Brunet, and S. A. Narod. 2000. BRCA1 and BRCA2 mutation analysis of 208 Ashkenazi Jewish women with ovarian cancer. Am. J. Hum. Genet. 66, 1259-1272.

Mullan, P. B., J. E. Quinn, P. M. Gilmore, S. McWilliams, H. Andrews, C. Gervin, N. McCabe, S. McKenna, P. White, Y. H. Song, S. Maheswaran, E. Liu, D. A. Haber, P. G. Johnston, and D. P. Harkin. 2001. BRCA1 and GADD45 mediated G2/M cell cycle arrest in response to antimicrotubule agents. Oncogene. 20, 6123-6131.

Murdoch, J., E. A. Van Kirk, and W. J. Murdoch. 1999. Hormonal control of urokinase plasminogen activator secretion by sheep ovarian surface epithelial cells. Biol. Reprod. 61, 1487-1491.

Murdoch, W. J. 1996. Ovarian surface epithelium, ovulation and carcinogenesis. Biol. Rev. Camb. Philos. Soc. 71, 529-543.

Murdoch, W. J. and A. C. McDonnel. 2002. Roles of the ovarian surface epithelium in ovulation and carcinogenesis. Reproduction. 123, 743-750.

Nagy, A., M. Gertstenstein, K. Vintersten, and R. Behringer, 2003. Manipulating the Mouse Embryo: A Laboratory Manual, 3. New York: Cold Spring Harbor Laboratory Press.

Narod, S. A. and J. Boyd. 2002. Current understanding of the epidemiology and clinical implications of BRCA1 and BRCA2 mutations for ovarian cancer. Curr Opin Obstet. Gynecol. 14, 19-26.

Nelson, H. D., L. H. Huffman, R. Fu, and E. L. Harris. 2005. Genetic risk assessment and BRCA mutation testing for breast and ovarian cancer susceptibility: systematic evidence review for the U.S. Preventive Services Task Force. Ann. Intern. Med. 143, 362-379.

Neuhausen, S. L. 2000. Founder populations and their uses for breast cancer genetics. Breast Cancer Res. 2, 77-81.

Neuhausen, S. L. and C. J. Marshall. 1994. Loss of heterozygosity in familial tumors from three BRCA1-linked kindreds. Cancer Res. 54, 6069-6072.

Niemann, T. H., T. L. Trgovac, V. R. McGaughy, G. S. Lewandowski, and L. J. Copeland. 1998. Retinoblastoma protein expression in ovarian epithelial neoplasms. Gynecol. Oncol. 69, 214-219.

Obata, K. and H. Hoshiai. 2000. Common genetic changes between endometriosis and ovarian cancer. Gynecol. Obstet. Invest. 50 Suppl 1, 39-43.

Okamura, H. and H. Katabuchi. 2001. Detailed morphology of human ovarian surface epithelium focusing on its metaplastic and neoplastic capability. Ital. J. Anat. Embryol. 106, 263-276.

Ong, A., S. L. Maines-Bandiera, C. D. Roskelley, and N. Auersperg. 1999. An ovarian adenocarcinoma line derived from SV40/E-cadherin-transfected normal human ovarian surface epithelium. Int. J. Cancer. 85, 430-437.

Ouchi, T., A. N. Monteiro, A. August, S. A. Aaronson, and H. Hanafusa. 1998. BRCA1 regulates p53-dependent gene expression. Proc. Natl. Acad. Sci. U. S. A. 95, 2302-2306.

Pal, T., J. Permuth-Wey, J. A. Betts, J. P. Krischer, J. Fiorica, H. Arango, J. Lapolla, M. Hoffman, M. A. Martino, K. Wakeley, G. Wilbanks, S. Nicosia, A. Cantor, and R. Sutphen. 2005. BRCA1 and BRCA2 mutations account for a large proportion of ovarian carcinoma cases. Cancer.

Papageorgiou, T. and C. A. Stratakis. 2002. Ovarian tumors associated with multiple endocrine neoplasias and related syndromes (Carney complex, Peutz-Jeghers syndrome, von Hippel-Lindau disease, Cowden's disease). Int J Gynecol. Cancer. 12, 337-347.

Park, T. W. and W. C. Kuhn. 2004. Neoadjuvant chemotherapy in ovarian cancer. Expert. Rev. Anticancer Ther. 4, 639-647.

Pejovic, T., J. E. Yates, H. Y. Liu, L. E. Hays, Y. Akkari, Y. Torimaru, W. Keeble, R. K. Rathbun, W. H. Rodgers, A. E. Bale, N. Ameziane, C. M. Zwaan, A. Errami, P. Thuillier, F. Cappuccini, S. B. Olson, J. M. Cain, and G. C. Bagby, Jr. 2006. Cytogenetic instability in ovarian epithelial cells from women at risk of ovarian cancer. Cancer Res. 66, 9017-9025.

Perego, P., S. Romanelli, N. Carenini, I. Magnani, R. Leone, A. Bonetti, A. Paolicchi, and F. Zunino. 1998. Ovarian cancer cisplatin-resistant cell lines: multiple changes including collateral sensitivity to Taxol. Ann. Oncol. 9, 423-430.

Petricoin, E. F., A. M. Ardekani, B. A. Hitt, P. J. Levine, V. A. Fusaro, S. M. Steinberg, G. B. Mills, C. Simone, D. A. Fishman, E. C. Kohn, and L. A. Liotta. 2002. Use of proteomic patterns in serum to identify ovarian cancer. Lancet. 359, 572-577.

Ponz de, L. M., P. Benatti, A. Percesepe, G. Rossi, A. Viel, M. Santarosa, M. Pedroni, and L. Roncucci. 1999. Clinical and molecular diagnosis of hereditary non-polyposis colorectal cancer: problems and pitfalls in an extended pedigree. Ital. J Gastroenterol. Hepatol. 31, 476-480.

Prat, J., A. Ribe, and A. Gallardo. 2005. Hereditary ovarian cancer. Hum. Pathol. 36, 861-870.

Purdie, D. M., C. J. Bain, V. Siskind, P. M. Webb, and A. C. Green. 2003. Ovulation and risk of epithelial ovarian cancer. Int. J. Cancer. 104, 228-232.

Qazi, F. and W. P. McGuire. 1995. The treatment of epithelial ovarian cancer. CA Cancer J. Clin. 45, 88-101.

Quinn, J. E., R. D. Kennedy, P. B. Mullan, P. M. Gilmore, M. Carty, P. G. Johnston, and D. P. Harkin. 2003. BRCA1 functions as a differential modulator of chemotherapy-induced apoptosis. Cancer Res. 63, 6221-6228.

Ramus, S. J., L. G. Bobrow, P. D. Pharoah, D. S. Finnigan, A. Fishman, M. Altaras, P. A. Harrington, S. A. Gayther, B. A. Ponder, and L. S. Friedman. 1999. Increased frequency of TP53 mutations in BRCA1 and BRCA2 ovarian tumours. Genes Chromosomes. Cancer. 25, 91-96.

Rangarajan, A., S. J. Hong, A. Gifford, and R. A. Weinberg. 2004. Species- and cell type-specific requirements for cellular transformation. Cancer Cell. 6, 171-183.

Reedy, M. B., T. Hang, H. Gallion, S. Arnold, and S. A. Smith. 2001. Antisense inhibition of BRCA1 expression and molecular analysis of hereditary tumors indicate that functional inactivation of the p53 DNA damage response pathway is required for BRCA-associated tumorigenesis. Gynecol. Oncol. 81, 441-446.

Risch, H. A. 1998. Hormonal etiology of epithelial ovarian cancer, with a hypothesis concerning the role of androgens and progesterone. J Natl. Cancer Inst. 90, 1774-1786.

Risma, K. A., C. M. Clay, T. M. Nett, T. Wagner, J. Yun, and J. H. Nilson. 1995. Targeted overexpression of luteinizing hormone in transgenic mice leads to infertility, polycystic ovaries, and ovarian tumors. Proceedings of the National Academy of Science USA. 92, 1322-1326.

Robanus-Maandag, E., M. Dekker, d. van, V, M. L. Carrozza, J. C. Jeanny, J. H. Dannenberg, A. Berns, and R. H. te. 1998. p107 is a suppressor of retinoblastoma development in pRb-deficient mice. Genes Dev. 12, 1599-1609.

Rosen, E. M., S. Fan, and I. D. Goldberg. 2001. BRCA1 and prostate cancer. Cancer Invest. 19, 396-412.

Rossing, M. A., M. T. Tang, E. W. Flagg, L. K. Weiss, and K. G. Wicklund. 2004. A case-control study of ovarian cancer in relation to infertility and the use of ovulation-inducing drugs. Am. J. Epidemiol. 160, 1070-1078.

Russell, P. A., P. D. Pharoah, F. K. De, S. J. Ramus, I. Symmonds, A. Wilson, I. Scott, B. A. Ponder, and S. A. Gayther. 2000. Frequent loss of BRCA1 mRNA and protein expression in sporadic ovarian cancers. Int. J. Cancer. 87, 317-321.

Salazar, H., A. K. Godwin, M. B. Daly, P. B. Laub, W. M. Hogan, N. Rosenblum, M. P. Boente, H. T. Lynch, and T. C. Hamilton. 1996. Microscopic benign and invasive

malignant neoplasms and a cancer-prone phenotype in prophylactic oophorectomies [see comments]. J. Natl. Cancer Inst. 88, 1810-1820.

Sanders, E. J., P. H. Torkkeli, and A. S. French. 1997. Patterns of cell death during gastrulation in chick and mouse embryos. Anat. Embryol. (Berl). 195, 147-154.

Sauer, B. 1998. Inducible gene targeting in mice using the Cre/lox system. Methods. 14, 381-392.

Schildkraut, J. M., P. J. Schwingl, E. Bastos, A. Evanoff, and C. Hughes. 1996. Epithelial ovarian cancer risk among women with polycystic ovary syndrome. Obstetrics and Gynecology. 88, 554-559.

Schlosshauer, P. W., C. J. Cohen, F. Penault-Llorca, C. R. Miranda, Y. J. Bignon, J. Dauplat, and L. Deligdisch. 2003. Prophylactic oophorectomy: a morphologic and immunohistochemical study. Cancer. 98, 2599-2606.

Schrock, E., P. Badger, D. Larson, M. Erdos, A. Wynshaw-Boris, T. Ried, and L. Brody. 1996. The murine homolog of the human breast and ovarian cancer susceptibility gene Brca1 maps to mouse chromosome 11D. Hum. Genet. 97, 256-259.

Schuetz, A. W. and C. Lessman. 1982. Evidence for follicle wall involvement in ovulation and progesterone production by frog (Rana pipiens) follicles in vitro. Differentiation. 22, 79-84.

Seeley, S. L., E. E. Bosco, E. Kramer, L. M. Parysek, and E. S. Knudsen. 2007. Distinct roles for RB loss on cell cycle control, cisplatin response, and immortalization in Schwann cells. Cancer Lett. 245, 205-217.

Sgagias, M. K., K. U. Wagner, B. Hamik, S. Stoeger, R. Spieker, L. J. Huber, L. A. Chodosh, and K. H. Cowan. 2004. Brca1-deficient murine mammary epithelial cells have increased sensitivity to CDDP and MMS. Cell Cycle. 3, 1451-1456.

Sharan, S. K., M. Wims, and A. Bradley. 1995. Murine Brca1: sequence and significance for human missense mutations. Hum. Mol. Genet. 4, 2275-2278.

Shen, S. X., Z. Weaver, X. Xu, C. Li, M. Weinstein, L. Chen, X. Y. Guan, T. Ried, and C. X. Deng. 1998. A targeted disruption of the murine Brca1 gene causes gamma-irradiation hypersensitivity and genetic instability. Oncogene. 17, 3115-3124.

Shimizu, Y., E. Akagaki, K. Hirota, M. Kono, S. Miura, and Y. Okudaira. 1985. [Analysis of CA 125 assay system and its diagnostic significance in gynecologic tumors]. Nippon Sanka Fujinka Gakkai Zasshi. 37, 2813-2820.

Shimizu, Y., H. Fujiwara, E. Akagaki, K. Hirota, M. Kono, T. Irie, S. Miura, and Y. Okudaira. 1986. [Significance of CA 125 antigen levels in patients with ovarian cancer]. Gan To Kagaku Ryoho. 13, 46-52.

Silverberg, S. G. 2000. Histopathologic grading of ovarian carcinoma: a review and proposal. Int J Gynecol. Pathol. 19, 7-15.

Simpson, K. J., M. R. Wati, A. J. Deans, G. J. Lindeman, and M. A. Brown. 2004. MMTV-trBrca1 mice display strain-dependent abnormalities in vaginal development. Int. J. Dev. Biol. 48, 675-678.

Singhal, P. and S. Lele. 2006. Intraperitoneal chemotherapy for ovarian cancer: where are we now? J Natl Compr. Canc. Netw. 4, 941-946.

Siskind, V., A. Green, C. Bain, and D. Purdie. 1997. Breastfeeding, menopause, and epithelial ovarian cancer. Epidemiology. 8, 188-191.

Somasundaram, K., H. Zhang, Y. X. Zeng, Y. Houvras, Y. Peng, H. Zhang, G. S. Wu, J. D. Licht, B. L. Weber, and W. S. El-Deiry. 1997. Arrest of the cell cycle by the tumour-suppressor BRCA1 requires the CDK-inhibitor p21WAF1/CiP1. Nature. 389, 187-190.

Sood, A. K., J. I. Sorosky, M. Dolan, B. Anderson, and R. E. Buller. 1999. Distant metastases in ovarian cancer: association with p53 mutations. Clin. Cancer Res. 5, 2485-2490.

Sorlie, T., T. I. Andersen, I. Bukholm, and A. L. Borresen-Dale. 1998. Mutation screening of BRCA1 using PTT and LOH analysis at 17q21 in breast carcinomas from familial and non-familial cases. Breast Cancer Res Treat. 48, 259-264.

St-Onge, L., P. A. Furth, and P. Gruss. 1996. Temporal control of the Cre recombinase in transgenic mice by a tetracycline responsive promoter. Nucleic Acids Res. 24, 3875-3877.

Stewart, J. J., J. T. White, X. Yan, S. Collins, C. W. Drescher, N. D. Urban, L. Hood, and B. Lin. 2006. Proteins associated with Cisplatin resistance in ovarian cancer cells identified by quantitative proteomic technology and integrated with mRNA expression levels. Mol Cell Proteomics. 5, 433-443.

Stewart, T. A., P. K. Pattengale, and P. Leder. 1984. Spontaneous mammary adenocarcinomas in transgenic mice that carry and express MTV/myc fusion genes. Cell. 38, 627-637.

Strange, R., F. Li, S. Saurer, A. Burkhardt, and R. R. Friis. 1992. Apoptotic cell death and tissue remodelling during mouse mammary gland involution. Development. 115, 49-58.

Stratakis, C. A., T. Papageorgiou, A. Premkumar, S. Pack, L. S. Kirschner, S. E. Taymans, Z. Zhuang, W. H. Oelkers, and J. A. Carney. 2000. Ovarian lesions in Carney complex: clinical genetics and possible predisposition to malignancy. J Clin. Endocrinol. Metab. 85, 4359-4366.

Szabo, C. I. and M. C. King. 1997. Population genetics of BRCA1 and BRCA2. Am. J. Hum. Genet. 60, 1013-1020.

Szabo, C. I., T. Worley, and A. N. Monteiro. 2004. Understanding germ-line mutations in BRCA1. Cancer Biol Ther. 3, 515-520.

Takahashi, M., J. Kigawa, Y. Minagawa, H. Itamochi, M. Shimada, S. Kamazawa, S. Sato, R. Akeshima, and N. Terakawa. 2000. Sensitivity to paclitaxel is not related to p53-dependent apoptosis in ovarian cancer cells. Eur. J. Cancer. 36, 1863-1868.

Tan, O. L., P. R. Hurst, and J. S. Fleming. 2005. Location of inclusion cysts in mouse ovaries in relation to age, pregnancy, and total ovulation number: implications for ovarian cancer? J. Pathol. 205, 483-490.

Tashiro, H., K. Miyazaki, H. Okamura, A. Iwai, and M. Fukumoto. 1992. c-myc over-expression in human primary ovarian tumours: its relevance to tumour progression. Int. J. Cancer. 50, 828-833.

Taylor, R. R., R. I. Linnoila, J. Gerardts, M. G. Teneriello, J. D. Nash, R. C. Park, and M. J. Birrer. 1995. Abnormal expression of the retinoblastoma gene in ovarian neoplasms and correlation to p53 and K-ras mutations. Gynecol. Oncol. 58, 307-311.

Thangaraju, M., S. H. Kaufmann, and F. J. Couch. 2000. BRCA1 facilitates stress-induced apoptosis in breast and ovarian cancer cell lines. Journal of Biological Chemistry. 275, 33487-33496.

Thompson, M. E., R. A. Jensen, P. S. Obermiller, D. L. Page, and J. T. Holt. 1995. Decreased expression of BRCA1 accelerates growth and is often present during sporadic breast cancer progression. Nat. Genet. 9, 444-450.

Tibbetts, R. S., D. Cortez, K. M. Brumbaugh, R. Scully, D. Livingston, S. J. Elledge, and R. T. Abraham. 2000. Functional interactions between BRCA1 and the checkpoint kinase ATR during genotoxic stress. Genes Dev. 14, 2989-3002.

Ting, N. S. and W. H. Lee. 2004. The DNA double-strand break response pathway: becoming more BRCAish than ever. DNA Repair (Amst). 3, 935-944.

Tonin, P., B. Weber, K. Offit, F. Couch, T. R. Rebbeck, S. Neuhausen, A. K. Godwin, M. Daly, J. Wagner-Costalos, D. Berman, G. Grana, E. Fox, M. F. Kane, R. D. Kolodner, M. Krainer, D. A. Haber, J. P. Struewing, E. Warner, B. Rosen, C. Lerman, B. Peshkin, L. Norton, O. Serova, W. D. Foulkes, J. E. Garber, and . 1996. Frequency of recurrent BRCA1 and BRCA2 mutations in Ashkenazi Jewish breast cancer families. Nat. Med. 2, 1179-1183.

Vanderhyden, B. C. 2005. Loss of ovarian function and the risk of ovarian cancer. Cell Tissue Res. 322, 117-124.

Vooijs, M., d. van, V, R. H. te, and A. Berns. 1998. Flp-mediated tissue-specific inactivation of the retinoblastoma tumor suppressor gene in the mouse. Oncogene. 17, 1-12.

Wang, A., R. Schneider-Broussard, A. P. Kumar, M. C. MacLeod, and D. G. Johnson. 2000a. Regulation of BRCA1 expression by the Rb-E2F pathway. Journal of Biological Chemistry. 275, 4532-4536.

Wang, C., A. Horiuchi, T. Imai, S. Ohira, K. Itoh, T. Nikaido, Y. Katsuyama, and I. Konishi. 2004. Expression of BRCA1 protein in benign, borderline, and malignant epithelial ovarian neoplasms and its relationship to methylation and allelic loss of the BRCA1 gene. J. Pathol. 202, 215-223.

Wang, Y., D. Cortez, P. Yazdi, N. Neff, S. J. Elledge, and J. Qin. 2000b. BASC, a super complex of BRCA1-associated proteins involved in the recognition and repair of aberrant DNA structures. Genes Dev. 14, 927-939.

Wang, Y., L. A. Krushel, and G. M. Edelman. 1996. Targeted DNA recombination in vivo using an adenovirus carrying the cre recombinase gene. Proc. Natl. Acad. Sci. U. S. A. 93, 3932-3936.

Watson, P. and B. Riley. 2005. The tumor spectrum in the Lynch syndrome. Fam. Cancer. 4, 245-248.

Weaver, Z., C. Montagna, X. Xu, T. Howard, M. Gadina, S. G. Brodie, C. X. Deng, and T. Ried. 2002. Mammary tumors in mice conditionally mutant for Brca1 exhibit gross genomic instability and centrosome amplification yet display a recurring distribution of genomic imbalances that is similar to human breast cancer. Oncogene. 21, 5097-5107.

Werness, B. A., A. M. Afify, K. L. Bielat, G. H. Eltabbakh, M. S. Piver, and J. M. Paterson. 1999. Altered surface and cyst epithelium of ovaries removed prophylactically from women with a family history of ovarian cancer. Hum. Pathol. 30, 151-157.

Wong, A. S., S. L. Maines-Bandiera, B. Rosen, M. J. Wheelock, K. R. Johnson, P. C. Leung, C. D. Roskelley, and N. Auersperg. 1999. Constitutive and conditional cadherin expression in cultured human ovarian surface epithelium: influence of family history of ovarian cancer. Int. J. Cancer. 81, 180-188.

Woodworth, C. D., E. Michael, L. Smith, K. Vijayachandra, A. Glick, H. Hennings, and S. H. Yuspa. 2004. Strain-dependent differences in malignant conversion of mouse skin tumors is an inherent property of the epidermal keratinocyte. Carcinogenesis. 25, 1771-1778.

Woolas, R. P., M. R. Conaway, F. Xu, I. J. Jacobs, Y. Yu, L. Daly, A. P. Davies, K. O'Briant, A. Berchuck, J. T. Soper, and . 1995. Combinations of multiple serum markers are superior to individual assays for discriminating malignant from benign pelvic masses. Gynecol. Oncol. 59, 111-116.

Woolas, R. P., F. J. Xu, I. J. Jacobs, Y. H. Yu, L. Daly, A. Berchuck, J. T. Soper, D. L. Clarke-Pearson, D. H. Oram, and R. C. Bast, Jr. 1993. Elevation of multiple serum markers in patients with stage I ovarian cancer. J Natl Cancer Inst. 85, 1748-1751.

Wu, L. C., Z. W. Wang, J. T. Tsan, M. A. Spillman, A. Phung, X. L. Xu, M. C. Yang, L. Y. Hwang, A. M. Bowcock, and R. Baer. 1996. Identification of a RING protein that can interact in vivo with the BRCA1 gene product. Nat. Genet. 14, 430-440.

Xing, D. and S. Orsulic. 2006. A mouse model for the molecular characterization of brca1-associated ovarian carcinoma. Cancer Res. 66, 8949-8953.

Xu, B., S. Kim, and M. B. Kastan. 2001a. Involvement of Brca1 in S-phase and G(2)-phase checkpoints after ionizing irradiation. Mol. Cell Biol. 21, 3445-3450.

Xu, X., W. Qiao, S. P. Linke, L. Cao, W. M. Li, P. A. Furth, C. C. Harris, and C. X. Deng. 2001b. Genetic interactions between tumor suppressors Brca1 and p53 in apoptosis, cell cycle and tumorigenesis. Nat. Genet. 28, 266-271.

Xu, X., K. U. Wagner, D. Larson, Z. Weaver, C. Li, T. Ried, L. Hennighausen, A. Wynshaw-Boris, and C. X. Deng. 1999a. Conditional mutation of Brca1 in mammary epithelial cells results in blunted ductal morphogenesis and tumour formation. Nat. Genet. 22, 37-43.

Xu, X., Z. Weaver, S. P. Linke, C. Li, J. Gotay, X. W. Wang, C. C. Harris, T. Ried, and C. X. Deng. 1999b. Centrosome amplification and a defective G2-M cell cycle checkpoint induce genetic instability in BRCA1 exon 11 isoform-deficient cells. Mol. Cell. 3, 389-395.

Yancik, R. 1993. Ovarian cancer: Age contrasts in incidence, histology, disease stage at diagnosis, and mortality. Cancer. 71 Suppl., 517-523.

Yoshida, K. and Y. Miki. 2004. Role of BRCA1 and BRCA2 as regulators of DNA repair, transcription, and cell cycle in response to DNA damage. Cancer Sci. 95, 866-871.

Yu, H. 2002. Regulation of APC-Cdc20 by the spindle checkpoint. Curr. Opin. Cell Biol. 14, 706-714.

Zahir, N. and V. M. Weaver. 2004. Death in the third dimension: apoptosis regulation and tissue architecture. Curr. Opin. Genet. Dev. 14, 71-80.

Zhou, C., J. L. Smith, and J. Liu. 2003. Role of BRCA1 in cellular resistance to paclitaxel and ionizing radiation in an ovarian cancer cell line carrying a defective BRCA1. Oncogene. 22, 2396-2404.

Zweemer, R. P., P. A. Shaw, R. M. Verheijen, A. Ryan, A. Berchuck, B. A. Ponder, H. Risch, J. R. McLaughlin, S. A. Narod, F. H. Menko, P. Kenemans, and I. J. Jacobs. 1999. Accumulation of p53 protein is frequent in ovarian cancers associated with BRCA1 and BRCA2 germline mutations. J. Clin. Pathol. 52, 372-375.